Universidad Autónoma de Madrid
Departamento de Bioquímica

Antitumorigenic mechanisms of action of Peroxisome Proliferator-Activated Receptor γ (PPARγ) ligands in breast cancer

TESIS DOCTORAL

JORGE DORADO PÉREZ

Madrid, 2.009

Departamento de Bioquímica
Facultad de Medicina
Universidad Autónoma de Madrid

Antitumorigenic mechanisms of action of Peroxisome Proliferator-Activated Receptor γ (PPARγ) ligands in breast cancer

Memoria que presenta

Jorge Dorado Pérez

Licenciado en Bioquímica

para optar al Grado de Doctor

Director:

Ana María Pérez Castillo

Instituto de Investigaciones Biomédicas "Alberto Sols"

CSIC-UAM

MINISTERIO
DE CIENCIA
E INNOVACIÓN

CSIC

UAM UNIVERSIDAD AUTÓNOMA DE MADRID

INSTITUTO DE INVESTIGACIONES BIOMÉDICAS
"ALBERTO SOLS"

ANA MARÍA PÉREZ CASTILLO, Profesor de Investigación del Consejo Superior de Investigaciones Científicas, con destino en el Instituto de Investigaciones Biomédicas "Alberto Sols"

CERTIFICO:

Que el trabajo que se recoge en la presente Memoria, titulada "Antitumorigenic mechanisms of action of Peroxisome Proliferator-Activated Receptor γ (PPARγ) ligands in breast cancer", que presenta D. **JORGE DORADO PÉREZ**, Licenciado en Bioquímica, para optar al Grado de Doctor por la Universidad Autónoma de Madrid, ha sido realizado bajo mi dirección en el Instituto de Investigaciones Biomédicas "Alberto Sols". Considero, además, que el mencionado trabajo reúne la originalidad y calidad científica requerida para ser presentado como Tesis Doctoral en el Departamento de Bioquímica de la Facultad de Medicina de la Universidad Autónoma de Madrid.

Y para que conste a todos los efectos, expido el presente certificado.

Madrid, 28 de septiembre de 2.009

Dra. Ana Pérez Castillo
Director de la Tesis
Profesor de Investigación
CSIC

VºBº Dr. Leandro Sastre Garzón
Tutor de la Tesis
Profesor Honorario
Departamento de Bioquímica
Universidad Autónoma de Madrid

c/ Arturo Duperier nº 4
28029 MADRID
TELÉFONO: 91 585 44 00
FAX: 91 585 44 01

A Juan Pérez de Lucas, mi abuelo.

Porque ya sé sumar.

AGRADECIMIENTOS

AGRADECIMIENTOS

Esta memoria recopila parte del trabajo realizado a lo largo de seis años. Quien la lea podrá valorar el fruto de todo este tiempo lleno de experimentos, de enseñanzas y de ciencia al fin y al cabo, aunque después de recopilar, analizar y ordenar todos los resultados creo que uno se convierte en el mejor crítico posible de su trabajo. Lo que no verá es todo lo que ha habido detrás de estos resultados, y ya que han sido muchas las personas que han colaborado a que todo este trabajo saliera adelante creo que se merecen un hueco entre estas líneas, porque ellos también son partícipes de estos resultados. Además, no quiero dejar pasar esta oportunidad de resaltar públicamente lo importantes que han sido determinadas personas en mi trabajo, ya sea por su implicación directa en él o por lo importantes que son en mi vida, con lo que ello supone para mi trabajo. Sé que los agradecimientos son breves, pero espero que no resulten escasos a ojos de nadie. A veces lo más corto es lo que más dice.

En primer lugar agradecer a la Dra. Ana Pérez Castillo haber confiado en mi y haberme dado la oportunidad de formar parte de su equipo. Gracias por mantener esa confianza en todo momento, por dejarme libertad, creer en mi trabajo, preocuparse por mi futuro y muy especialmente por tener esa relación tan cercana. Gracias, Ana. Dar las gracias también al Dr. Ángel Santos por estar siempre dispuesto a ayudar, por sus críticas para mejorar, su buen humor y su visión tan especial de la ciencia. Gracias al Dr. Leandro Sastre por ejercer como Tutor de este trabajo, por las facilidades que ha dado durante la realización del mismo y por su predisposición, siempre con una sonrisa.

A todas las personas que forman parte de este laboratorio. A Miguel, por todo el trabajo que sirvió de base al mío. A Jinny y John por su recibimiento cuando llegué, por estar siempre dispuestos a enseñarme y ayudarme. A unas cuantas personas a quienes aprecio y quiero muchísimo… A Marta, por enseñarme casi todo lo que ha permitido hacer esta tesis. Por hacerlo siempre con una sonrisa y por ser un modelo de científica y de persona. Por haber tenido la suerte de compartir westerns, nesteas y di-le-que-nos con una de las personas que más me ha marcado en la vida. A Maicha, por todos los buenos momentos y tantos cambios que hemos compartido en estos años, por todo lo que me has enseñado en el laboratorio, por tu alegría. A Claudia, por sufrir conmigo la prostaglandina, por ser tan re-buena persona; no me acostumbro a no tenerte por aquí. A Jose, por las risas y los bailes entre el trabajo duro, por hacer del laboratorio un lugar agradable donde no hay compañeros sino amigos. A Diana, por las conversaciones, por los zumos, las chocitas y el FGF. A Marina, por tener siempre la frase para cambiar un mal día, por sus detalles, por hacernos sentir tan importantes para alguien. A Sandra, por mantener el espíritu del viejo 1.9. Y gracias también a los nuevos: a Jimena, por trasmitir su energía, y a Elena, por sus ganas y su decisión.

Gracias también a Alberto Álvarez Barrientos, Pilar Torralbo, Elvira Arza y Raquel Nieto, a Mariano Vitón, José Manuel Ligos y Pedro Lastres por tantos experimentos de citometría, por sus enseñanzas, por implicarse tan profundamente y por los buenos ratos

(¿verdad, Raquel?). Gracias también al CNIC por recibirnos durante seis meses, por poner sus medios a nuestra disposición y hacernos sentir mejor que en casa.

A todos los vecinos de laboratorio a los que debo tantos buenos momentos. Gracias a los chicos del 1.11: Vane, María, Vero, Pipe, Inma, Julio, Gallarda y Ascen por los buenos ratos, los vídeos musicales, makoki, los karaokes…; a los del 1.10: Fátima, David, María Ángeles, Jacin, Sara, Quilla, Carol, Ana y Tere, por los ratos dentro y fuera de cultivos, en Pamplona…; al 1.13: a Héctor, Sonia, Eva (cuando bailamos?), Giacomo… A Carmen, Mari Carmen, Dani (lo que da de sí una feria…).

Gracias también a todo el personal del IIB que ha facilitado y hecho más ameno el trabajo. A María Teresa Macías, Raquel Pina y Cristina Requejo del Servicio de Protección Radiológica por su profesionalidad y eficiencia; a Fernando Nuñez, Carmina Fernández, Ruth e Iliana de Animalario; a Javi Merino, Guti y Nani de Informática; a Javi y Ricardo de Imagen, a Mari Carmen de Administración, Jose de Almacén (graciaxx), Fernando y Mari Paz (sin ella una tesis no es lo mismo) de Biblioteca y Gabriel y Carlos de Recepción.

Tampoco me olvido de mis compañeros de Bioquímica. Gracias a María Salazar, Amaya, Isa, María Jurado y Ángel, aparte de los que ya han tenido su espacio, por tantas y tantas risas y buenos momentos. A mis amigos de Biología: Irene, Paula, Cris, Lucía, Jose, Dani y Álex por los ánimos y por estar tan pendientes en todo momento. Lo mismo digo de mis biólogas: Raquel, Martina, Sara, Marta, María, Mariajo y Rosa, gracias por todos los ánimos. Y por supuesto gracias a Daniel Herranz, a David Marsán y a Rubén y María por estar siempre tan cerca.

Una pequeña mención para el Dr. Enrique Panero Grimau, por ser un ejemplo de profesionalidad y sabiduría, y al Dr. Roberto Marco, por sus consejos, sus locuras espaciales y todos los momentos y personas que surgieron de ellas.

A Isa, por animarme y darme fuerza en todo momento, por volcarte en mi, por las vueltas de tuerca, por tu paciencia y tu comprensión, y por estar siempre a mi lado y hacerme tan feliz. Gracias. Te quiero.

A mi familia. A mi abuela, por tantísimo cariño. A mis primos, por llenar la casa de alegría, por las carreras, las risas y los juegos. A Miguel y a mi Titi, por preocuparse tanto por mi, por meterse, por los trasteros, de pequeño y de mayor, por buscar siempre lo mejor para mi y tratarme y quererme como a un hijo. A mis hermanos, por ser dos pilares fundamentales en mi vida, por su cariño y por importarles tanto. A mis padres, por todo lo que se han sacrificado por mi, por mi educación y la de mis hermanos, por nuestro futuro, porque llegara hasta aquí, por anteponernos a ellos mismos, por desvivirse por nosotros y por hacernos sentir tan queridos. Gracias. Os quiero mucho.

Gracias a todos por haberme acompañado y ayudado a lo largo de esta etapa. Ahora toca pensar en nuevos horizontes, porque, en palabras de Springsteen,

‘Tramps Like Us,
Baby, We Were Born To Run’

RESUMEN

RESUMEN

En este trabajo hemos analizado el mecanismo de acción tumorogénica de los ligandos del Receptor Activado por Proliferadores Peroxisomales γ (PPARγ) 15-deoxi-Δ^{12-14}-PGJ_2 **(**15d-PGJ_2), rosiglitazona y pioglitazona en células humanas de cáncer de mama. Nuestros datos muestran que el tratamiento con estos compuestos reduce la viabilidad, inhibe la proliferación y favorece la apoptosis en varias líneas celulares de carcinoma mamario, y atribuyen por vez primera efectos similares a los miembros de la familia de compuestos denominados tiadiazolidinonas (TDZDs). Además, hemos determinado que algunos de sus efectos son llevados a cabo, al menos en el caso del agonista natural 15d-PGJ_2, por defosforilación de ErbB2 y ErbB3 a través de un incremento en la actividad fosfatasa de la fosfatasa 1 con dominios de homología a Src (SHP-1). Por otro lado, demostramos que 15d-PGJ_2 es responsable de inducir en células de cáncer de mama parada de ciclo celular en la fase G_2/M así como una desestructuración significativa de la red de microtúbulos mediante su unión directa a tubulina. También mostramos los efectos antineoplásicos de los ligandos de PPARγ en el crecimiento y la auto-renovación de las células madre humanas de cáncer de mama. Por último, hemos evaluado la fiabilidad del perfil de expresión $CD44^{+}/CD24^{-/bajo}$ como marcador de células madre humanas de cáncer de mama y de la "side population" como modelo de las mismas.

SUMMARY

SUMMARY

In this work we have analyzed the antitumorigenic mechanism of action of the Peroxisome Proliferator-Activated Receptor γ (PPARγ) ligands 15-deoxi-Δ^{12-14}-PGJ_2 (15d-PGJ_2), rosiglitazone and pioglitazone on human breast cancer cells. Our data show that treatment with these compounds reduces cell viability, induces inhibition of proliferation and promotes apoptosis in several breast carcinoma cell lines, and attribute for the first time similar effects to members of the thiadiazolidinones (TDZDs) family of compounds. In addition, we determined that some of their effects are exerted, at least in the case of the natural agonist 15d-PGJ_2, through an increase in the phosphatase activity of Src-Homology-2 domain-containing phosphatase 1 (SHP-1), by dephosphorylation of ErbB2 and ErbB3. In addition, we show that 15d-PGJ_2 is responsible for inducing cell cycle arrest of breast cancer cells in the G_2/M phase of the cell cycle and a significant dysruption of the microtubule network following its direct binding to tubulin. Furthermore, we show antineoplastic effects of PPARγ ligands on growth and self-renewal of human breast cancer stem cells. Finally, we have evaluated the reliability of $CD44^+/CD24^{-/low}$ expression profile as a marker and of the 'side population' as a working model for human breast cancer stem cells.

ÍNDICE

ÍNDICE

ABREVIATURAS

ABBREVIATIONS

15d-PGJ$_2$	15-deoxi-$\Delta^{12,14}$-PGJ$_2$
ABCG2	ATP-Binding Cassette, Subfamily G Member 2
AF-1	Activation Function-1
ALDH	Aldehyde dehydrogenase
aP2	Adipocyte fatty acid binding protein
ATP	Adenosine triphosphate
APC	Allophycocyanin
BDP1	Brain-Derived Phosphatase-1
bFGF	Basic Fibroblast Growth Factor
BrdU	5-Bromo-2-deoxy-uridine
BSA	Bovin Serum Albumin
CBP-1	CREB-binding protein-1
COX	Cyclooxygenase
DAPI	4,6-diamidino-2-phenylindole
DEP1	Density-Enhanced-Phosphatase 1
DNA	Deoxyribonucleic acid
DR1	Direct Repeat 1
DTT	Dithiotreitol
ECL	Enhanced Chemoluminiscence
EDTA	Ethylenediaminetetraacetic acid
EGF	Epidermal Growth Factor
EGFP	Enhanced Green Fluorescent Protein
EGFR	Epidermal Growth Factor Receptor
EGTA	Ethyleneglycoltetraacetic acid
ErbB	Erythroblastic Leukemia Viral Oncogene Homolog

FACS	Fluorescence-Activated Cell Sorting
FBS	Fetal Bovine Serum
FITC	Fluoresceinisothiocyanate
FTC	Fumitremorgin C
HPLC	High Performance Liquid Chromatography
IKK	IKB Kinase
iNOS	Inducible Nitric Oxide Synthase
iRNA	Interference RNA
LPL	Lipoprotein lipase
MAPK	Mitogen-Activated Protein Kinase
M-MLV RT	Moloney Murine-Leukaemia Virus Reverse Transcriptase
MRM	Multiple Reaction Monitoring
mRNA	Messenger RNA
MS	Mass spectrometry
MT	Microtubule
MTT	3-[4,5-dimethylthiazol-2-yl]-2,5-diphenyl tetrazolium bromide
NCoR1-2	Nuclear Co-Repressors 1-2
NF-kB	Nuclear Factor-kB
NRG	Neuregulin
NSAID	Non-Steroideal Anti-Inflammatory Drug
PAGE	Polyacrilamide Gel Electrophoresis
PBS	Phosphate-buffered saline
PCR	Polymerase Chain Reaction
PE	Phycoeritrin
PGZ	Pioglitazone
PI	Propidium Iodide
PI3K	Phosphatidylinositol 3-kinase

PMSF	Phenylmethylsulphonyl fluoride
PPAR	Peroxisome Proliferator-Activated Receptor
PPRE	PPAR Response Element
PTB	Phosphotyrosine Binding
PTP	Protein Tyrosine Phosphatase
Q-PCR	Quantitative PCR
RIP140	Receptor Interacting Protein 140
RNA	Ribonucleic acid
RSG	Rosiglitazone
RXR	Retinoid X Receptor
SD	Standard Deviation
SDS	Sodium Dodecyl Sulfate
SH2	Src-homology-2
SHP-1	SH2-domain containing phosphatase-1
SHP-2	SH2-domain containing phosphatase-2
SMRT1-2	Silencing Mediator for Retinoid and Thyroid Hormone Receptors
SP	Side Population
SRC-1	Steroid receptor coactivator-1
STAT5	Signal transducer and activator of transcription 5
TBS	Tris-buffered saline
TGF-α	Transforming Growth Factor-α
TNF-α	Tumor Necrosis Factor-α
TZD	Thiazolidinedione
TDZD	Thiadiazolidinones
TDZD-8	4-benzyl-2-methyl-1,2,4-thiadiazolidine-3,5-dione
WB	Western-blot

INTRODUCTION

1.- CANCER

Cancer is a disease defined by uncontrolled cell expansion, dedifferentiation of the abnormally-dividing cells and migration and invasiveness of surrounding and distant tissues. The cause for the deregulation of proliferation at the origin of cancer lies in accumulative sequential mutations that occur as a result of both genetic instability and environmental offences, generating important molecular alterations within the cell that interfere with its proliferation.

Cell proliferation is controlled by a balance between proliferative and antiproliferative signals to which the cell is submitted. When a cell proliferates it undergoes a repetitive cycle of duplication of the genetic information and division, which is known as cell cycle. The cell first duplicates its DNA content to generate two identical copies. This defines the S phase of the cell cycle (S for synthesis). Then, each copy is segregated to one of the two daughter cells resulting from cell division. Segregation and cell division define the M phase (M for mitosis). Mitosis is further subdivided in subphases that reflect how chromosome segregation occurs. To prepare for synthesis and mitosis, the cell undergoes two previous gap phases, called G_1 and G_2, respectively.

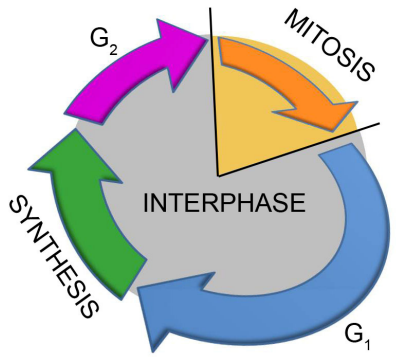

Figure 1. **The phases of the cell cycle.**
When cells proliferate they duplicate their DNA content and segregate the copies into the daughter cells. DNA duplication occurs during the S phase, and cell division marks the M phase. These processes are separated by gap phases (G_1 and G_2). The period comprising G_1, S and G_2 phases, in which the cell prepares for mitosis, is known as interphase.

To integrate the stimuli that induce or oppose proliferation, the cell possesses signalling pathways that transform both external and internal signals into a cellular response. To achieve this, the cell accounts for signal receptors in charge of receiving the signal. This is the case, of ErbB receptors, that will be discussed later on. Through a complex system of lipid and protein recruitment and interaction, where post-transductional modifications such as phosphorylation play a crucial role, the cell activates transcription factors that will bind to the promoter of target genes and regulate their transcription, giving thus an appropriate response to the stimuli. Misfunctioning of these mechanisms may lead to aberrant proliferative responses and, in some cases, to cancer.

With more than 3 million new cases and 1.7 million deaths each year, cancer represents the second most important cause of death in Europe, after cardiovascular disease. Depending on the tissue where it originates, cancer can be further classified in carcinoma, if it arises from the epithelium, or sarcoma if it originates from mesoderm. Leukaemias are neoplasties which start in blood precursors, whereas lymphomas and myelomas begin in cells of the immune system. Currently, the most common form of diagnosed cancer is breast cancer (13.5% of all cancer cases), followed by colorectal cancer (12.9%) and lung cancer (12.1%). Regarding the number of deaths from cancer, breast carcinoma is, after lung cancer and colorectal cancer, the third most common cause of death considering both sexes and the leading cause in women (Ferlay et al., 2007).

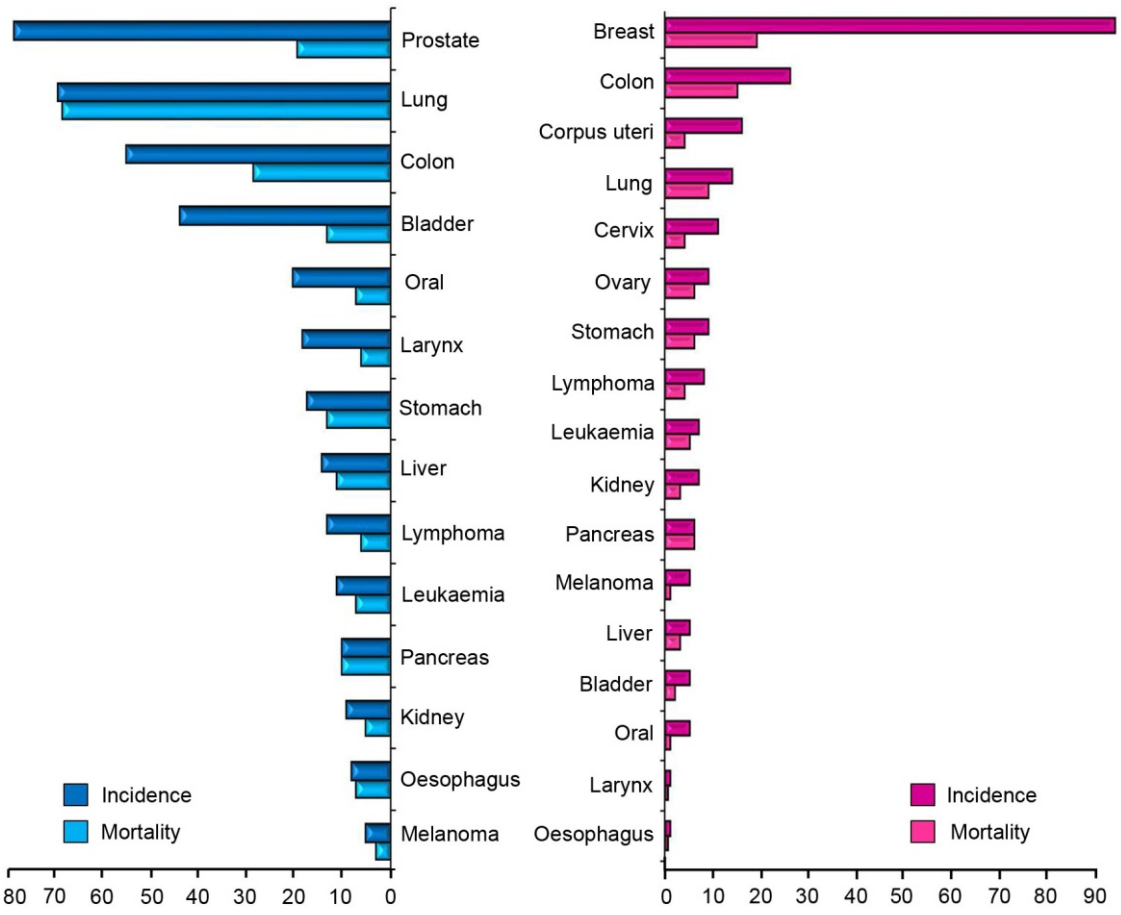

Figure 2. **Incidence and mortality of most common cancer types in Spain.**
Data from year 2006. Related to 100,000 inhabitants.
Source: International Agency for Research on Cancer

2.- BREAST CANCER

The mammary gland originates as an appendage of the skin during foetus development. Epithelial cells proliferate within the so-called stroma, surrounding connective tissue composed of extracellular matrix, fibroblasts, blood and lymphoid vessels, nerves and inmmune cells. As a result, a rudimentary tree-shaped net of ducts is generated. During puberty, the exposure of the epithelial cells to oestrogen and progesterone causes elongation and side branching of the ducts, at whose end epithelial cells form alveoli, giving the mammary gland its final configuration. Alveoli are in charge of producing milk upon pregnancy and secrete it into the lumen of the ducts. In the resulting mature mammary gland, epithelial cells are organized in two strata: some of the epithelial cells are adjacent to the lumen, and are thus named luminal, whereas the so-called basal myoepithelial cells form a mesh-like structure between the luminal cells and the basement membrane (Hennighausen and Robinson, 2005).

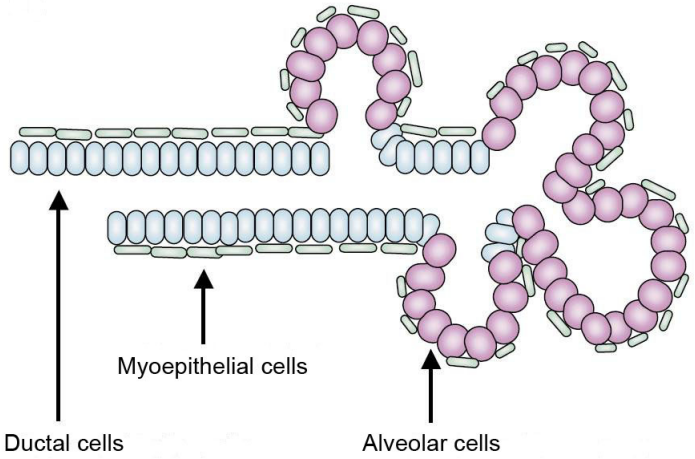

Figure 3. **Organization of the mature mammary gland.** Cells are classified in ductal or alveolar depending of their localization. In addition, cells in contact with the lumen are considered basal, and cells in contact with the basement membrane are known as myoepithelial. Source: (Woodward et al., 2005).

Depending on which structure of the mammary gland is affected by a neoplastic lesion, breast cancer is classified on luminal or basal cancer or alternatively in ductal or lobular cancer, when ducts or alveoli are affected, respectively. In its early stage, cancer cells form a neoplastic mass, which remains embedded in the tissue where it has been originated, but separated from the surrounding tissue by the basement membrane. At this moment, the carcinoma is called '*in situ'*. However, during cancer progression, the basement membrane is progressively degradated and tumour cells invade the stroma. Cancer is then classified as 'invasive'. Most breast tumours arise from the duct epithelium, with invasive ductal carcinomas, accounting for over 70% of diagnosed breast cancers.

In order to efficiently eradicate cancer cells, elucidation of the mechanisms underlying tumour progression and identification of new therapeutic agents is of crucial importance. Studies from our laboratory and other groups have shown that ligands for the Peroxisome Proliferator-Activated Receptor γ (PPARγ) have important antitumorigenic effects on breast cancer cells, placing them as important therapeutic agents to fight breast cancer.

3.- PPARs

Peroxisome Proliferator-Activated Receptors (PPARs) are ligand-inducible transcription factors that belong to the superfamily of the nuclear hormone receptors, which includes receptors for steroid hormones, bile acids, retinoic acids, and thyroid hormones (Evans, 1988). These receptors are multi-domain transcription factors that bind to specific DNA sequences and induce transcription of target genes. They have a N-terminal domain that contains at least one constitutively active transactivation region known as 'activation function-1' (AF-1) together with sites for phosphorylation and docking of regulatory proteins, a highly conserved central domain responsible for DNA binding and heterodimerization, a domain which acts as a flexible hinge region and a C-terminal domain which serves as docking site for cofactors and contains a nuclear localization signal and a ligand-dependent transactivation function referred to as AF-2.

PPARs bind to consensus sequences known as PPAR Response Elements (PPRE) in the promoter of their target genes. These sequences consist of a directly repeating core site separated by one nucleotide (NNN-AGGTCA-N-AGGTCA), and are thus called 'direct repeat 1' (DR1) (Palmer et al., 1995). PPREs have been identified, among others, in genes coding for acylcoenzyme A oxidase, cytochrome P450 4A6, and adipocyte P2. To recognize a PPRE, PPARs must form a heterodimer with the retinoid X receptor (RXR), which is a common DNA binding partner of the thyroid/steroid receptor family that binds 9-cis retinoic acid (Mangelsdorf et al., 1992). Once bound to the PPRE, PPAR activates transcription via a mechanism that involves the recruitment of coactivators, such as CREB-binding protein (CBP-1), steroid receptor coactivator 1 (SRC-1), and receptor interacting protein 140 (RIP140) and corepressors such as nuclear co-repressors 1-2 (NCoR1-2) and silencing mediator for retinoid and thyroid hormone receptors 1-2 (SMRT1-2).

There are three PPAR isotypes: PPARα, PPARβ (also called PPARδ, due to parallel characterization) and PPARγ (Keller and Wahli, 1993; Sertznig et al., 2007). PPARα and PPARβ are deeply implicated in energy homeostasis. PPARα controls transcription of genes involved in mitochondrial β-oxidation of free fatty acids, stimulates gluconeogenesis, ketone-body synthesis and cholesterol uptake by the liver (Bragt and Popeijus, 2008), whereas PPARβ participates in fatty acid oxidation and in myelinization and lipid metabolism in the brain (Basu-Modak et al., 1999). Conversely to PPARγ, for whom a deep implication in cancer has been established, PPARα and PPARβ are mainly in charge of fatty acid metabolism, with few and not fully-elucidated implications on tumorigenesis.

3.1.- PPARγ

The gene encoding for PPARγ (NR1C3) has been identified under six isoforms in humans, named PPARγ1-5 and PPARγ7. PPARγ1 and PPARγ2 differ only in 84 additional nucleotides at the 5' end of PPARγ2 gene, that encode for 28 additional aminoacids. This causes the ligand-independent activation domain of PPARγ2 to be five to ten times more effective than that of PPARγ1. The rest of the isoforms are different transcripts, but encode for the same protein than PPARγ1. Therefore, there are only two resulting proteins: PPARγ1 and PPARγ2, caused by different promoter usage and alternative splicing. PPARγ is highly expressed in white and brown adipocytes, immune system and at lower levels in skeletal muscle, liver and bone marrow stromal cells, fibroblasts and epithelial cells.

PPARγ regulates adipocyte differentiation and lipid storage and release. In fact, one of the earliest events in the differentiation of adipocytes is PPARγ expression (Tontonoz et al., 1994). Moreover, PPARγ regulates multiple genes implicated in lipid metabolism, including lipoprotein lipase (LPL), adipocyte fatty acid binding protein (aP2), acyl-CoA synthase, and fatty acid transport protein. In addition, PPARγ regulates insulin homeostasis, as activation of PPARγ leads to improvement of insulin sensitivity, and a subsequent increase in glucose uptake.

PPARγ has been shown to have antineoplastic effects in several carcinomas (Grommes et al., 2004). The ability of PPARγ to inhibit the proliferation of fibroblasts during adipose differentiation first suggested that this receptor might be capable of reducing

malignant behaviour in neoplastic lesions. This was first examined in human liposarcoma, a malignancy of the adipose lineage. Most liposarcomas have been found to express higher levels of PPARγ than other sarcomas, and cells grown from liposarcomas were found to have a dramatic differentiation response to PPARγ ligands (Tontonoz et al., 1997). Based on these findings, later studies reported that PPARγ activation inhibits proliferation and induces apoptosis of malignant cells from different lineages such as gastric carcinoma (Sato et al., 2000), colorectal carcinoma (Kubota et al., 1998), pancreatic carcinoma (Elnemr et al., 2000), hepatocellular carcinoma and non-small-cell lung cancer (Keshamouni et al., 2004). More recently, its antineoplastic capacities have been proved in glioma (Grommes et al., 2006). In addition, PPARγ ligands have been reported to inhibit angiogenesis and neovascularisation both *in vitro* and *in vivo* (Panigrahy et al., 2002). Altogether, these observations suggest that induction of differentiation and apoptosis by activation of PPARγ may represent a promising novel therapeutic approach for cancer as already demonstrated for liposarcoma. In accordance with this, we and others have obtained evidence that activation of PPARγ by different ligands results in a more differentiated, less malignant state, a reduction in growth rate and an enhancement of apoptosis of several breast cancer cell lines. Specifically we have shown that the PPARγ ligand 15-deoxi-$\Delta^{12\text{-}14}$-Prostaglandin J_2 almost completely blocks phosphorylation and subsequent activation of the ErbB receptor tyrosine kinase family and, therefore, plays a suppressive regulatory role in the tumour growth of human breast carcinoma cells that express these receptors (Pignatelli et al., 2001).

3.2.- PPARγ ligands

PPARγ can be activated upon binding of a wide variety of hydrophobic ligands. Unsaturated fatty acids are commonly found among the natural activators of PPARγ. These are dietary components that, in general terms, are good activators of all PPAR subtypes, especially the 18-20 carbon unsaturated fatty acids. However, the highest activation rate of PPARγ is achieved by the endogenous eicosanoid 15-deoxi-$\Delta^{12\text{-}14}$-prostaglandin J_2 (15d-PGJ_2), with proven antiproliferative effects on several carcinoma types. There are also synthetic molecules capable of significantly activating PPARγ. This group of synthetic activators includes the group of insulin sensitizers known as thiazolidinediones (TZDs) and the non-steroideal anti-inflammatory drugs (NSAIDs).

3.2.1.- Thiazolidinediones

Thiazolidinediones (TZDs) are insulin sensitizers that improve glucose uptake and lower hyperglycaemia and hyperinsulinaemia. Thus, they have been used in the treatment for type II *diabetes mellitus*, although some reports suggest that they could increase the risk of heart failure (Home et al., 2009).

This group of synthetic PPARγ ligands, which includes among others rosiglitazone, pioglitazone, ciglitazone and troglitazone, has also been reported to inhibit the growth and promote apoptosis in different types of carcinomas. Activation of PPARγ by rosiglitazone, for example, induces inhibition of cell growth and/or induction of apoptosis in prostate cancer, hepatocellular carcinoma and breast carcinoma (Grommes et al., 2004). Similar effects have been observed upon treatment with pioglitazone in gastric cancer and breast carcinoma (Sohda et al., 1990). Troglitazone, another member of the family of the TZDs, exhibits antineoplastic effects in a wide variety of tumours, both *in vitro* and *in vivo*. Considering breast cancer, troglitazone has been reported to inhibit proliferation of breast carcinoma cells (Elstner et al., 1998) and cause regression or stasis of breast tumours in rats (Pighetti et al., 2001). Conversely, a phase II study conducted on patients with advanced refractory breast cancer was not able to report benefit from treatment with troglitazone (Burstein et al., 2003). However this study had to be concluded in advance due to withdrawal of troglitazone from clinical use as significant adverse events of severe liver toxicity were reported.

3.2.2.- Thiadiazolidinones (TDZDs)

The compounds of the family of the thiadiazolidinones (TDZDs) show structure similarity with the TZDs group of PPARγ ligands that includes rosiglitazone and pioglitazone, among others. Although these compounds were originally developed as non-ATP competitive inhibitors of GSK-3β (Martinez et al., 2002), data from our group indicate that they are efficient activators of PPARγ receptors. Moreover, our data reflect that inhibitors of PPARγ impair the effects exerted by TDZDs, strongly suggesting that their action is mediated by this receptor (Luna-Medina et al., 2005). In addition, TDZDs have been shown to have potent anti-inflammatory effects, including downregulation of cycloxygenase type 2 (COX-2), a property shared with the natural PPARγ ligand 15d-PGJ_2.

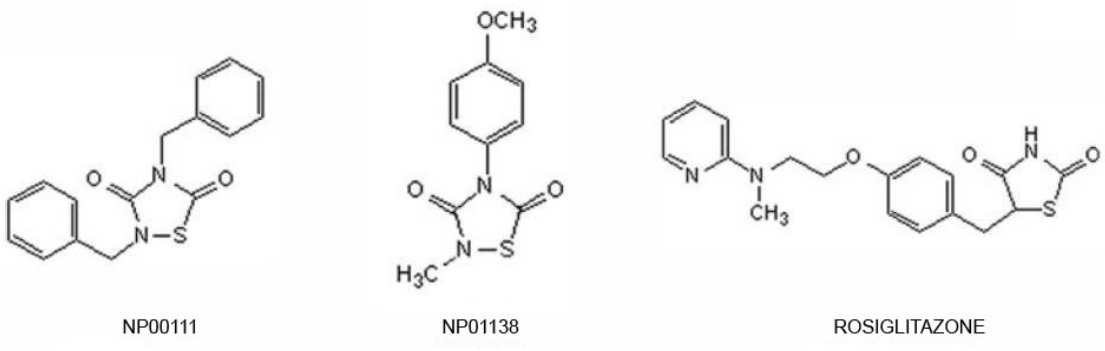

Figure 4. **Structure of the thiadiazolidinones compounds NP00111 and NP01138 and the thiazolidinedione rosiglitazone.**

Although TDZDs have been reported by us as well as other authors to promote cytoprotective effects in several tissues (Luna-Medina et al., 2007), it has been recently shown that one of these compounds, known as TDZD-8, causes death of leukaemia stem cells (Guzman et al., 2007), suggesting a possible role in cancer therapy.

3.2.3.- Non-Steroideal Anti-Inflammatory Drugs (NSAIDs)

Non-Steroideal Anti-Inflammatory Drugs (NSAIDs) such as indometacin and ibuprofen are cyclooxygenase inhibitors that also bind and activate PPARγ *in vitro* at high concentrations, causing terminal adipocyte differentiation (Lehmann et al., 1997). Some of them are also activators of PPARα, inducing peroxisomal activity in hepatocytes.

3.2.4.- 15-deoxi-Δ^{12-14}-Prostaglandin J_2

Prostaglandins are derivatives of arachidonic acid liberated from membrane phospholipids by phospholipase A_2 (Straus and Glass, 2001). Upon release, arachidonic acid is converted by the enzyme cyclooxygenase (COX, also known as PGH synthase) to PGH_2, an unstable intermediate that will be enzimatically processed. Depending on the enzyme that catalyses the reaction, PGH_2 will originate one of the different biologically active prostanoids: PGD_2, PGE_2, $PGF_{2\alpha}$, PGI_2, or thromboxane A_2. Each of them will be the precursor of a series of derivatives with biological effects. Thus, PGD_2 spontaneously undergoes chemical dehydratation to form PGJ_2. Prostaglandins from the J series contain an electrophilic carbonyl moiety in their cyclopentenone ring that is responsible for their reactivity with other molecules. PGJ_2 can undergo further dehydratation by loss of the 15-hydroxyl group, which, coupled with migration of the 13,14-double bond, results in the formation of 15-deoxi-Δ^{12-14}-PGJ_2 (15d-PGJ_2), that contains a second potentially reactive electrophilic carbon on one of its side chains.

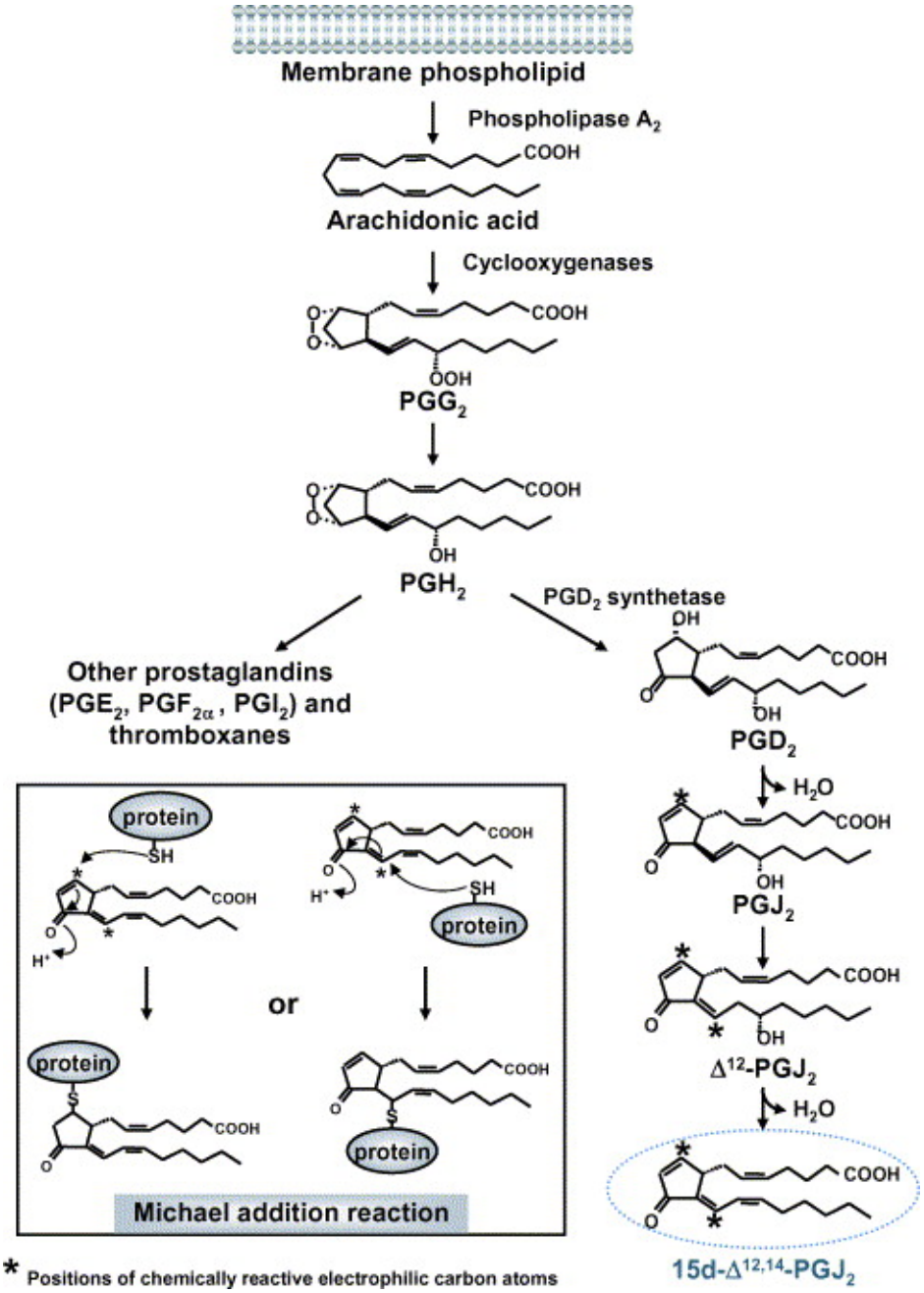

Figure 5. **Schematic representation of the synthesis pathway of 15d-$\Delta^{12\text{-}14}$PGJ$_2$.**
Source: (Kim and Surh, 2006)

15d-PGJ$_2$ plays an important role in adipogenesis, as it is an inducer of adipocyte differentiation (Forman et al., 1995; Kliewer et al., 1995). In addition, 15d-PGJ$_2$ is a potent anti-inflammatory agent capable of repressing the expression of inducible nitric oxide synthase (iNOS), tumour necrosis factor-α (TNFα) and COX-2 in activated monocytes (Ricote et al., 1998) and inhibiting the production of inflammatory cytokines (Jiang et al., 1998). Moreover, 15d-PGJ$_2$ enhances platelet production (O'Brien et al., 2009) and protects against oxidative stress.

15d-PGJ_2 has also been shown to have important antineoplastic effects *in vitro* and *in vivo* on prostate carcinoma, gastric cancer, colon carcinoma, glioma, breast carcinoma and pancreatic cancer (Grommes et al., 2004). These effects comprise inhibition of growth, promotion of apoptosis, and arrest of the cell cycle, an effect attributed to downregulation of cyclin D1. In the later years, 15d-PGJ_2 has emerged as an inhibitor of angiogenesis (Fu et al., 2006) and its induction of apoptosis has been related to activation of p53 (Ho et al., 2008). In agreement with all this data, we have recently shown that 15d-PGJ_2 inhibits breast cancer cell proliferation, induces apoptosis and causes mitochondrial dysfunction, suggesting that the anti-neoplastic effects of 15d-PGJ_2 can be triggered by multiple mechanisms (Pignatelli et al., 2005).

Some of the anticancer effects exerted by 15d-PGJ_2 are based on its ability to activate PPARγ. However, other effects are not mediated by PPARγ, but are due to the capacity of 15d-PGJ_2 to directly interact with other proteins. The presence of two highly reactive electrophilic centres in 15d-PGJ_2 allows the formation of covalent adducts via a Michael addition reaction with nucleophiles such as cysteine thiol groups present in proteins (Kim and Surh, 2006). This is the mechanism by which 15d-PGJ_2 binds several transcription factors, such as nuclear factor-kB (NF-kB) (Straus et al., 2000) and the β-subunit of the IKB kinase (IKK) complex (Rossi et al., 2000) and regulates their transcriptional activity. In a similar way, 15d-PGJ_2 interacts with cell signal transducers, thus interfering in central signalling pathways. This is the case, among others, of H-Ras, to whom 15d-PGJ_2 directly binds, inducing its activation (Oliva et al., 2003).

4.- Erythroblastic leukemia viral oncogene homologues (ErbBs)

The ErbB family of proteins are transmembrane receptors with intrinsic tyrosine kinase activity in their intracellular domain that allows them to transfer phosphate groups to tyrosine residues contained in cellular substrates. This family, that takes its name from the homology of one of its members to the erythroblastoma viral gene product, v-erbB, comprises four receptors (ErbB1-4, also known as HER1-4) with several extracellular ligands, all of them containing a conserved epidermal growth factor (EGF) domain (Hynes and Lane, 2005). These ligands are classified in three groups:

· EGF, transforming growth factor-α and amphiregulin, which bind to ErbB1.

· Betacellulin, heparin-binding EGF and epiregulin, which bind both EGFR and ErbB4.

· Neuregulins (NRG), bind only ErbB4 (NRG3, NRG4) or also ErbB3 (NRG1, NRG2).

ErbBs exist as inactive transmembrane monomers in tissues of neural, epithelial and mesenchymal origin. Ligand binding to their extracellular domain initiates a conformational rearrangement in the receptor leading to its homo or heterodimerization. Then, each member of the dimer uses its intracellular protein tyrosine kinase domain to phosphorylate its partner on its cytosolic domain, inducing thus its activation (Citri and Yarden, 2006). Interestingly, ErbB2 and Erb3 are non-autonomous: no ligand has been identified for ErbB2, and ErbB3 is defective in kinase activity. Despite this lack of autonomy, both ErbB2 and ErbB3 form heterodimeric complexes with other ErbBs that are capable of generating potent cellular signals. Moreover, they can heterodimerize with each other to form an ErbB2/ErbB3 complex that gives rise to one of the most potent oncogenic signals described (Holbro et al., 2003a).

ErbB1, ErbB2 and ErbB3 are all implicated in the development and progression of cancer. Patients with cancer whose tumours have alterations in ErbB receptors tend to have a more aggressive disease, and predicts a poor clinical outcome. The role of ErbB4 in oncogenesis is less clear. Current data indicate that this receptor might be involved in inhibition of cell growth rather than proliferation.

- ErbB1

ErbB1 binds to multiple ligands, although his ability to bind the epidermal growth factor has caused that this receptor is commonly named epidermal growth factor receptor (EGFR). Upon binding, ErbB1 can form homodimers as well as three functional heterodimers. Knock-out studies of genes coding for specific ligands of ErbB1 demonstrated a marked functional redundancy between the ligands: knock-out mice of EGF show no significant phenotype, and alterations in transforming growth factor-α (TGF-α) knock-out mice are restricted to eye abnormalities.

Gene amplification leading to ErbB1 overexpression is often found in human cancers, together with mutations and deletions that result in constitutive kinase activity (Holbro et al., 2003b). Furthermore, in many tumours EGF-related growth factors are produced by the tumour cells themselves or by surrounding stromal cells, leading to constitutive ErbB1 activation. Aberrantly increased ErbB1 signalling has been reported in glioblastomas, lung carcinomas, prostate cancer and breast carcinoma..

- ErbB2

ErbB2 (also referred as neu and HER2) is the preferred heterodimeric partner of the other three ErbB family members. Although no direct ligand has been identified for this receptor to date, it exits in a conformational state that is constitutively active for dimerization. ErbB2-containing heterodimers have a higher affinity and broader specificity than other heterodimeric receptor complexes, and the ErbB2/ErbB3 heterodimer is considered the most potent ErbB complex with respect to strength of interaction, ligand-induced tyrosine phosphorylation and downstream signalling (Baselga and Swain, 2009).

ERBB2 amplification and overexpression have been observed in several types of human tumours such as ovarian cancer, gastric carcinoma, salivary gland tumours and in 20-30% of human breast cancers (Slamon et al., 1989). Moreover, this expression profile is associated with a poor prognosis. Overexpression promotes spontaneous ErbB2 dimerization in the absence of a ligand and constitutive receptor activation, leading to aberrantly increased levels of ErbB2-mediated signalling, which promotes tumorigenesis. According to this, results from our group show that proliferation and survival of human breast cancer cells is due to activation of phosphatidylinositol 3-kinase (PI3K) and mitogen-activated protein kinase (MAPK) signalling cascades respectively, as a result of signalling through the ErbB2/ErbB3 heterodimer (Pignatelli et al., 2001).

- ErbB3

ErbB3 can bind to four different ligands but lacks intrinsic tyrosine kinase activity, as it is unable to bind adenosine triphosphate (ATP). This is the reason why ErbB3 cannot homodimerize. Nonetheless, the cytoplasmic domain of ErbB3 undergoes tyrosine phosphorylation upon heterodimerization, and this allows the recruitment and activation of PI3K, which promotes tumour proliferation. ErbB3 is the preferred dimerization partner when signalling occurs through the PI3K pathway, probably because although ErbB1 and ErbB2 can interact with and activate PI3K through adaptor proteins, binding via ErbB3 is direct and the resulting activation is of PI3K pathway is more intense (Hellyer et al., 1998).

Alterations in ErbB3 signalling have been reported in breast carcinoma, ovarian cancer, lung and prostate carcinoma, among others. In all these cases, but especially in breast cancer, ErbB3 is commonly expressed along with ErbB2 (Lee-Hoeflich et al., 2008). Interestingly, amplification of ErbB3 alone has also been observed in lung cancer, and growing data indicate that ErbB3 expression is upregulated in breast cancer in order to compensate for the inhibition of other members of the ErbB family (Sergina et al., 2007).

- ErbB4

ErbB4 shows a high similarity to ErbB1 in ligand specificity and recruitment of adaptor proteins. Interestingly, although ErbB4 acts mainly as a receptor tyrosine kinase in plasma-membrane signalling processes, it also undergoes catalytic cleavage generating a chaperone that facilitates the translocation into the nucleus of several transcription factors such as signal transducer and activator of transcription 5 (STAT5) (Williams et al., 2004). More recent studies on the still poorly unknown functions of ErbB4 indicate that suppression of its function leads to inhibition of cell growth in breast cancer (Hollmen et al., 2009).

5.- PROTEIN PHOSPHOTYROSINE PHOSPHATASES

Phosphotyrosine phosphatases (PTPs) are proteins in charge of dephosphorylating tyrosine residues. Since protein tyrosine phosphorylation is a key event in the activation of signalling cascades, PTPs constitute a key regulatory mechanism in signal modulation (Tonks, 2006). In the case of ErbB-mediated signalling, several phosphatases have been implicated in the regulation of the pathway, a property that is based on the presence within the phosphatase of domains capable of recognizing and binding phosphorylated tyrosines. This is the case of Src-homology-2 (SH2) and phosphotyrosine binding (PTB) domains. Thus, for example, EGFR is bound and dephosphorylated by PTP1B phosphatase, RPTPσ, density-enhanced phosphatase 1 (DEP1) and SH2-domain containing phosphatase-1 (SHP-1) (Ostman and Bohmer, 2001), whereas ErbB2 has been shown to be dephosphorylated by the PEST-motif containing brain-derived phosphatase 1 (BDP1) (Gensler et al., 2004) and positively regulated by the SH2-domain containing phosphatase-2 (SHP-2) (Zhou and Agazie, 2009).

- SHPs

SHPs are a family of cytosolic tyrosine phosphatases which contain SH2 domains. This family comprises SHP-1, SHP-2, corkscrew (Csw) from *Drosophila* and PTP-2 from *Caenorhabditis elegans*. SHP-1 and SHP-2 have highly homologous primary structures (55% identity). Both consist of two SH2 domains and a tyrosine phosphatase domain followed by a highly basic C-terminal tail that contains phosphorylation sites (Tyr536 and Tyr564 for SHP-1) and regulates substrate recognition and activity (Pei et al., 1994; Zhang et al., 2003). Interestingly, this regulatory C-terminal tail is the region where SHP-1 and SHP-2 show lower sequence homology (about 15% identity), a fact that could explain their divergences in distribution, functions and targets. Regardless of their structure similarity, SHP-1 and SHP-2 differ greatly in cellular distribution and biological function. SHP-1 is predominantly expressed in haematopoietic and epithelial cells, and behaves as a negative regulator of several receptor tyrosine kinases. In contrast, SHP-2 is expressed ubiquitously in cells with various origins and acts primarily as a positive regulator (Plutzky et al., 1992), with functions antagonizing those of SHP-1 in several systems (Qu et al., 2001).

SHP1

SHP-1, also known as PTP1C, SH-PTP1, HCP and PTPN6, is present under different isoforms in haematopoietic and epithelial cells (Poole and Jones, 2005), where it acts as a negative regulator of cell signalling. SHP-1 has been proposed to antagonize growth-promoting signals initiated by receptor tyrosine kinases, since mice lacking SHP-1 protein show hyperproliferation of myeloid and lymphoid progenitors and enhanced response to growth factors (Tapley et al., 1997). In addition, SHP-1 messenger RNA (mRNA) and protein levels are decreased in most lymphomas and leukaemias (Oka et al., 2001) and forced expression of SHP-1 in lymphoma and leukaemia cell lines results in decreased proliferation (Bruecher-Encke et al., 2001). Similar results have been obtained in other cancer types, including breast cancer, where transfection of SHP-1 inhibits the growth of the SHP-1-deficient HTB26 cell line (Wu et al., 2003), thereby confirming the implication of this phosphatase in opposing cell growth.

In breast cancer cells, SHP-1 dephosphorylates several receptor tyrosine kinases such as EGFR (Tomic et al., 1995), platelet-deriver growth factor receptor (PDGF) (Yu et al., 1998) and ErbB2 (Vogel et al., 1993), suggesting that the antiproliferative effect of the

phosphatase is related to silencing of the signalling pathways initiated by these receptors. In fact, overexpression of SHP-1 leads to a decrease in the phosphorylation level of EGFR and viceversa (Keilhack et al., 1998).

One peculiarity of SHP-1 is that phosphorylation on its C-terminal region determines its activation. Phosphorylation on Tyr536 by the insulin receptor tyrosine kinase has been reported to induce its activation (Uchida et al., 1994). Similarly, SHP-1 experiences an increase in its catalytic activity upon phosphorylation on tyrosine by Src (Frank et al., 2004) and in human platelets upon phosphorylation on both tyrosine and serine residues (Li et al., 1995). The C-terminal tail of SHP-1 also accounts for a nuclear localization signal, which is blocked in the native protein but becomes active upon stimulation with EGF and causes traslocation of SHP-1 from the cytosol to the nucleus in monkey embryonic kidney COS7 cells. Conversely, SHP-1 presents a cytosolic distribution in H9 hematopoietic cells (He et al., 2005) and in several cancer cell lines studied (human epithelial carcinoma A431 and human colonic adenocarcinoma HT29 cells), independently of EGF stimulation.

SHP-2

Regardless of its sequence similarity, SHP-2 (PTP1D, PTP2C, SH-PTP2, Syp or PTPN11) exerts functions antagonizing those of SHP-1. SHP-2 directly binds several receptor tyrosine kinases such as EGFR and ErbB2 and acts as a positive regulator of their signalling, thus promoting cell growth and survival. In fact, its activation is a requirement in certain systems to achieve activation of PI3K or MAPK pathways (Wu et al., 2001). Moreover, SHP-2 has been reported to promote cell transformation (Agazie et al., 2003) through positively regulating ErbB2 signalling (Zhou and Agazie, 2009).

- BDP1

BDP1 is a phosphatase enriched in PEST sequences, which are characterized by their high content in proline (P), glutamic acid (E), serine (S) and threonine (T). BDP1 has been reported to negatively regulate ErbB2 activation in breast cancer cell lines, leading to reduced activation of MAPKs (Gensler et al., 2004).

6.- CANCER STEM CELLS

Traditionally, cancer was believed to follow a clonal evolution model by which stochastic mutations accumulate in a cell or in a group of cells over-time, providing these cells with a growth advantage over the adjacent tissue that favours their expansion as competition during natural selection occurs. Thus, any cell would have the potential to originate a tumour. However, there is increasing evidence that supports that cancer follows a stem cell model, that posits that tumorigenesis is driven by a subset of cells with unlimited proliferative potential resulting from their capacity to undergo asymmetric divisions that produce an exact copy of the cell (self-renewal) and a daughter cell that differentiates. Thereby, cells within a tumour would be functionally heterogeneous, as only few cells would be responsible for the progression of the tumour by generating the diverse cells that comprise it. Although both models are not mutually exclusive, transplantation studies of single cells into immunodeficient mice indicate that only cells which expressed a determined combination of surface markers were able to regenerate the whole tumour (Bhatia et al., 1997). These cancer stem cells have been described in several malignancies after serial transplantation studies, and the membrane antigens that characterize them vary depending on the tissue of origin. Therefore, they have been described as $CD44^{+}/CD24^{-/low}$ in breast cancer (Al-Hajj et al., 2003) and $CD133^{+}$ in colon carcinoma (O'Brien et al., 2007), lung carcinoma and glioma (Singh et al., 2004).

Together with xenografts, cultures in non-adherent conditions have contributed to the prospective identification of cancer stem cells. When grown as suspension cultures, only cells with stem properties survive and proliferate, originating spheres which represent the progeny of a single stem cell and are enriched in progenitor cells (Ponti et al., 2005). This property of being capable to grow under non-adherent conditions is shared with normal tissue stem cells (Dontu et al., 2003). Interestingly, several studies report that spheres are preferentially generated *in vitro* by cells comprised in the side population, a minor subpopulation of cells detected by flow cytometry thanks to their capacity to differentially efflux the fluorescent DNA-binding dye Hoechst 33342 due to their overexpression of the multidrug resistance transporter ATP-binding cassette G2 (ABCG2) (Goodell et al., 1996).

However, great controversy surrounds both the techniques employed to define the markers and their accurateness. Big divergences have been observed in orthotopic xenograft models depending on the mouse strain used (Quintana et al., 2008) and on the experimental conditions, such as use of humanized microenvironments or artificial matrices e.g. Matrigel. Similarly, the $CD44^{+}/CD24^{-/low}$ phenotype defined for breast cancer stem cells does not correlate with poor prognosis, a fact that has lead other groups to propose alternative markers such as aldehyde dehydrogenase-1 (ALDH1) (Ginestier et al., 2007).

Prospective identification and isolation of cancer stem cells is a main challenge in the actual scientific scope, since to be efficient, therapies must eradicate this subset of cells responsible of the driving and progression of tumorigenesis. In case any of these cells persists after treatment the tumour will relapse. Thus, assessment of the antitumorigenic properties of a drug in the cancer stem population is of crucial relevance to determine its potential as therapeutic agent.

In this work, we have further analyzed the mechanism of action of PPARγ ligands in breast cancer cells and their effect on the cancer stem cell population.

INTRODUCCIÓN

1.- CÁNCER

El cáncer es una enfermedad caracterizada por expansión celular descontrolada, desdiferenciación de las células con división anómala y migración e invasividad de los tejidos circundantes y distantes. La causa de esta desregulación de la proliferación que da origen al cáncer radica en la acumulación de sucesivas mutaciones que aparecen como resultado de inestabilidad genética y daños causados por el ambiente y generan importantes alteraciones moleculares en la célula que interfieren con su proliferación.

La proliferación celular está controlada por un equilibrio entre señales proliferativas y antiproliferativas. Cuando una célula prolifera entra en un ciclo continuo de duplicación de la información genética y división que se conoce como ciclo celular. La célula primero duplica su contenido en ADN para generar dos copias idénticas. Este hecho define la fase S del ciclo célular (S de síntesis). Entonces, cada copia es segregada a sendas células hijas resultantes de la división celular. La segregación y la división celular definen la fase M (de mitosis). La mitosis se divide a su vez en subfases que reflejan cómo ocurre la segregación. Para prepararse para la síntesis y la mitosis, la célula pasa por sendas fases previas de preparación, denominadas G_1 y G_2.

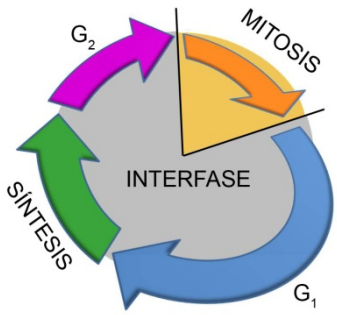

Figura 1. **Las fases del ciclo celular.**
Cuando las células proliferan duplican su contenido en ADN y segregan las copias en las células hijas. La duplicación del ADN ocurre durante la fase S, y la división celular marca la fase M. Estos procesos están separados por fases espaciadoras (G_1 y G_2 respectivamente). El periodo que comprende las fases G_1, S y G_2, durante el que la célula se prepara para la mitosis, se denomina interfase.

Para integrar los estímulos que inducen o se oponen a la proliferación la célula cuenta con vías de señalización que transforman las señales externas e internas en una respuesta celular. Para ello, la célula posee receptores de señales encargados de captar la señal, como es el caso de los receptores ErbB, a los que nos referiremos más adelante. Mediante un complejo sistema de reclutamiento e interacción de lípidos y proteínas donde las modificaciones post-transduccionales juegan un papel primordial, la célula activa factores de transcripción que se unirán al promotor de determinados genes diana y regularán su transcripción, dando de esta manera una respuesta apropiada al estímulo.

El mal funcionamiento de estos mecanismos puede acarrear respuestas proliferativas erróneas y, en algunos casos, cáncer.

Con más de 3 millones de nuevos casos y 1,7 millones de muertes cada año, el cáncer representa la segunda causa de muerte en Europa, después de las enfermedades cardiovasculares. Dependiendo de su origen el cáncer puede ser clasificado en carcinoma, si deriva de epitelio, o sarcoma, si se origina del mesodermo. Las leucemias se inician en precursores sanguíneos y los linfomas y los mielomas comienzan en células del sistema inmune. Actualmente, el tipo de cáncer más comúnmente diagnosticado es el cáncer de mama (con el 13,5% de todos los casos de cáncer), seguido de cáncer colorrectal (12,9%) y de pulmón (12,1%). Teniendo en cuenta el número de muertes debidas a cáncer, el carcinoma mamario es, después del cáncer de pulmón y el colorrectal, la tercera causa más común de muerte si consideramos ambos sexos y la primera en el caso de mujeres (Ferlay et al., 2007).

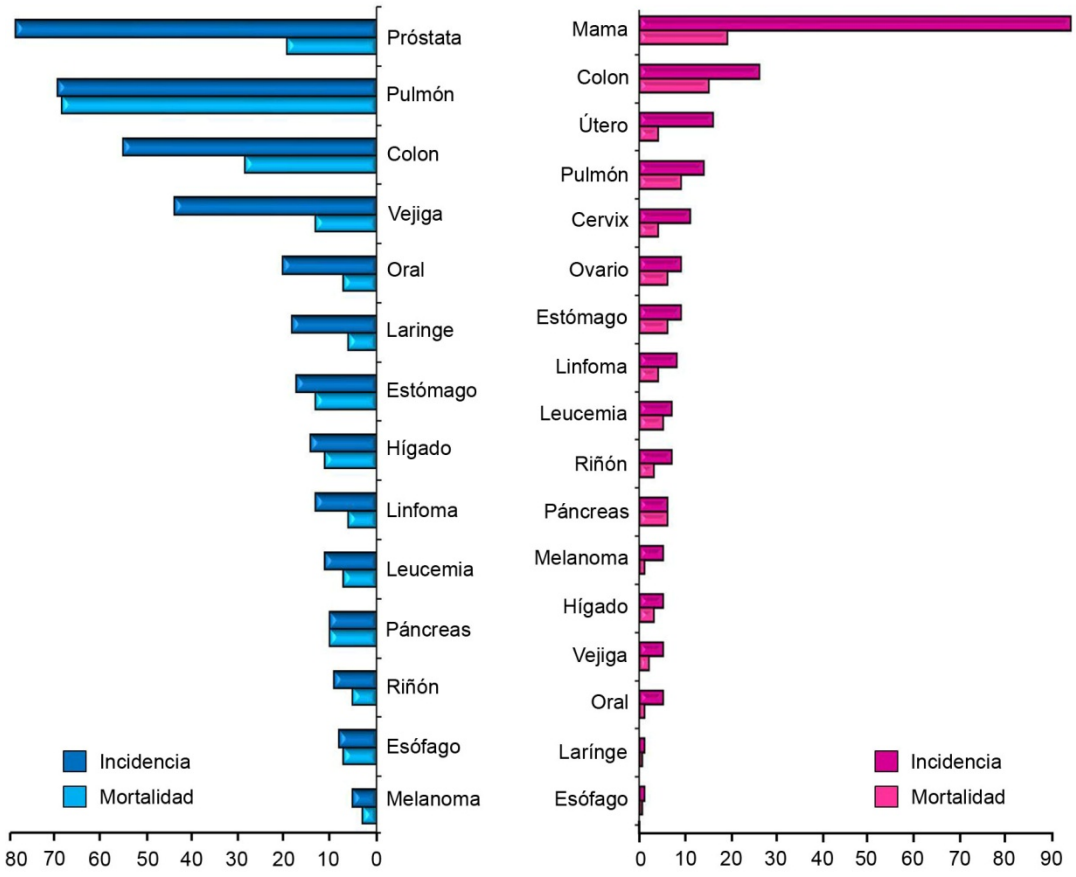

Figura 2. **Incidencia y mortalidad del cáncer en España.**
Datos del año 2006. Referidos a 100.000 habitantes.
Fuente: International Agency for Research on Cancer

2.- CÁNCER DE MAMA

La glándula mamaria se origina como un apéndice de la piel durante el desarrollo fetal. Las células epiteliales proliferan dentro del estroma, tejido conectivo circundante compuesto por matriz extracelular, fibroblastos, vasos sanguíneos y linfáticos, nervios y células del sistema inmune. Como resultado, se genera una primitiva red de ductos en forma de árbol. Durante la pubertad, la exposición de las células epiteliales a estrógeno y progesterona causa la elongación y la ramificación de los ductos, en cuya parte final las células epiteliales forman los alveolos, que producirán leche durante el embarazo, secretándola a la luz de los ductos. En la glándula mamaria adulta resultante las células epiteliales se organizan en dos estratos: algunas de las células epiteliales quedan adyacentes a la luz, y son llamadas por ello luminales, mientras que otras, llamadas células mioepiteliales, forman una estructura en forma de malla entre las células luminales y la membrana basal (Hennighausen and Robinson, 2005).

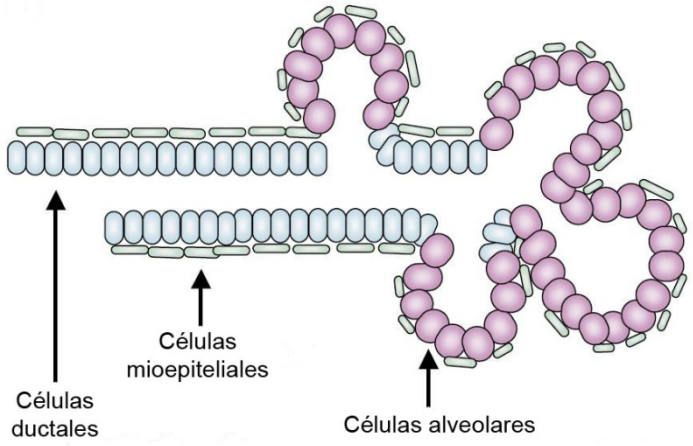

Figura 3. **Organización de la glándula mamaria adulta.** Las células se clasifican en ductales o alveolares según su localización. Además, las células en contacto con la luz son denominadas basales y las que están en contacto con la membrana basal mioepiteliales. Fuente: (Woodward et al., 2005)

Dependiendo de qué estructura de la glándula mamaria esté afectada por una lesión neoplásica, el cáncer de mama se clasifica en cáncer luminal o basal, o, alternativamente, en ductal o lobular cuando los ductos o los alveolos están afectados, respectivamente. En su etapa temprana, las células cancerosas forman una masa neoplásica que permanece incluida en el tejido donde se originó, pero separada del tejido circundante por la membrana basal. En este estado, el carcinoma es denominado "*in situ*". Durante la progresión del cáncer, la membrana basal es degradada progresivamente, y las células cancerosas invaden el estroma. El cáncer es clasificado entonces como "invasivo". La mayoría de los tumores de mama derivan de ductos del epitelio, siendo los carcinomas ductales invasivos los más frecuentes, al constituir más del 70% de los tumores diagnosticados.

Con el fin de erradicar de modo eficaz las células cancerígenas, desenmascarar los mecanismos que determinan la progresión tumoral así como identificar nuevos agentes terapéuticos y su mecanismo de acción es de vital importancia. Estudios de nuestro laboratorio junto con los de otros grupos muestran que los ligandos del Receptor Activado por Proliferadores Peroxisomales γ (PPARγ) poseen importantes efectos antitumorigénicos en células de cáncer de mama, lo que los sitúa como importantes agentes terapéuticos en la lucha contra el cáncer de mama.

3.- PPARs

Los Receptores Activados por Proliferadores Peroxisomales (PPARs) son factores de transcripción inducibles por ligando que pertenecen a la superfamilia de los receptores de hormonas nucleares, que agrupa a los receptores de esteroides, ácidos biliares, ácido retinoico y hormonas tiroideas (Evans, 1988). Estos receptores son factores de transcripción multi-dominio que se unen a secuencias específicas del DNA llamadas elementos de respuesta e inducen así la transcripción de sus genes diana. Cuentan con un dominio N-terminal que contiene al menos una región de transactivación constitutivamente activa denominada "función de activación-1" (AF-1) junto a sitios para la fosforilación y el anclaje de proteínas reguladoras, un dominio central altamente conservado responsable de llevar a cabo la unión al ADN y la heterodimerización, un dominio flexible que actúa de bisagra y un dominio C-terminal que sirve como lugar de anclaje de cofactores y contiene una secuencia de localización nuclear y una función de transactivación dependiente de ligando llamada AF-2.

Los PPARs se unen a secuencias consenso en el promotor de sus genes diana denominadas Elementos de Respuesta a PPAR (PPRE). Estas secuencias consisten en repeticiones directas separadas por un nucleótido (NNN-AGGTCA-N-AGGTCA), por lo que son llamadas "repeticiones directas-1" (DR1) (Palmer et al., 1995). Se han identificado PPREs entre otros en genes que codifican para la acilcoenzima A oxidasa, el citocromo P450 4A6 y aP2. Para reconocer un PPRE, los PPARs deben formar previamente un heterodímero con el receptor X retinoide (RXR), el cual es un miembro de la familia de los receptores tiroideos/esteroideos que une ácido 9-cis retinoico y es frecuentemente copartícipe de la unión a ADN de otros factores de transcripción (Mangelsdorf et al., 1992). Una vez unido al PPRE, PPAR activa la transcripción mediante un mecanismo que involucra el reclutamiento de complejos coactivadores,

como la proteína de unión a CREB (CBP-1), el coactivador 1 del receptor de esteroides (SRC-1), la proteína 140 de interacción con receptores (RIP140) y correpresores como los correpresores nucleares 1-2 (NCoR1-2) y el mediador silenciador de los receptores 1-2 de hormonas retinoides y tiroideas (SMRT1-2).

Existen tres isotipos de PPAR: PPARα, PPARβ (también llamado PPARδ, debido a caracterización paralela) y PPARγ (Keller and Wahli, 1993; Sertznig et al., 2007). PPARα y PPARβ están profundamente implicados en la homeostasis energética. PPARα controla la transcripción de genes que participan en la β-oxidación mitocondrial de ácidos grasos libres presentes en el plasma, estimula la gluconeogénesis, la síntesis de cuerpos cetónicos y la captación de colesterol por el hígado (Bragt and Popeijus, 2008), mientras que PPARβ participa en la oxidación de ácidos grasos y en la mielinización y el metabolismo lipídico en el cerebro (Basu-Modak et al., 1999). Contrariamente a lo que sucede con PPARγ, para quien se ha establecido una profunda implicación en cáncer, PPARα y PPARβ intervienen principalmente en el metabolismo de ácidos grasos, con pocas y no claramente descritas implicaciones en tumorigénesis.

3.1.- PPARγ

El gen que codifica para PPARγ (NR1C3) ha sido identificado bajo seis isoformas en humanos, llamadas PPARγ1-5 y PPARγ7. PPARγ1 y PPARγ2 se diferencian sólo por la existencia de 84 nucleótidos adicionales en el extremo 5' del gen PPARγ2, los cuales codifican para 28 aminoácidos adicionales. Esto hace que el dominio de activación independiente de ligando de PPARγ2 sea de cinco a diez veces más eficiente que el de PPARγ1. El resto de isoformas son distintos transcritos, pero codifican la misma proteína que PPARγ1, de modo que sólo hay dos proteínas resultantes: PPARγ1 y PPARγ2, causadas por distinto uso de promotor y procesado alternativo de los exones. PPARγ se expresa de manera abundante en tejido adiposo blanco y marrón y en células del sistema inmune. También se encuentra, aunque en menor medida, en músculo esquelético, hígado y células del estroma de la médula ósea, fibroblastos y células epiteliales.

PPARγ regula la diferenciación de adipocitos y el almacenamiento y la liberación de lípidos. De hecho, su expresión es uno de los eventos iniciales en la diferenciación de los adipocitos (Tontonoz et al., 1994). Además, PPARγ regula la expresión de multitud

de genes implicados en el metabolismo lipídico, incluyendo la lipoproteína lipasa (LPL), la proteína de unión a ácidos grasos (aP2), la acil-CoA sintasa, y la proteína transportadora de ácidos grasos. A ello se suma que PPARγ regula la homeostasis de glucosa, ya que mejora la sensibilidad a insulina, aumentando así la captación de glucosa.

Se ha demostrado que PPARγ tiene efectos antineoplásicos en varios tipos de carcinoma (Grommes et al., 2004). La capacidad de PPARγ de inhibir la proliferación de fibroblastos durante la diferenciación adipocítica sugirió que este receptor podía ser capaz de reducir la transformación celular, capacidad que fue evaluada inicialmente en liposarcoma humano. Se ha observado que la mayoría de los liposarcomas expresan cantidades más elevadas de PPARγ que otros sarcomas, y que células crecidas de liposarcomas diferencian en respuesta a ligandos de PPARγ (Tontonoz et al., 1997). Basándose en estas observaciones, estudios posteriores describieron que la activación de PPARγ inhibe la proliferación e induce la apoptosis de células tumorales de distintos linajes, como es el caso del carcinoma gástrico (Sato et al., 2000), colorrectal (Kubota et al., 1998), pancreático (Elnemr et al., 2000), hepatocelular y del cáncer de pulmón no microcítico (Keshamouni et al., 2004). Recientemente esta capacidad antineoplásica ha sido demostrada también en glioma (Grommes et al., 2006). Además, se ha descrito que PPARγ inhibe la angiogénesis y la neovascularizacion tanto *in vitro* como *in vivo* (Panigrahy et al., 2002). Todo ello sugiere que la inducción de diferenciación y apoptosis por la activación de PPARγ puede constituir un prometedor abordaje terapéutico del cáncer, tal y como ha sido demostrado en el caso del liposarcoma. De acuerdo con esto, nuestro grupo, así como otros laboratorios, ha obtenido evidencias de que la activación de PPARγ por diferentes ligandos conduce a un estado más diferenciado y menos transformado, una reducción en la tasa de crecimiento y un aumento de la apoptosis de varias líneas celulares de cáncer de mama. Concretamente, nuestros datos demuestran que el ligando natural de PPARγ 15-deoxi-Δ^{12-14}-Prostaglandina J_2 bloquea casi completamente la fosforilación y consiguiente activación de los receptores tirosina kinasa ErbB y, de este modo, juega un papel supresor del crecimiento tumoral en células humanas de cáncer de mama que expresan estos receptores (Pignatelli et al., 2001).

3.2.- Ligandos de PPARγ

PPARγ puede ser activado por la unión de una amplia variedad de ligandos hidrofóbicos. Entre los activadores naturales de PPARγ se encuentran los ácidos grasos insaturados, componentes de la dieta que, en términos generales, son buenos activadores de todos los subtipos de PPAR, especialmente en el caso de los ácidos grasos insaturados de 18-20 carbonos. Sin embargo, la mayor activación de PPARγ se logra por unión del eicosanoide endógeno 15-deoxi-Δ^{12-14}-Prostaglandina J_2 (15d-PGJ_2), que tiene efectos antiproliferativos en varios tipos de carcinoma. También existen moléculas sintéticas capaces de activar PPARγ significativamente. Este grupo de activadores sintéticos incluye el grupo de sensibilizadores a insulina conocido como tiazolidinedionas (TZDs) y los compuestos anti-inflamatorios no esteroideos (NSAIDs).

3.2.1.- Tiazolidinedionas (TZDs)

Las tiazolidinedionas (TZDs) son sensibilizadores a insulina que mejoran la captación de glucosa y disminuyen la hiperglucemia y la hiperinsulinemia. Por ello han sido utilizados en el tratamiento contra la *diabetes mellitus* tipo II, a pesar de que algunos datos sugieren que pueden incrementar el riesgo de fallo cardiaco (Home et al., 2009).

Se ha descrito que este grupo de ligandos sintéticos de PPARγ que incluye, entre otros, rosiglitazona, pioglitazona, ciglitazona y troglitazona, inhibe el crecimiento y promueve la apoptosis en distintos carcinomas. La activación de PPARγ por rosiglitazona, por ejemplo, inhibe el crecimiento celular y/o induce apoptosis en cáncer de próstata, hepatocelular y mamario (Grommes et al., 2004). Efectos similares han sido observados tras el tratamiento con pioglitazona en cáncer gástrico y de mama (Sohda et al., 1990). La troglitazona, a su vez, posee efectos antineoplásicos en una gran variedad de tumores, tanto *in vitro* como *in vivo*. En lo que concierne al cáncer de mama, la troglitazona inhibe la proliferación de las células de carcinoma mamario (Elstner et al., 1998) y causa regresión o estasis de tumores mamarios en rata (Pighetti et al., 2001). Por el contrario, un ensayo clínico en fase II llevado a cabo en pacientes con cáncer de mama refractario avanzado no vislumbró beneficio alguno tras el tratamiento con troglitazona (Burstein et al., 2003). Sin embargo, hemos de tener en cuenta que este estudio terminó anticipadamente ya que la troglitazona fue retirada del uso clínico al apreciarse eventos adversos de toxicidad hepática severa.

3.2.2.- Tiadiazolidinonas (TDZDs)

Los compuestos de la familia de las tiadiazolidinonas (TDZDs) poseen estructura similar a la del grupo de los ligandos de PPARγ TZDs, que incluye rosiglitazona y pioglitazona entre otros. Aunque estos compuestos fueron desarrollados inicialmente como inhibidores no competitivos de GSK-3β (Martinez et al., 2002), datos obtenidos por nuestro grupo indican que son activadores eficientes del receptor PPARγ. Además, nuestros datos muestran que inhibidores de PPARγ bloquean los efectos llevados a cabo por las TDZDs, sugiriendo que la activación de estas está mediada por este receptor (Luna-Medina et al., 2005). Por otro lado, se ha demostrado que las TDZDs tienen potentes efectos anti-inflamatorios, entre ellos la regulación negativa de la ciclooxigenasa tipo 2 (COX-2), una propiedad que también posee el ligando natural de PPARγ 15d-PGJ_2.

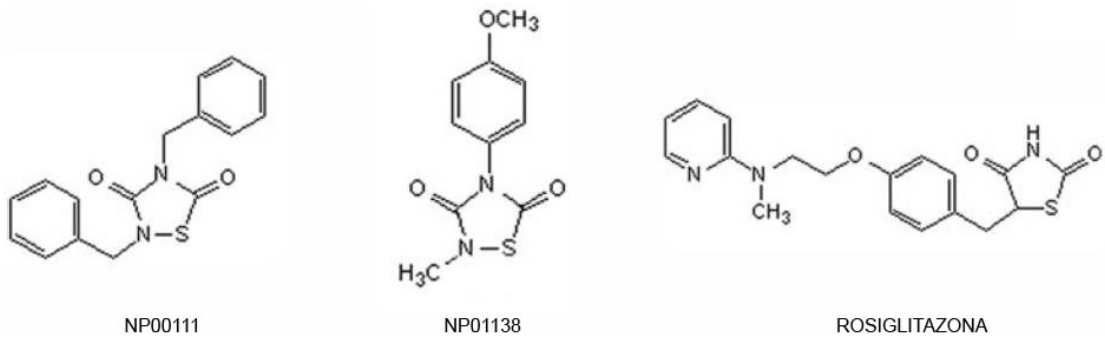

Figura 4. **Estructura de los compuestos tiadiazolidinonas NP00111 y NP01138 y de la tiazolidinediona rosiglitazona.**

Aunque tanto nosotros como otros grupos hemos descrito que las TDZDs promueven efectos citoprotectores en varios tejidos (Luna-Medina et al., 2007), se ha demostrado recientemente que uno de estos compuestos, conocido como TDZD-8, causa la muerte de células madre de leucemia (Guzman et al., 2007), sugiriendo una posible uso de este compuesto en terapia contra el cáncer.

3.2.3.- Compuestos Anti-Inflamatorios No Esteroideos (NSAIDs)

Los compuestos anti-inflamatorios no esteroideos (NSAIDs) como el indometacino, ibuprofeno, fenoprofeno y ácido flufémico son inhibidores de la ciclooxigenasa que también se unen y activan PPARγ *in vitro* a altas concentraciones, provocando diferenciación terminal de adipocitos (Lehmann et al., 1997). Algunos de ellos también son activadores de PPARα, capaces de inducir actividad peroxisomal en hepatocitos.

3.2.4.- 15-deoxi-$\Delta^{12\text{-}14}$-Prostaglandina J_2

Las prostaglandinas (PGs) son derivados del ácido araquidónico que es liberado de los fosfolípidos de membrana por la fosfolipasa A_2 (Straus and Glass, 2001). Al ser liberado, el ácido araquidónico es convertido por la enzima ciclooxigenasa (COX, también llamada PGH sintasa) a PGH_2, que es procesado enzimáticamente para dar lugar, dependiendo del enzima que catalice la reacción, a PGD_2, PGE_2, $PGF_{2\alpha}$, PGI_2, o tromboxano A_2. Cada uno de estos prostanoides es el precursor de una serie de derivados con efectos biológicos. Así, PGD_2 se deshidrata espontáneamente originando PGJ_2. Las prostaglandinas de la serie J poseen un residuo carbonilo electrofílico en su anillo de ciclopentano que es responsable de su reactividad con otras moléculas. PGJ_2 puede sufrir una mayor deshidratación y perder su grupo 15-hidroxilo, lo que unido a la migración del doble enlace 13-14, resulta en la formación de 15-deoxi-$\Delta^{12\text{-}14}$-PGJ_2 (15d-PGJ_2), que contiene un segundo carbono electrofílico potencialmente reactivo.

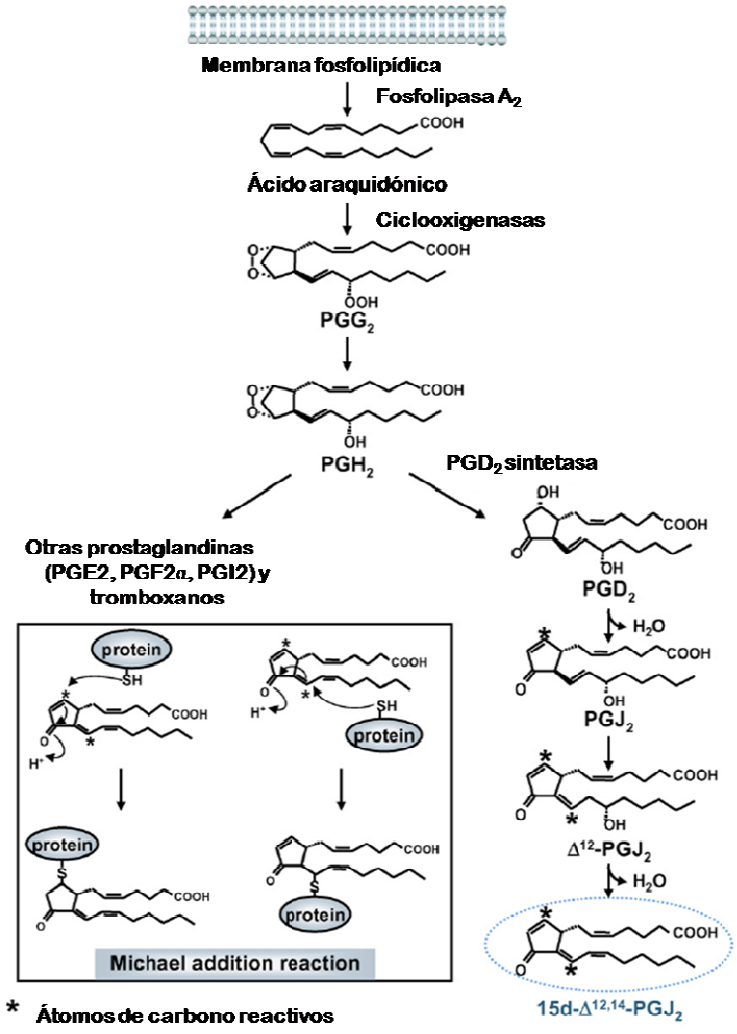

Figura 5. **Representación esquemática de la vía de síntesis de 15-deoxi-$\Delta^{12\text{-}14}$-PGJ_2**
Fuente: (Kim and Surh, 2006)

La 15d-PGJ_2 posee un papel muy importante en la adipogénesis, puesto que es un inductor de la diferenciación de adipocitos (Forman et al., 1995; Kliewer et al., 1995). Por otro lado, la 15d-PGJ_2 es un potente agente inductor capaz de reprimir la expresión de la sintasa inducible de óxido nítrico (iNOS), el factor α de necrosis tumoral (TNFα) y COX-2 en monocitos activados (Ricote et al., 1998), al mismo tiempo que inhibe la producción de citoquinas inflamatorias (Jiang et al., 1998). Además, la 15d-PGJ_2 promueve la producción plaquetaria (O'Brien et al., 2009) y protege del estrés oxidativo.

Se ha descrito que 15d-PGJ_2 posee importantes efectos antineoplásicos *in vitro* e *in vivo* en varios tipos de cáncer, como el carcinoma de próstata, el cáncer gástrico, el carcinoma de colon, el glioma, el carcinoma mamario y el pancreático (Grommes et al., 2004). Estos efectos incluyen la inhibición del crecimiento y la apoptosis, y, en algunos casos, se ha descrito que esta prostaglandina causa parada del ciclo celular mediante reducción de la cantidad de ciclina D1. En los últimos años 15d-PGJ_2 ha emergido como un inhibidor de angiogénesiss (Fu et al., 2006) y se ha establecido que la inducción de apoptosis por 15d-PGJ_2 es causada por la activación de p53 (Ho et al., 2008). De acuerdo con todos estos datos, nuestro grupo ha demostrado recientemente que 15d-PGJ_2 inhibe la proliferación de células de cáncer de mama, induce su apoptosis y causa malfuncionamiento de la mitocondria, lo que indica que el efecto antineoplásico de 15d-PGJ_2 puede ser debido a múltiples mecanismos (Pignatelli et al., 2005).

Algunos de los efectos anticancerígenos ejercidos por 15d-PGJ_2 se basan en su capacidad de activar PPARγ. Sin embargo, otros efectos no están mediados por PPARγ, sino que son debidos a la capacidad de 15d-PGJ_2 de interaccionar directamente con otras proteínas. La presencia de dos centros electrofílicos altamente reactivos en 15d-PGJ_2 permite la formación de aductos covalentes mediante reacciones de adición de Michael con nucleófilos tales como los grupos tiol de las cisteínas presentes en las proteínas (Kim and Surh, 2006). Por este mecanismo 15d-PGJ_2 se une a varios factores de transcripción, tales como el factor nuclear kB (NF-kB) (Straus et al., 2000) y la subunidad β del complejo IKB kinasa (IKK) (Rossi et al., 2000), regulando así su actividad transcripcional. De modo similar, 15d-PGJ_2 interacciona con transductores de señales celulares, interfiriendo de este modo en vías centrales de señalización. Tal es el caso, entre otros, de H-Ras, a quien 15d-PGJ_2 se une directamente, induciendo su activación (Oliva et al., 2003).

4.- Homólogos del oncogen de leucemia eritroblástica viral (ErbBs)

La familia de proteínas ErbB son receptores transmembrana con actividad tirosina kinasa intrínseca en su dominio intracelular, la cual les permite transferir grupos fosfato a residuos de tirosina de sustratos celulares. Esta familia toma su nombre de la homología de uno de sus miembros con el producto del gen de eritroblastoma viral, v-erbB, y agrupa cuatro receptores (ErbB1-4, también denominados HER1-4). Estos receptores cuentan con varios ligandos extracelulares, que poseen un dominio conservado del factor de crecimiento epidérmico (EGF) (Hynes and Lane, 2005). Dichos ligandos se clasifican en tres grupos:

· EGF, factor de crecimiento transformante α y anfirregulina, que se unen a ErbB1.

· Betacelulina, EGF de union a heparina y epirregulina, que se unen a EGFR y ErbB4.

· Neurregulinas (NRG), que se unen a ErbB3 y ErbB4 (NRG1 y NRG2) o sólo a ErbB4 (NRG3 y NRG4).

Los receptores ErbB existen como monómeros transmembrana inactivos. Se expresan en varios tipos de tejido epitelial, mesenquimal y de origen neural. La unión de ligando a su dominio extracelular inicia un cambio conformacional en el receptor que ocasiona su homo o heterodimerización. Entonces, casa miembro del dímero usa su dominio tirosina kinasa intracelular para fosforilar al otro, induciendo así su activación (Citri and Yarden, 2006). Curiosamente, ni ErbB2 ni ErbB3 no son autónomos: no se ha identificado ningún ligando para ErbB2 y ErbB3 carece de actividad kinasa. A pesar de esta falta de autonomía, tanto ErbB2 como ErbB3 forman con otros ErbBs complejos heterodiméricos que son capaces de generar potentes señales celulares. De hecho, pueden heterodimerizar entre ellos para formar el complejo ErbB2/ErbB3 que da lugar a una de las señales oncogénicas más potentes que se han descrito (Holbro et al., 2003a).

ErbB1, ErbB2 y ErbB3 están implicados en el desarrollo y la progresión del cáncer. Los pacientes con cáncer cuyos tumores tienen alteraciones en receptores ErbB tienen tendencia a una enfermedad más agresiva, y correlaciona con un mal pronóstico. El papel de ErbB4 en oncogénesis no es tan evidente. Los datos actuales parecen indicar que este receptor está implicado en la inhibición del crecimiento celular más que en la proliferación.

- ErbB1

ErbB1 une múltiples ligandos, aunque su capacidad para unir el factor de crecimiento epidérmico (EGF) ha hecho que este receptor sea comúnmente denominado receptor del factor de crecimiento epidérmico (EGFR). Al unirse el ligando, ErbB1 puede formar homodímeros así como tres heterodímeros funcionales. Estudios de supresión de los genes que codifican para ligandos específicos de ErbB1 han demostrado la existencia de una marcada redundancia funcional entre estos ligandos. Así, ratones carentes de EGF no muestran ningún fenotipo, y las alteraciones en los ratones carentes de factor de crecimiento transformante α (TGF-α) se limitan a anomalías en los ojos.

La amplificación génica que causa sobre-expresión de ErbB1 es frecuente en cánceres humanos, junto a mutaciones y deleciones que conllevan actividad kinasa constitutiva (Holbro et al., 2003b). Lo que es más, en muchos tumores factores de crecimiento relacionados con EGF son producidos por las propias células tumorales o por las células del estroma circundante, causando la activación constitutiva de ErbB1. La señalización de ErbB1 incrementada aberrantemente ha sido descrita en glioblastomas, carcinoma de pulmón, cáncer de próstata, carcinoma mamario y tumores gastrointestinales.

- ErbB2

ErbB2 (también denominada neu o HER2) es receptor con el que heterodimerizan preferencialmente los otros miembros de la familia ErbB. Aunque no se ha identificado ningún ligando directo de este receptor, se halla en un estado conformacional que le predispone a la heterodimerización. Los heterodímeros que contienen ErbB2 tienen una mayor afinidad y especificidad que otros complejos, y el heterodímero ErbB2/ErbB3 está considerado como el complejo ErbB más potente en lo que se refiere a fuerza de interacción, fosfoorilación en tirosina, y señalización (Baselga and Swain, 2009).

La amplificación de ErbB2 y su sobre-expresión han sido descritas en cáncer de ovario, carcinoma gástrico, tumores de glándula salivar y en el 20-30% de los cánceres de mama (Slamon et al., 1989). Además, este patrón de expresión está asociado a un mal pronóstico. La sobre-expresion promueve la dimerización espontánea de ErbB2 en ausencia de ligando y la activación constitutiva del receptor, dando lugar a una señalización mediada por ErbB2 aberrantemente elevada, lo que promueve la tumorigénesis. En consonancia con esto, resultados de nuestro grupo indican que la

proliferación y la supervivencia de las células humanas de cáncer de mama son debidas a la activación de las cascadas de señalización de la fosfatidilinositol 3-kinasa (PI3K) y la proteína kinasa activada por mitógenos (MAPK), respectivamente, como resultado de la señalización mediante el heterodímero ErbB2/ErbB3 (Pignatelli et al., 2001).

- ErbB3

ErbB3 pude unir cuatro diferentes ligandos, pero carece de actividad tirosina kinasa intrínseca, ya que es incapaz de unir adenosíntrifosfato (ATP). Esta es la razón por la cual ErbB3 no puede homodimerizar. Aun así, el dominio citoplásmico de ErbB3 es fosforilado en tirosina cuando el receptor heterodimeriza, y esto permite el reclutamiento y la activación de PI3K, que promueve la proliferación tumoral. ErbB3 es el monómero preferido para la dimerización cuando la señalización ocurre mediante la vía de PI3K, probablemente porque aunque ErbB1 y ErbB2 pueden interaccionar y activar PI3K a través de proteínas adaptadoras, la unión mediante ErbB3 es directa y la activación resultante de la vía de PI3K es más intensa (Hellyer et al., 1998).

Alteraciones en la señalización por ErbB3 han sido descritas en cáncer de mama, ovario, pulmón y próstata, entre otros. En todos estos casos, pero especialmente en cáncer de mama, ErbB3 es expresado generalemente junto a ErbB2 (Lee-Hoeflich et al., 2008). La amplificación de ErbB3 ha sido observada en cáncer de pulmón y cada vez un mayor número de datos indican que la expresión de ErbB3 puede ser incrementada para compensar la inhibición de otros miembros de la familia ErbB (Sergina et al., 2007).

- ErbB4

ErbB4 muestra una gran similitud con ErbB1 en la especificidad de ligandos y en el reclutamiento de proteínas adaptadoras una vez iniciada la señalización. Aunque ErbB4 actúa principalmente como un receptor tirosina quinasa en procesos de señaización en membrana plasmática, también es capaz de sufrir un procesado proteolítico que genera una chaperona que facilita la traslocación de ciertos factores de trascripción como el factor de transcripción activador de la transpcripción y transductor de la señal 5 (STAT5) al núcleo (Williams et al., 2004). Estudios recientes de las todavía poco conocidas funciones de ErbB4 indican que la supresión de su función conduce a la inhibición del crecimiento celular en cáncer de mama (Hollmen et al., 2009).

5.- PROTEINAS FOSFOTIROSINAS FOSFATASAS

Las proteínas fosfotirosinas fosfatasas (PTPs) son proteínas encargadas de defosforilar residuos de tirosina. Dado que la fosforilación en tirosina de proteínas es un evento clave en la activación de cascadas de señalización, las PTPs constituyen un mecanismo regulatorio esencial en la modulación de señales (Tonks, 2006). En el caso de la señalización mediada por ErbB, varias fosfatasa han sido implicadas en la regulación de la vía, una característica que se basa en la presencia en la fosfatasa de dominios capaces de reconocer y unir tirosinas fosforiladas. Este es el caso de los dominios tipo 2 de homología a Src (SH2) y de unión a fosfotirosina (PTB). Así, por ejemplo, EGFR es unido y defosforilado por la fosfatasa PTP1B, RPTPσ, la fosfatasa 1 de densidad incrementada (DEP1) y la fosfatasa 1 con dominios SH2 (SHP-1) (Ostman and Bohmer, 2001), mientras que ErbB2 es defosforilada por la fosfatasa 1 derivada de cerebro con motivo PEST (BDP1) (Gensler et al., 2004) y regulada positivamente por la fosfatasa 2 con dominios SH2 (SHP-2) (Zhou and Agazie, 2009).

- SHPs

Las SHPs son una familia de fosfatasas de tirosina citosólicas que poseen dominios SH2. Esta familia agrupa a las fosfatasas SHP-1, SHP-2, corkscrew (Csw) de *Drosophila* y PTP-2 de *Caenorhabditis elegans*. SHP-1 y SHP-2 tienen una alta homología en su estructura primaria (55% de semejanza). Ambas cuentan con dos dominios SH2 y un dominio proteína tirosina fosfatasa seguido de una cola C-terminal básica que contiene sitios de fosforilación (Tyr536 y Tyr564 para SHP-1) y determina la identificación del sustrato y la actividad (Pei et al., 1994; Zhang et al., 2003). Curiosamente, esta región reguladora C-terminal es la zona donde SHP-1 y SHP-2 presentan una menor homología de secuencia (en torno al 15%), un hecho que podría explicar sus divergencias en distribución, función y dianas. A pesar de su estructura similar, SHP-1 y SHP-2 difieren enormemente en su distribución en la célula y en su función biológica. SHP-1 se expresa abundantemente en células hematopoyéticas y epiteliales, y se comporta como un regulador negativo de varios receptores tirosina kinasa. En cambio, SHP-2 se expresa ubicuitamente en células con diverso origen y actúa como un regulador positivo (Plutzky et al., 1992), con funciones que antagonizan las de SHP-1 en algunos casos (Qu et al., 2001).

SHP-1

SHP-1, también conocida como PTP1C, SH-PTP1, HCP y PTPN6 está presente bajo diferentes isoformas en células hematopoyéticas y epiteliales (Poole and Jones, 2005), donde actúa como un regulador negativo de la señalización celular. De hecho, SHP-1 juega un papel clave en antagonizar las señales promotoras de crecimiento iniciadas por tirosina kinasas, puesto que ratones carentes de proteína SHP-1 muestran hiperproliferación de progenitores mieloides y linfoides así como una mayor respuesta ante factores de crecimiento (Tapley et al., 1997). Además, la cantidad de RNA mensajero (RNAm) y proteína de SHP-1 se encuentra disminuida en la mayoría de linfomas y leucemias (Oka et al., 2001), y la expresión forzada de SHP-1 en líneas celulares de linfoma y leucemia causa una reducción de su proliferación (Bruecher-Encke et al., 2001). Resultados similares se han obtenido en otros tipos de cáncer, incluyendo el cáncer de mama, donde la transfección de SHP-1 inhibe el crecimiento de la línea celular carente de SHP-1 HTB26 (Wu et al., 2003), confirmando de este modo la implicación de esta fosfatasa en la oposición al crecimiento celular. En células de cáncer de mama, SHP-1 defosforila varios receptores tirosina kinasa, como EGFR (Tomic et al., 1995), el receptor de crecimiento derivado de plaquetas (PDGF) (Yu et al., 1998) y ErbB2 (Vogel et al., 1993), lo que sugiere que el efecto antiproliferativo de la fosfatasa guarda relación con el silenciamiento de vías de señalización iniciadas por estos receptores. De hecho, la sobre-expresión de SHP-1 conduce a una reducción de la fosforilación de EGFR y viceversa (Keilhack et al., 1998).

Una peculiaridad de SHP-1 es que la fosforilación de su región C-terminal determina su activación. La fosforilación de SHP-1 en Tyr536 por el receptor tirosina kinasa de insulina se ha demostrado que induce su activación (Uchida et al., 1994). De modo similar, SHP-1 experimenta un aumento de su actividad catalítica al ser fosforilada en tirosina por Src (Frank et al., 2004) y en plaquetas humanas al ser fosforilada a la vez en residuos de tirosina y serina (Li et al., 1995). La cola C-terminal de SHP-1 también posee una secuencia de localización nuclear, que está bloqueada en la proteína nativa pero se activa al ser estimulada con EGF y causa la traslocacion de SHP-1 del citosol al núcleo en células embrionarias de riñón de mono (He et al., 2005) y en varias líneas celulares de cáncer estudiadas (las líneas de carcinoma epitelial humano A431 y de adenocarcinoma humano de colon HT29), de manera independiente de estimulación con EGF.

SHP-2

A pesar de su similitud de secuencia, SHP-2 (PTP1D, PTP2C, SH-PTP2, Syp o PTPN11) ejerce funciones antagónicas a las de SHP-1. Se ha descrito que SHP-2 interacciona directamente con varios receptores tirosina kinasa como EGFR y ErbB2 y actúa como regulador positivo de su señalización, promoviendo de este modo el crecimiento y la supervivencia celular en diferentes tipos celulares. De hecho, su activación es un requisito en ciertos sistemas para lograr la activación de las vías de PI3K y MAPK (Wu et al., 2001). Además, se ha descrito que SHP-2 promueve la transformación celular (Agazie et al., 2003) mediante la regulación positiva de la señalización por ErbB2 (Zhou and Agazie, 2009).

- BDP1

BDP1 es una fosfatasa rica en secuencias PEST, que se caracterizan por su alto contenido en prolina (P), ácido glutámico (E), serina (S) y treonina (T). Se ha descrito que BDP1 regula negativamente la activación de ErbB2 en líneas celulares de cáncer de mama, lo que causa una reducción en la activación de MAPKs (Gensler et al., 2004).

6.- CANCER STEM CELLS

Tradicionalmente se consideraba que el cáncer seguía un modelo de evolución clonal, por el cual mutaciones estocásticas se acumulan a lo largo del tiempo en una célula o grupo de ellas, confiriendo a estas células una ventaja proliferativa sobre el tejido adyacente, lo que favorece su expansión en la selección natural por competición. Consecuentemente, cualquier célula tiene el potencial de originar un tumor. Sin embargo, cada vez hay más datos que apoyan que el cáncer sigue un modelo de célula madre, según el cual la tumorogénesis viene dada por un grupo de células con potencial proliferativo ilimitado debido a su capacidad de división asimétrica, por la cual generan una célula copia exacta de sí mismas (auto-renovación) y otra célula hija que diferencia. Así pues, las células de un tumor son funcionalmente heterogéneas, ya que sólo unas pocas son responsables de la progresión del tumor. Aunque ambos modelos no son mutuamente excluyentes, estudios de trasplante de células aisladas en ratones inmunosuprimidos indican que sólo células que expresan un determinado patrón de marcadores e superficie son capaces de regenerar el tumor entero (Bhatia et al., 1997). Estas células madre de cáncer han sido descritas en varias neoplasias tras estudios de trasplantes seriados, y los antígenos de membrana que las caracterizan varían

dependiendo del tejido de origen. Así pues, han sido descritas como $CD44^{+}/CD24^{-/bajo}$ en cáncer de mama (Al-Hajj et al., 2003) y como $CD133^{+}$ en carcinoma de colon (O'Brien et al., 2007), carcinoma de pulmón y glioma (Singh et al., 2004).

Junto con los xenotrasplantes, el cultivo en condiciones no adherentes ha contribuido a la identificación de las células madre de cáncer. Cuando son crecidas como cultivos en suspensión, sólo las células con propiedades de célula madre sobreviven y proliferan, originando esferas que representan la progenie de una sola célula madre y están enriquecidas en células progenitoras (Ponti et al., 2005). Esta propiedad es compartida con las células madre de tejido normal, no cancerígeno (Dontu et al., 2003). Curiosamente, algunos estudios indican que las esferas son generadas *in vitro* principalmente por células presentes en la "side population", una subpoblación de células detectada por citometría de flujo gracias a su capacidad de expulsar de manera diferente el compuesto fluorescente denominado Hoechst 33342, que se une al ADN celular. La expulsión diferencial de este compuesto radica en la sobre-expresión en estas células del transportador de resistencia a drogas llamado grupo de unión de ATP G2 (ABCG2) (Goodell et al., 1996).

Sin embargo, una gran controversia rodea tanto las técnicas empleadas para definir los marcadores como su precisión, ya que hay grandes divergencias en los resultados obtenidos en los modelos de xenotrasplante dependiendo de la cepa de ratón utilizada (Quintana et al., 2008) y de las condiciones experimentales, así como del uso de microambientes o matrices articificiales como Matrigel. Del mismo modo, el perfil $CD44^{+}/CD24^{-/bajo}$ definido para las células madre de cáncer de mama no correlaciona con peor pronóstico, lo que ha llevado a proponer marcadores alternativos como la enzyma aldehídodeshidrogenasa 1 (ALDH1) (Ginestier et al., 2007).

La identificación y el aislamiento de las células madre de cáncer es un desafío primordial en el actual horizonte científico, ya que para ser eficaces las terapias deben erradicar esta subpoblación de células responsable del inicio y la progresión de la tumorogénesis. En caso de que alguna de estas células persista tras el tratamiento el tumor volverá a resurgir. Por ello, la evaluación de las propiedades antitumorogénicas de un compuesto en la población de células madre de cáncer es de crucial importantcia para determinar su potencial como agente terapéutico.

En este trabajo hemos analizado aun más el mecanismo de acción de los ligandos de PPARγ en células de cáncer de mama y su efecto en la población de células madre de cáncer.

OBJECTIVES

OBJECTIVES

1.- Assessment of the effects of PPARγ ligands 15-deoxi-Δ^{12-14}-Prostaglandin J_2, rosiglitazone and pioglitazone on viability, proliferation and apoptosis of human breast cancer cells.

2.- Evaluation of the effects of thiadiazolidinones (TDZDs) on growth of human breast cancer cells.

3.- Study and characterization of the mechanism of action of 15d-Prostaglandin J_2 on ErbB2 and ErbB3 dephosphorylation.

4.- Study and characterization of the mechanism of action of 15d-Prostaglandin J_2 on cell cycle progression and microtubule dynamics.

5.- Evaluation of the antitumorigenic effects of PPARγ ligands on human breast cancer stem cells.

MATERIALS and METHODS

MATERIALS AND METHODS

Cell culture

MCF-7, MDA-MB-231, SKBR3 and T47D human breast cancer cell lines were obtained from American Type Culture Collection (ATCC) (catalogue numbers HTB-22, HTB-26, HTB-30 and HTB-133, respectively). MCF-7, MDA-MB-231 and SKBR3 cells are derived from pleural effusions of breast adenocarcinomas, whereas T47D derives from pleural effusion of a ductal carcinoma. All cell lines were cultured in Roswell Park Memorial Institute (RPMI) medium (Gibco, Invitrogen, CA, USA) supplemented with 2mM glutamine, 40 µg/mL gentamicin, 0.5 µg/µL fungizone and 10% fetal bovine serum (FBS) (Gibco, Invitrogen, CA, USA) at 37ºC and 5% CO_2.

Drug administration

Experimental cultures were usually grown in regular 10% FBS RPMI or in regular RPMI supplemented with 5% dextran-charcoal stripped FBS. After 24 hours of growth in these conditions, cells were submitted to the treatments specified in Table 1.

Drug	Abbreviation	Supplier	Reference	Working concentration
15-deoxi-$\Delta^{12,14}$-prostaglandin J_2	15d-PGJ_2	Cayman Chemical MI, USA	18570	10 µM
Human Neuregulin-β1	NRG1	Peprotech Inc., NJ, USA	100-03	30 nM
Nocodazole	-----	Sigma-Aldrich Co., MO, USA	M1404	1 µM
Pioglitazone	PGZ	Actos. Lilly. London, UK	-----	10 µM
Rosiglitazone	RSG	Cayman Chemical MI, USA	71740	30 µM
TDZD-8	-----	Sigma-Aldrich Co., MO, USA	T8325	10 µM
NP00111	-----	Noscira, SPAIN		10 µM
NP01138				
NP031112				
NP031115				
NP031122				

Table 1.- **List of treatments administered in the study and working concentrations.**

Cell viability

Cell viability was measured using the 3-[4,5-dimethylthiazol-2-yl]-2,5-diphenyl tetrazolium bromide (MTT) assay (Roche Diagnostic GmbH, Basel, Switzerland), based on the ability of viable cells to reduce yellow MTT to blue formazan. Cells were cultured in 96-well microtitre plates (8,000 cells/well) and exposed to drugs during different periods of time. Then, cells were incubated with MTT (0.5 mg/mL, 4 hours) and subsequently solubilized in 5% DMSO/5 mM HCl for at least 2 hours at dark. MTT reduction was quantified by absorbance measurement at 550 nm.

Proliferation assay

Cells were seeded onto 96-well plates at a density of 8,000 cells/well. After 24 hours of growth in normal medium, cells were switched to RPMI containing 5% dextran-charcoal stripped FBS and grown for 24 hours after which drugs were added. Cells were grown for 24 hours in the presence of 0.5 mCi radiolabelled [^{3}H]thymidine and harvested. [^{3}H]radioactivity was measured in a solid scintillation counter.

Alternatively, a colorimetric assay based on incorporation of the thymidine analogue 5-Bromo-2-deoxy-uridine (BrdU) was used. Briefly, 8,000 cells/well are plated in a 96-well culture plate and switched after 24 hours of growth to medium supplemented with 5% stripped FBS. Treatments are then added and, after incubation for further 24 hours, DNA synthesis is assayed with the ELISA BrdU Assay Kit (Roche Diagnostic GmbH, Basel, Switzerland) according to the manufacturer's guidelines. Absorbance measurements were obtained using a Varioscan (Thermo Electron Corp.) plate reader.

Apoptosis assay

To calculate the extent of cell death, $0.5x10^6$ cells were grown in RPMI for 24 hours before switching to medium supplemented with 5% stripped-FBS for another 24 hours previous to the addition of the corresponding treatments. For analyses, both the floating cells in the supernatant and the adhered ones were collected from each plate. Apoptotic cells were assayed by analyzing annexin-V conjugated to fluoresceinisothiocyanate (annexin-V-FITC) (Bender MedSystems, Vienna, Austria) to determine the translocation of phosphatidylserine from the inside to the outside of the plasma membrane. Cell staining was performed according to the manufacturer's instructions.

Cell cycle analysis

MCF-7 cells treated with 10 μM 15dPG-J_2 or 30 μM rosiglitazone in RPMI medium for 24 hours were fixed in 70% ethanol/phosphate buffer saline (PBS), pelleted and resuspended in buffer containing 10 μg/ml RNAse A and 0.01 mg/ml propidium iodide (PI). Cell cycle distribution was determined by flow cytometric analysis in a Cyan MLE-R cytometer (DAKO-Cytomation, Glastrup, Denmark). Data analysis was performed using the Summit Software (DAKO).

Activation of human PPRE

Semiconfluent cultures were transfected with the reporter plasmid pPPRE-tk-luc, containing three PPARγ consensus binding sites upstream of a minimal promoter. Transfection was performed using Lipofectamine2000 (Gibco, Invitrogen, CA, USA) according to the manufacturer's protocol. Cells received 0.2 μg of luciferase reporter plasmid and were harvested 24 hours after treatment with 10 or 20 μM 15d-PGJ_2 or TDZD-8, for determination of luciferase and β-galactosidase (to assess transfection efficiency) activities. Each experiment was repeated at least three times in triplicate.

Soft agar colony assays

Anchorage-independent growth was determined by suspending 50,000 cells in 0.3% Noble Agar (Sigma-Aldrich Co., MO, USA) in 10% FBS RPMI medium in 60 mm plates over a bottom layer of 0.5% agar in medium. Cells were allowed to grow for 20 days with feeding every 2.5 days. At this time, NRG1 and 15d-PGJ_2 were added where appropriate. Colonies were stained with p-iodotetrazolium violet. Experiments were carried out three times in duplicate.

Western-Blot

Cells were washed twice with ice-cold PBS, and detached from the culture dish with a cell scraper in presence of 175 μL (for a 6-cm diameter plate) of extraction buffer (PBS containing 1% Nonidet P-40, 0.5% sodium deoxycholate, 0.1% sodium dodecyl sulfate [SDS] and 1mM phenylmethylsulphonyl fluoride [PMSF], 1mM sodium orthovanadate and 0.1 mM sodium pyrophosphate). Cells were then disrupted by repeated aspiration through a 21-gauge needle, incubated on ice for 30 min and spun at 12,000 g for 20 min. Supernatants were separated and 20 micrograms of total cellular protein were

loaded onto each lane of a 10% SDS-polyacrilamide gel. After electrophoresis, proteins were transfered to Protran nitrocellulose membranes (Whatman, NJ, USA) at 90 mA overnight in transfer buffer (25 mM Tris, pH 8.3; 190 mM glycine; 20% methanol; 0.5% SDS). Protein loading and transference were checked by Red Ponceau staining. Blots were then blocked with 5% dry non-fat milk or 3% bovine serum albumin (BSA) in Tris-buffered saline (TBS) (20 mM Tris-HCl, pH 7.6; 130 mM NaCl; 0.1% Tween-20) containing 0.5% Tween-20 for 60 min and probed with appropiate antibodies (see Table 2). After washing, membranes were incubated with peroxidase-conjugated secondary antibodies and immunoreactive bands were visualized using the Amersham enhancement chemiluminiscence system (ECL) (GE Healthcare, Buckinghamshire, UK). Blots were reprobed with different antibodies after stripping for 30 min in a buffer of 62.5 mM Tris-HCl (pH 6.7), 100 mM β-mercaptoethanol and 2% SDS.

Antibodies

Antibody	Origin	Clonality	Reference	Manufaturer
Alexa	various			Vector Laboratories, CA, USA
BDP-1	rabbit	polyclonal	-----	Donated by Dr. Axel Ullrich
Biotin	goat	polyclonal	BA9500	Vector Laboratories, CA, USA
CD24:PE	mouse	monoclonal	555428	BD Pharmingen
CD44:FITC	mouse	monoclonal	555478	BD Pharmingen
ErbB2	mouse	monoclonal	610161	BD Transduction Laboratories
Pericentrin	rabbit	polyclonal	PRB-432C	Covance, CA, USA
RC-20:HRPO	mouse	monoclonal	610023	BD Transduction Laboratories
SHP-1	rabbit	polyclonal	SC-287	Santa Cruz Biotechnology Inc.
SHP-2	rabbit	polyclonal	SC-424	Santa Cruz Biotechnology Inc.
α-tubulin	mouse	monoclonal	T9026	Sigma, MO, USA
β-tubulin	mouse	monoclonal	T8660	Sigma, MO, USA

Table 2. **Antibodies used in western-blot, immunoprecipitation and microscopy.**

Quantitative-PCR (Q-PCR)

In order to detect changes in SHP-1, SHP-2 and BDP1 mRNA expression, MCF-7 cells treated or not for 24 hours with 15d-PGJ_2 were lysed in guanidinium thiocyanate to proceed with RNA extraction with phenol chloroform. Quality and concentration of the RNA obtained was determined in an Agilent 2100 bioanalyzer (Agilent Technologies, CA, USA) and cDNA synthesis was performed using Moloney Murine-Leukaemia Virus Reverse Transcriptase (M-MLV RT) in the presence of random nucleotide

hexamers. Q-PCR was performed in an ABI PRISM 7900HT Fast Real-Time PCR (Applied Biosystems, CA, USA) and results were analyzed with SDS software using measurements of ribosomal 18S mRNA transcription as loading control. For amplification, Power SYBR Green PCR Master Mix (Applied Biosystems, CA, USA) was used, together with the following primers for each phosphatase:

BDP1: 5'-GAACGTGAGGAAGAACCGCTA-3' (forward)
5'-CGCGTCTGATCATAAGGCAG-3' (reverse)

SHP-1: 5'-ACTTCTCGCTCTCCGTCAGG-3' (forward);
5'-GGATCCGAATATGGGTCACCT-3' (reverse)

SHP-2: 5'-CCTGCCCTTTGATCATACCAG-3' (forward)
5'-TCATTGGGATCACCATCGTG-3' (reverse)

Immunoprecipitation

For immunoprecipitation assays, 600,000 cells were grown for 24 hours in complete medium, switched to serum-treated medium and exposed for different time to 15d-PGJ_2 (Cayman Chemical, MI, USA). Cells were then stimulated with NRG1 (30 nM) for 5 minutes, lysed in 500 ml of PBS containing 1% NP40, 0.5% sodium deoxycholate, 0.1% SDS and protease inhibitors, and spun at 12,000 *g* for 20 minutes. Protein concentration in the supernatant was determined by Bradford assay and equal amounts of protein from each sample were collected, precleared with Pansorbin (Calbiochem-Novabiochem Corp.) and incubated for 12 hours at 4°C with 1 μg of the appropriate antibodies (see Table 2). Protein-A-Sepharose was added to each sample and additionally incubated for 5 hours at 4°C. Beads were collected by microcentrifugation and washed five times with lysis buffer. Immunocomplexes were eluted by boiling for 3 min in SDS sample buffer (100 mM Tris, pH 6.8, 36% glycerol, 4% SDS, 0.01% bromophenol blue and 200 mM DTT) and subjected to SDS-PAGE. Proteins were then transferred to nitrocellulose membranes. The blots were blocked with 3% BSA in TBS-Tween buffer for 1 hour at room temperature and incubated with the horseradish peroxidase-coupled antiphosphotyrosine antibody RC-20 (Transduction Laboratories, Lexington, KY, USA) used at 1:2500 dilution in TBS-Tween with 3% BSA for 2 hours. After several washes, immunoreactive bands were visualized using Amersham ECL detection kit. Membranes were stripped and incubated with the corresponding antibodies for loading control.

Transfection of interference RNA (iRNA).

Semi-confluent MCF-7 cells were transfected using Lipofectamine2000 (Gibco, Invitrogen, CA, USA) according to the manufacturer's recommendations. Transfected iRNAs included a siGLO-RNA tagged with enhanced green fluorescent protein (EGFP) (Dharmacon, CO, USA; Catalogue number D-001630-01-05) that was used as a control of transfection efficiency, a non-targeting iRNA (Dharmacon, CO, USA; Catalogue number D-001210-01-05) used as control, and a mixture of four iRNAs directed against SHP-1 phosphatase, the so-called hPTPN6 SMARTpool (Dharmacon, CO, USA; Catalogue number M-009778-00). Optimal final iRNA concentration was determined on a dose curve assay analyzing the inhibition of SHP-1 achieved by growing concentrations of iRNA and the resulting cellular toxicity. A working concentration of 30 nM was probed to significantly silence SHP-1 expression without causing cell death. Twenty-four hours post-transfection, efficiency of iRNA incorporation was determined in the control plate by visual analysis in an Zeiss Axiovert 35 microscope of the ratio of cells showing green fluorescence due to siGLO-RNA. Efficiency was higher than 80% in all the experiments and fluorescence was observable for longer than 72 hours. Twenty-four hours after transfection, medium was shifted to RPMI supplemented with 5% stripped-FBS and 12 hours later treatments were added where appropriate.

Tyrosine phosphatase activity assay.

SHP-1 phosphatase activity was evaluated using the Universal Tyrosine Phosphatase Assay Kit (Takara Bio Inc., Shiga, Japan). SHP-1 protein was immunoprecipitated from MCF-7 cells as previously indicated once they had been treated with 15d-PGJ_2 and/or NRG1. Equal amounts of protein were used in the immunoprecipitation of SHP-1, and analysis of the phosphatase activity within each immunoprecipitate was performed following the manufacturer's instructions.

Immunofluorescence and confocal microscopy.

Confocal microscopy was used to detect cytoskeleton organization. MCF-7 cells were plated in glass coverslips in 24-well cell culture plates and grown in regular medium for 12 hours before switching to new medium with the corresponding treatment. Cells were then fixed for 10 min with methanol at –20°C, permeabilized with 0.1% Triton X-100 for 30 min at 37ºC and washed with PBS. After one hour incubation with the

appropriate primary antibody (see Table 2), cells were washed and incubated with 4,6-diamidino-2-phenylindole (DAPI), Alexa Fluor 488, Alexa Fluor 546, or Alexa Fluor 647 secondary antibodies (Molecular Probes, OR, USA) for 45 min at 37°C. Images were acquired using a Radiance 2100 laser scanning confocal microscope (Bio-Rad, Hercules, CA) using a 60x NA 1.40 oil immersion objective (Nikon). The images were obtained using a series of 0.5 μm (depth) spaced cell fluorescent slices (Z axis). Confocal microscope settings were adjusted to produce the optimum signal-to-noise ratio. Images were collected and processed using Lasersharp 2000 and Adobe Photoshop version 8.0, respectively.

For staining of mitochondria, cells were treated with 20 nM Mitotracker Red CMXRos (Molecular Probes, Leiden, The Netherlands) for 45 min, fixed for 10 min in methanol at -20ºC, and washed with PBS. Morphology was determined using a TCS SP2 laser scanning spectral confocal microscope (Leica Mycrosystems).

Separation of soluble and polymerized tubulins.

Separation of soluble and polymerized tubulins was carried out as described by Minotti et al (Minotti et al., 1991). Briefly, 12 hours after 15d-PGJ_2 (10 μM) or rosiglitazone (30 μM) treatment, MCF-7 cells were lysed using 120 μL of microtubule-stabilizing buffer [20 nM Tris-HCl (pH 6.8), 1 mM $MgCl_2$, 2 mM EGTA, 0.5% NP-40, 2 mM PMSF, 1 mM benzamidine]. After vortexing, 120 μg of protein were centrifuged at 13,000 rpm for 15 minutes at room temperature and soluble (supernatant) and polymerized (pellet) tubulin analyzed by SDS-PAGE.

Time-Lapse microscopy.

MCF-7 cells were plated and placed in a chamber in complete medium with CO_2 exchange at 37ºC. Cells were imaged every 1 min for 1-2 days using a 40x objective on an inverted microscope (Zeiss Axiovert 135 TV). Images were captured on a JVC (TK-C1481EG) digital video camera. Where indicated, 10 μM 15d-PGJ_2 or 30 μM rosiglitazone were added to live microscopy media. Resulting movies were collected and processed by using image analySIS software (Soft Imaging System) and exported as Quicktime (Apple Computer, Cupertino, CA) and are shown at 7 frames per second.

***In vitro* tubulin polymerization assay.**

In vitro tubulin assembly was evaluated using the HTS-Tubulin Polimerization Assay Kit (Cytoskeleton, Denver, CO), according to the manufacturer's instructions. Absorbance readings were taken at 340 nm every 30 s for 1 h, using a Varioscan (Thermo Electron Corporation) plate reader and data was processed using the Skanit 2.0 Research Edition software.

Biotinylated 15d-PGJ_2 pull down and western blot analysis.

For assessment of *in vivo* incorporation of 15d-PGJ_2 into α- and β-tubulin in intact cells, MCF-7 cells were incubated with 10 μM biotinylated 15d-PGJ_2 for 2 hours, lysed in lysis buffer [10 mM Tris-HCl (pH 7.5), 0.1 mM ethylenediaminetetraacetic acid (EDTA), 0.1 mM EGTA, 0.5% SDS, 0.1 mM 2-mercaptoethanol and 1mM PMSF], and biotinylated proteins were purified by adsorption onto Neutravidin beads (Pierce Biotechnology Inc., IL, USA), as indicated by the manufacturer's protocol. Proteins were detected by Western-blot using anti-α- and anti-β antibodies, as previously described.

Off line nanospray characterization of 15d-PGJ_2 by mass spectrometry (MS).

About 1 μL containing 5 μg of 15d-PGJ_2 was dissolved in 20 μl of 50% CH3CN, 0.5% acetic acid. 5 μL were introduced into the off line nanospray medium needle and infused using the Protana nanosprayTM ion source. Then, 15d-PGJ_2 was ionized into a triple quadrupole mass spectrometer (4000 Q Trap LC-MS/MS hybrid system, Applied Biosystems, MDS Sciex), and data were acquired for 2 min. The needle voltage was set at 1300 V, and the declustering potential was set at 50 V to minimize in-source fragmentation. A collision energy between 25 and 30 was used to induce the fragmentation of the 15d-PGJ_2 molecule.

Protein digestion and sample preparation for MS analysis.

Untreated or 15d-PGJ_2-treated microtubules were incubated with 1 μg trypsin (Promega Sequencing Grade) for 2 hours at 37ºC. Reaction mixtures were dried *in vacuo* and dissolved in 5% CH3CN, 0.5% CH3COOH, for later MS analysis.

Nano-HPLC and tandem triple-quadrupole MS analysis of peptides.

The tryptic peptides from control and 15d-PGJ_2-treated samples were injected with a Famos (LC Packings) autosampler onto a PepMapTM C18 reversed phase micro-column (300 μm ID x 5 mm) from LC Packings and washed to remove salts. Samples were eluted onto a C18 reversed phase nano-column (100 μm ID x 15 cm, Teknokroma, Mediterranea sea), which was developed with a CH3CN gradient (5-47.5% CH3CN over 45 min, followed by a 1 min increase to 85.5% CH3CN) generated by an Ultimate Nano-HPLC (LC Packings). A flow rate of ca. 300 nL min-1 was used to elute peptides from the nano-column to a New Objective PicoTip™ emitter nano-spray needle (3000 V) in a Protana nanospray ion source, and ions were analyzed with the 4000 Q-Trap system. In the enhanced resolution mode, the linear ion trap was scanned at m/z 250/s, and the ion of interest was selected in Q1 by precursor ion scanning. N2 was used as the curtain (value of 15) and collision gas (set to high).

Multiple Reaction Monitoring (MRM).

15d-PGJ_2-bound tryptic peptides from treated and untreated microtubules were analyzed in the MRM mode. Q1 was set on the m/z corresponding to charged parent ions from masses 1, 2, 3, and 4 previously observed (m/z at 644.4, 662.9, 726.4, and 989.9, respectively), and Q3 was set on specific fragment ions for each parent mass (m/z at 482.3 corresponding to y4 fragment ion for mass 1, m/z at 948.2 corresponding to 15d-PGJ_2-modified y6 fragment ion for mass 2, m/z at 841.4 corresponding to y7 fragment ion for mass 3, and m/z 1326.1 corresponding to doubly-charged, y25 fragment ion for mass 4). Collision energy was set to 30 eV.

MS data analysis.

All the chromatograms and MS/MS spectra from the 4000 Q Trap System were analyzed with Analyst 1.4.1 software (Applied Biosystems, CA, USA). Analyses of 15d-PGJ_2-binding to microtubules by MS were repeated with two independent samples.

Mammosphere culture.

Supernatants from exponentially growing cultures in 10 cm-diameter dishes were centrifuged in a Selecta Centroni-BL centrifuge at 1,000 r.p.m. (700 r.c.f.) for 5 min. Cells were resuspended and analyzed for single-cellularity. Viability was determined

using Trypan Blue dye (Sigma-Aldrich Co., MO, USA). Then, 2,000 viable cells/mL were plated in low-attachment plates (Falcon, BD Biosciences, CA, USA) in serum-free medium containing DMEM-HAM's-F12 1:1 supplemented with B27 (Gibco, Invitrogen, CA, USA), 20 ng/mL epidermal growth factor (EGF) and 20 ng/mL basic fibroblast growth factor (bFGF) (Peprotech Inc., NJ, USA). Medium was partially refreshed every 2.5 days, with addition of EGF and bFGF. To obtain secondary mammospheres, primary mammospheres were collected by centrifugation (400 r.p.m.) after 7-10 days, dissociated enzymatically (4 min trypsin-EDTA at 37ºC) and seeded as indicated.

Mammosphere forming efficiency.

To determine mammosphere forming efficiency, the number of mammospheres resulting from seeding 2,000 cels/mL as previously described was evaluated by direct observation on a Nikon Eclipse TS100 microscope.

Study of primary mammosphere growth.

Briefly, 2,000 viable cells per mL were plated in low-adherence plates as previously described. Mammosphere formation was followed during 12 days. Then, treatment was added. Treatment and growth factors were renewed each 2.5 days dissolved in medium to contribute to medium refreshment. After 12 days, mammospheres were counted and photographed.

Self-renewal studies.

Primary spheres were obtained from MCF-7 cells as previously indicated and allowed to grow for 5 days in non-adherent plates. Similarity in sphere number and size in the different wells at the beginning of the experiment was checked. Treatments were added where corresponding and spheres were allowed to grow for 5 additional days (days 6-10). Then, spheres were sedimented, washed with PBS,disaggregated until single cellularity and resuspended in mammosphere medium containing or not the corresponding treatment. Spheres were grown in this medium for 5 days (day 11-15) and were then photographed. Treatment and growth factors were renewed each 2.5 days.

Detection of $CD44^{+}/CD24^{-/low}$ expression profile by flow cytometry.

Typically, 600,000 cells from each cell line were plated in 10-cm diameter culture dishes in regular RPMI medium. Then, 24 hours later, supernatants were collected, and adherent cells were trypsinized for 3 min and included in the tube containing the corresponding supernatant. Cells were centrifuged at 1,000 r.p.m. 5 min and the pellet was then washed with PBS. Cells were counted and 10^6 cells were separated, centrifuged and resuspended in 100 µL PBS 1% FBS. Samples were incubated at dark with CD44 monoclonal antibody coupled to FITC (BD Pharmingen; cat.# 555478) and CD24 antibody coupled to APC (BD Pharmingen; cat.# 555428) for 15 min at room temperature with moderate shacking. Samples were centrifuged and washed with PBS before being analyzed in a MoFlo cytometre (Beckman-Coulter, CA, USA). Controls for each dye and cell type were included. To avoid divergences in the detection of the membrane antigens due to their enzymatic cleavage by trypsin, control plates where cells were detached using EDTA or Versene (Gibco, Invitrogen, CA, USA) were used, obtaining similar results than with trypsin.

Side population (SP) isolation.

Briefly, 10^6 cells were trysinized and resuspended in 500 µL PBS containing 1% FBS previously to addition of Hoechst 33342 (5 µg/mL) (Fluka, Sigma-Aldrich Co., MO, USA; cat. # 14533), and 10 µmol/mL Fumitremorgin C (FTC) (Sigma-Aldrich Co., MO, USA; cat. # F9054) in the case of control tubes. Incubation was done in an orbital shacker at 37ºC for 90 min protected from light. At the end of the incubation, samples were centrifuged, washed twice with chilled PBS and filtered through a 40-µm nylon mesh previously to fluorescence-activated cell sorting (FACS) in a FACS Aria SORP cytometre (BD Biosciences, CA, USA). Sorted SP and non-SP fractions were collected in 96-well plates.

Orthotopic xenograft model.

Typically, 6-week-old virgin nu/nu female mice (n=6) were anesthetized by an intraperitoneal (i.p.) injection of 0.3 mL ketamine/xylacine and 17β-oestradiol pellets (Innovative Research of America, FL, USA; cat. # NE-121) were implanted on the lateral side of their necks. Three days after pellet implantation, 200 SP or non-SP MCF-7 cells were resuspended in RPMI/Matrigel 1:1 and injected immediately after cell

sorting in the fat pad of the fourth mammary gland using a 27-gauge needle. Tumoral burden was estimated twice a week by palpation and tumour diameters were measured with calipers. Tumour volume was evaluated according to the equation: Volume = (Dxd2)/2, where 'D' is the major diameter of the tumour and 'd' the minor diameter. Experiments were performed in accordance with the European Communities Council, directives 86/609/EEC and 2007/526/CE.

Statistical analysis.

The data shown are the means ± standard deviation (SD) of at least three independent experiments. Statistical comparisons for significance between cells with different treatments were performed using the Student's t test. Significance is represented as *, $P < 0.05$; **, $P < 0.01$; ***, $P < 0.001$.

RESULTS

RESULTS

In the later years, increasing evidences of significant antineoplastic effects of PPARγ agonists in different cancer cell types have been reported (Grommes et al., 2004), placing these compounds as potential therapeutic agents for the treatment of this disease. Especially relevant is their antiproliferative and proapoptotic effect on breast cancer tumorigenesis, as it has been stated by several authors (Bonofiglio et al., 2006; Kim et al., 2006) and by previous work of our laboratory (Pignatelli et al., 2003; Pignatelli et al., 2001; Pignatelli et al., 2005). However, the mechanism by which PPARγ ligands exert their antineoplastic activity has not been yet fully elucidated. In this work we have further examined the mechanisms underlying the antitumorigenic effects of PPARγ ligands in breast carcinoma.

1.- PPARγ LIGANDS INHIBIT GROWTH OF HUMAN BREAST CANCER CELL LINES.

In this work, we first have further established the role of different PPARγ ligands on breast cancer cell proliferation, viability and apoptosis. With this aim, we have studied the effects caused by the natural PPARγ ligand 15-deoxi-$\Delta^{12,14}$-Prostaglandin J_2 (15d-PGJ_2) and by the synthetic agonists rosiglitazone (RSG) and pioglitazone (PGZ), since these compounds have been reported to potently activate PPARγ.

1.1.- PPARγ agonists significantly reduce viability of breast cancer cells.

To evaluate the effect on cell growth of PPARγ ligands we performed studies on viability of the human breast cancer cell lines SKBR3, MCF-7, T47D and MDA-MB-231 upon treatment with these compounds. Subconfluent cultures of these cell lines were treated with 10 μM 15d-PGJ_2, 30 μM rosiglitazone or 10 μM pioglitazone for 24 hours and cell viability was determined through colorimetric assessment of conversion of yellow 3-[4,5-dimethylthiazol-2-yl]-2,5-diphenyl tetrazolium bromide (MTT) to purple formazan by viable cells. As it is shown in Figure 1, the three compounds cause a significant decrease in cell viability, with 15d-PGJ_2 being responsible for the most dramatic effect, achieving a reduction of approximately 70% in cell viability independently of the cell line studied. Treatment with rosiglitazone and pioglitazone also leads to a decrease in viable cells, although the intensity of this effect at 24 hours is much lower than that of 15d-PGJ_2.

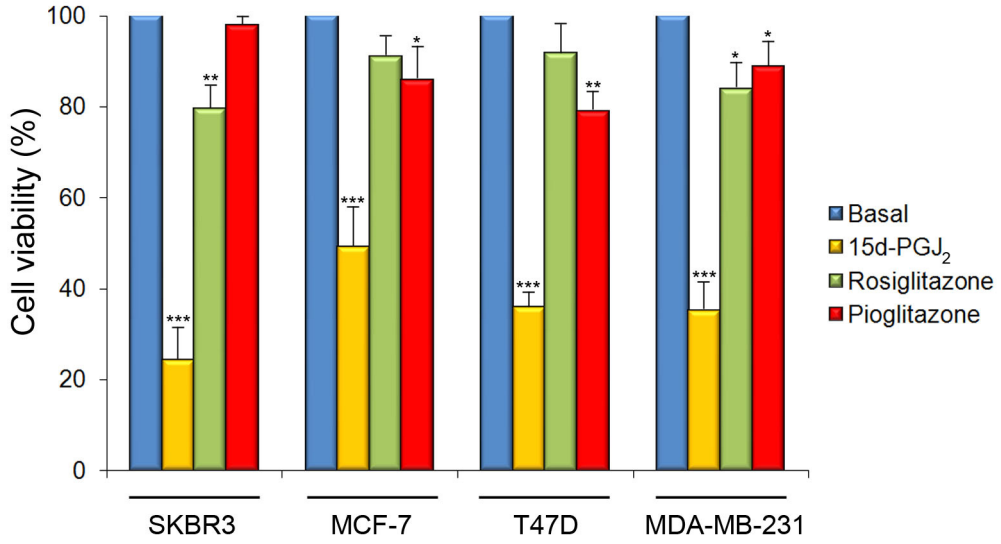

Figure 1. **Effect on cell viability of PPARγ ligands on human breast cancer cell lines.** Cells were incubated in the presence or absence of 15d-PGJ_2 (10 μM), rosiglitazone (30 μM) or pioglitazone (10 μM) for 24 hours, as commented in Materials and Methods. Cell viability was determined by MTT assay. Results show the means ± SD (standard deviation) of 5 independent experiments with 5 replicates each. *, $P < 0.05$; **, $P < 0.01$; *** $P < 0.001$.

1.2.- Treatment of breast cancer cells with PPARγ ligands leads to a significant reduction in cell proliferation.

To better characterize the inhibition of growth following treatment with 15d-PGJ_2, rosiglitazone or pioglitazone, we next analyzed whether the observed effect on viability was a result of impaired cell proliferation. With this purpose, incorporation of radiolabelled [^{3}H]thymidine or of its non-radiactive analogue 5-Bromo-2-deoxy-uridine (BrdU) in exponentially growing cultures of four different human breast cancer cell lines treated or not with PPARγ agonists was assessed in order to quantitatively measure cell proliferation. The results from incorporation of radioactive thymidine (Fig. 2A) and BrdU (Fig. 2B), indicate that 15d-PGJ_2, rosiglitazone and pioglitazone notably decrease cell proliferation in all the cell lines tested. In agreement with the results obtained on the evaluation of cell viability after treatment with PPARγ ligands, 15d-PGJ_2 is the compound that exerts the most potent effects on cell proliferation, being even almost capable of completely blocking proliferation in the highly proliferative SKBR3 cell line after 24 hours of treatment.

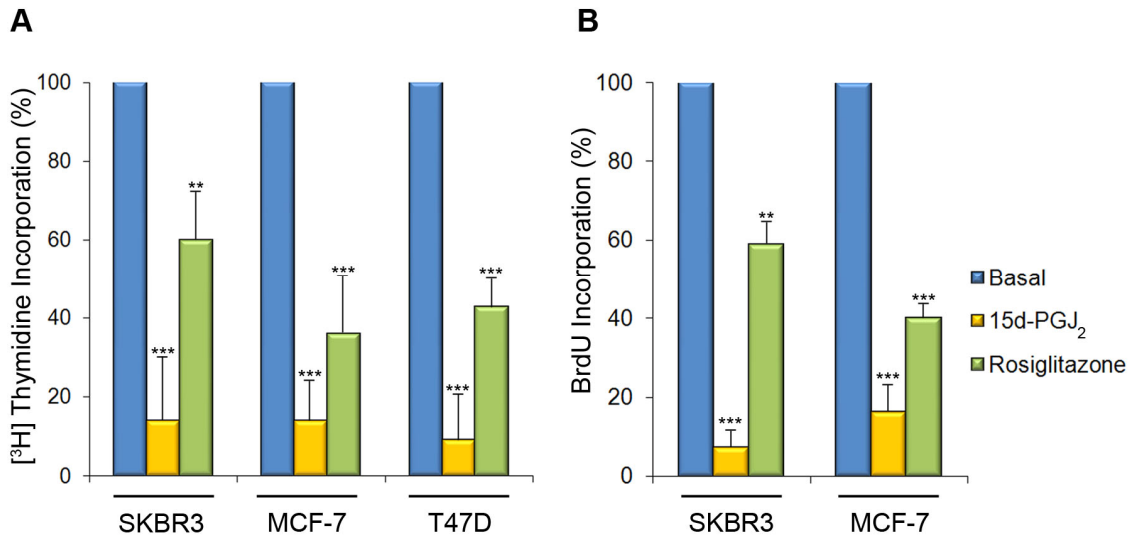

Figure 2. **Effect of PPARγ ligands on proliferation of human breast cancer cell lines.**
(A) Measurement of the incorporation of radiactive thymidine in SKBR3, MCF-7 and T47D cells treated during 24 hours in the presence of 10 µM 15d-PGJ_2 or 30 µM rosiglitazone. Results correspond to 6 independent experiments with 8 replicates each. **(B)** Incorporation of BrdU in cells treated as in (A). The graphic represents the means ± SD of three independent experiments. **, $P < 0.01$; *** $P < 0.001$.

1.2.- Inhibition of growth in breast cancer cells upon treatment with PPARγ ligands is accompanied by increased apoptosis.

Observation of the capacity of 15d-PGJ_2, rosiglitazone and pioglitazone to cause cell death in breast cancer cells raised the possibility of these compounds acting as inducers of apoptosis. To test this hypothesis, we performed studies of flow cytometry to evaluate the presence of phosphatidylserine in the outer layer of the cytoplasmic membrane. Exposure of phosphatidylserine at the cell surface is a characteristic trait of the apoptotic process that can be detected through staining of the cells with annexin V-FITC, a protein coupled to fluorescein capable of binding to phosphatidylserine. This method, in combination with the detection of the cells which are not stained by the dye propidium iodide (PI) that enters only death cells, is a suitable approach to assess induction of apoptosis in a cell culture.

MCF-7 cells were seeded on 60 mm-diameter culture dishes and allowed to grow for 24 hours before shifting medium to RPMI supplemented with 5% charcoal-stripped PBS. After 24 hours growing in these conditions, cells were treated with 10 µM 15d-PGJ_2, 30 µM rosiglitazone or 10 µM pioglitazone and both floating and adhered cells were collected for staining with Annexin V-FITC and PI using the human Annexin V-FITC

kit (Bender MedSystems, Vienna, Austria), according to manufaturer's guidelines. Treatment with 15d-PGJ_2 for 24 hours was shown to be capable of significantly increasing the number of apoptotic cells (21%) in comparison with non-treated cultures (6%) (Fig. 3), whereas rosiglitazone and pioglitazone exhibit a milder effect (10 and 8%, respectively).

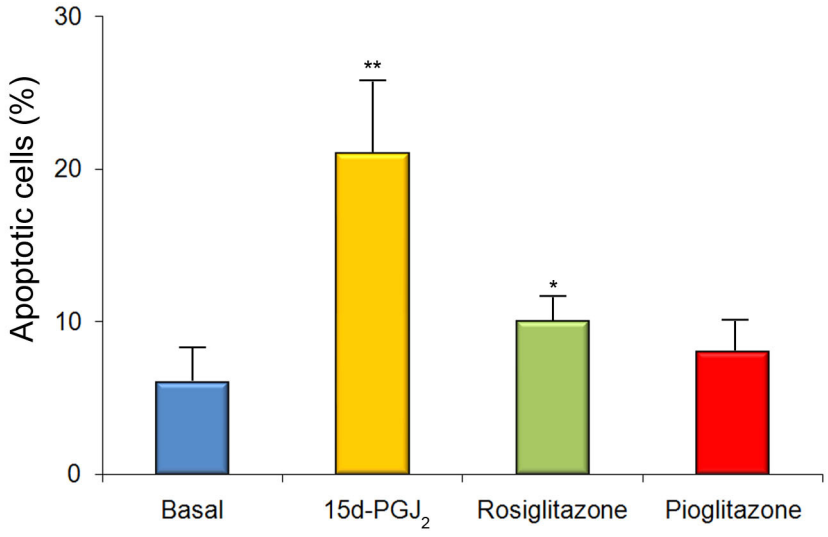

Figure 3. **Analysis of induction of apoptosis by PPARγ agonists.**
MCF-7 cells were treated with 10 μM 15d-PGJ_2, 30 μM rosiglitazone or 10 μM pioglitazone, afterwards the number of apoptotic cells was determined by Annexin V-FITC staining and FACS analysis. The graph represents the percentage of apoptotic cells in the cultures. *, $P < 0.05$; **, $P < 0.01$.

1.3.- Assessment of antineoplastic capacity of TDZDs in human breast cancer cells.

Based on the observation of the potent antineoplastic effects of several PPARγ ligands, we sought to identify new potential therapeutic agents that exert similar effects in human breast carcinoma. Since compounds of the family of the thiadiazolidinones (TDZDs) show structure similarity with the TZDs group of PPARγ ligands that includes rosiglitazone and pioglitazone, and considering that TDZDs action has been reported to be mediated by PPARγ (Luna-Medina et al., 2005), we evaluated the effects of TDZDs on cell growth.

1.4.- Effect of TDZD compounds on proliferation of human breast cancer cells.

First of all, we assessed the effect exerted by the members of the TDZDs family known as NP00111, NP01138, NP031112, NP031115, NP031122, and TDZD-8 on proliferation of breast cancer SKBR3, MCF-7 and T47D cells. With this purpose, cells

growing exponentially in 96-well culture plates were cultured for 24 hours in RPMI supplemented with 5% stripped FBS before addition of the different compounds at a final concentration of 10 μM. After 24 hours, 0.5 mCi radiolabelled [^{3}H]thymidine was added per well and incubation proceeded for another 24 hours. [^{3}H]radioactivity measurements obtained after harvesting are represented in Figure 4. As it can be observed, all compounds cause a decrease in cell proliferation, although the most notable effect is that exerted by TDZD-8 and NP031122, that provoke a reduction in proliferation of approximately 70% in MCF-7 cells when compared to control cells.

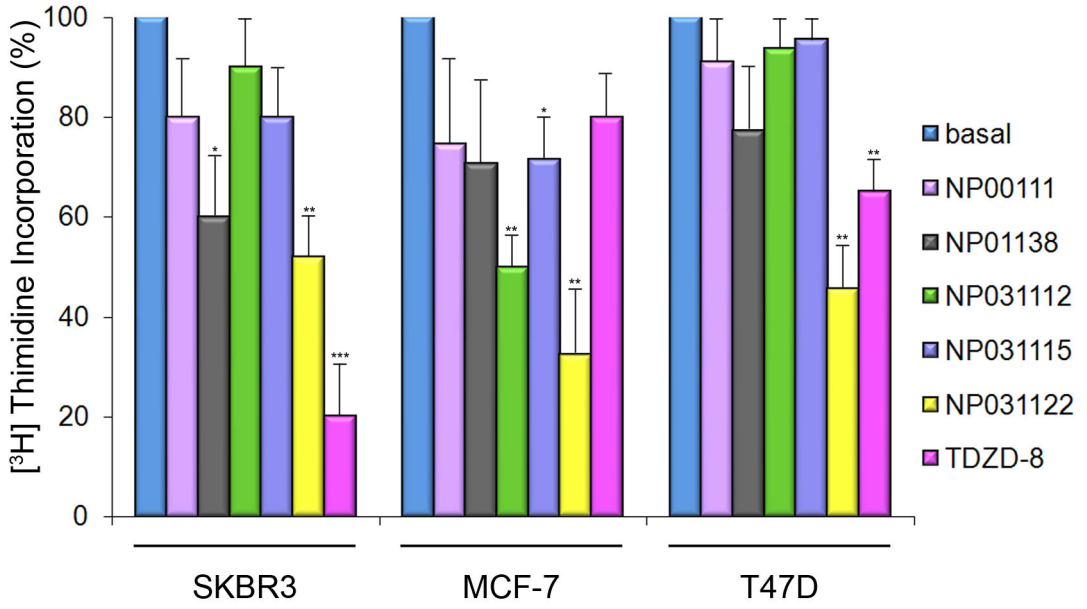

Figure 4. **Effect of TDZDs on proliferation of human breast cancer cell lines.**
SKBR3, MCF-7 and T47D cells were treated during 24 hours with the specified TDZDs at a concentration of 10 μM. After addition of 0.5 μCi of ^{3}H-thymidine cells were harvested and incorporation of radiactive timidine was measured. Results are representative of 5 independent experiments with 8 duplicates each. *, $P < 0.05$; **, $P < 0.01$; *** $P < 0.001$.

1.5.- TDZD-8 induces activation of a PPRE reporte gene together with reduction of cell viability and proliferation.

Since other members of the TDZD family have been shown to be capable of activating PPARγ, we first studied the ability of TDZD-8 to induce activation of a PPRE reporter gene. To this end, we performed transient transfections in MCF-7 and T47D cells of the reporter plasmid pPPRE-tk-luc, containing three PPARγ consensus binding sites. As shown in Figure 5, TDZD-8 is capable of inducing the expression of the reporter construct, suggesting that this compound efficiently activates PPARγ.

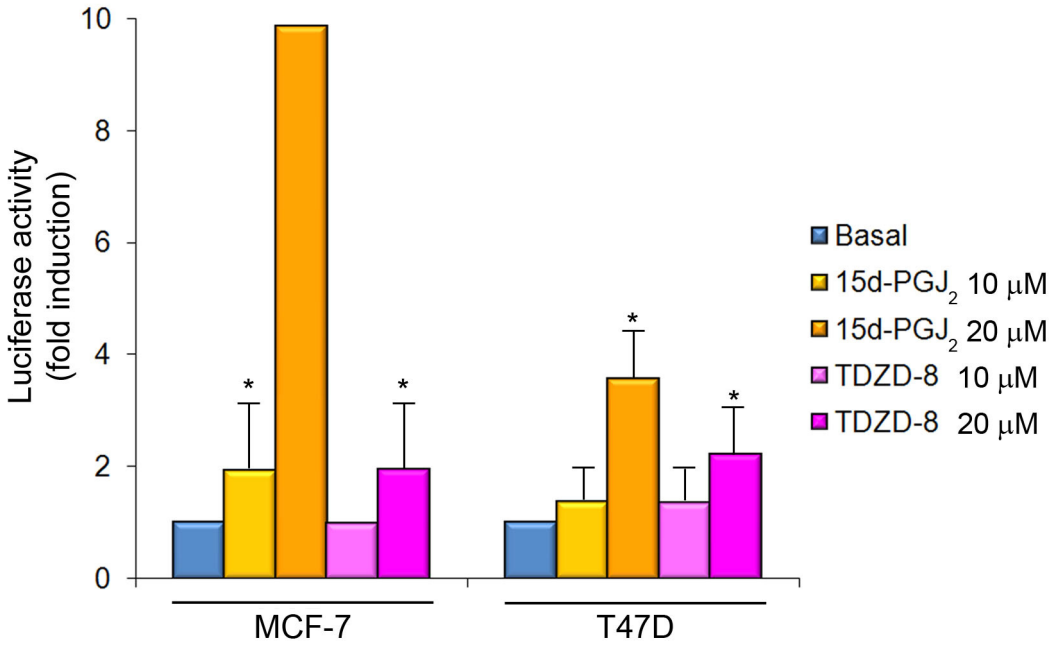

Figure 5. **Activation of a PPRE reporter gene by 15d-PGJ$_2$ and TDZD-8.**
MCF-7 cells were transfected with 0.2 μg of the PPRE-tk-luc reporter plasmid and harvested after 24 hours of treatment with growing concentrations of 15d-PGJ$_2$ or TDZD-8. Luciferase activity of cell lysates was determined. Data are expressed relative to the basal values and represent the means ± SD luciferase activity determined in triplicate in three independent experiments. *, $P < 0.05$.

We next evaluated the effects of TDZD-8 on breast cancer cell viability and proliferation. Regarding cell viability, transformation of yellow MTT to blue formazan by viable cells was measured in cultures of SKBR3, MCF-7, T47D and MDA-MB-231 cells treated or not with TDZD-8 at a concentration of 10 or 20 μM. Figure 6 shows the decrease in cell viability caused by treatment with TDZD-8. This reduction is significant in all the cell lines tested, although it is even more dramatic in the case of SKBR3 cell line, where viable cells after 24 hours of treatment are reduced to less than 20% of the original population.

Effects on proliferation were analyzed in MCF-7 and SKBR-3 cells by monitoring BrdU incorporation after 24 hours of treatment with growing concentrations of TDZD-8. As it can be observed in Figure 7, TDZD-8 causes a decrease in cell proliferation in both cell lines, although in line with the results obtained in cell viability, the effect is more pronounced in the SKBR3 cell line.

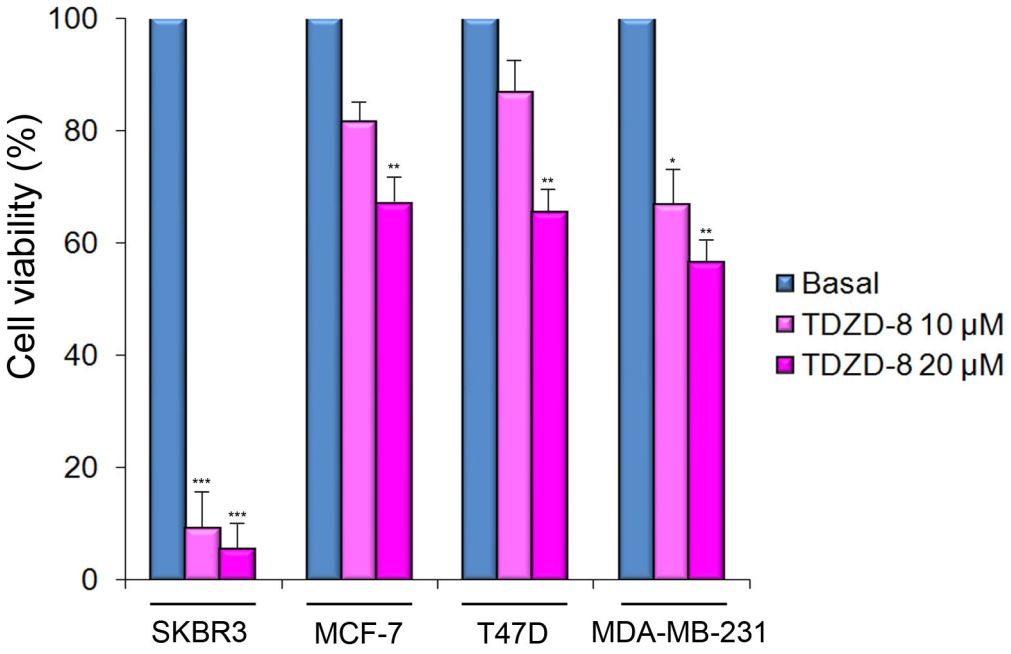

Figure 6. **Viability of cells treated with TDZD-8.**
Cell viability assayed in four different human breast cancer cell lines following 24 hours of treatment with growing concentrations of TDZD-8. Measurements indicate the means values ± SD of four independent MTT assays with 6 replicates each. *, P < 0.05; **, P < 0.01; *** P < 0.001.

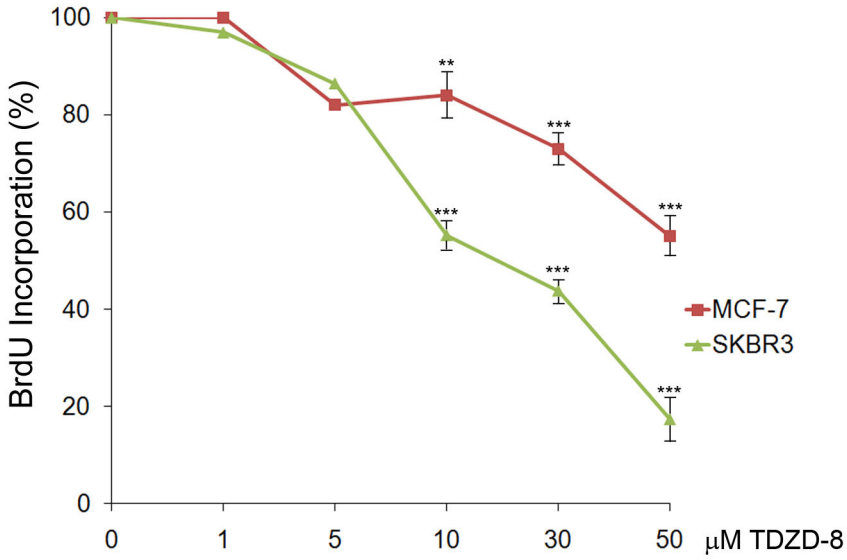

Figure 7. **Effect of TDZD-8 on cell proliferation.**
Measurement of BrdU incorporation after 16 hours of treatment with growing concentrations of TDZD-8. Represented results correspond to means values ± SD of three independent experiments. *, P < 0.05; **, P < 0.01; *** P < 0.001.

1.6.- NP031122 reduces MCF-7 transformation capacity.

To further assess the efficacy of NP031122, we performed colony-forming assays in soft agar to evaluate the clonogenicity of MCF-7 cells treated or not with NP031122. The ability of cells to exhibit anchorage independent growth and thus grow in a soft agar matrix, is a measure of cell transformation. We seeded MCF-7 cells in soft agar and 24 hours after seeding started to treat the cells with NRG1, that stimulates growth, NP031122 or a combination of both compounds. As it can be observed in Figure 8, MCF-7 control cells which had not been treated exhibit the ability to grow embedded in soft agar and originate numerous colonies. The number of colonies was increased upon treatment with NRG1 but decreases in presence of NP031122. When cells were treated at the same time with both NRG1 and NP031122, this TDZD reversed the proliferative

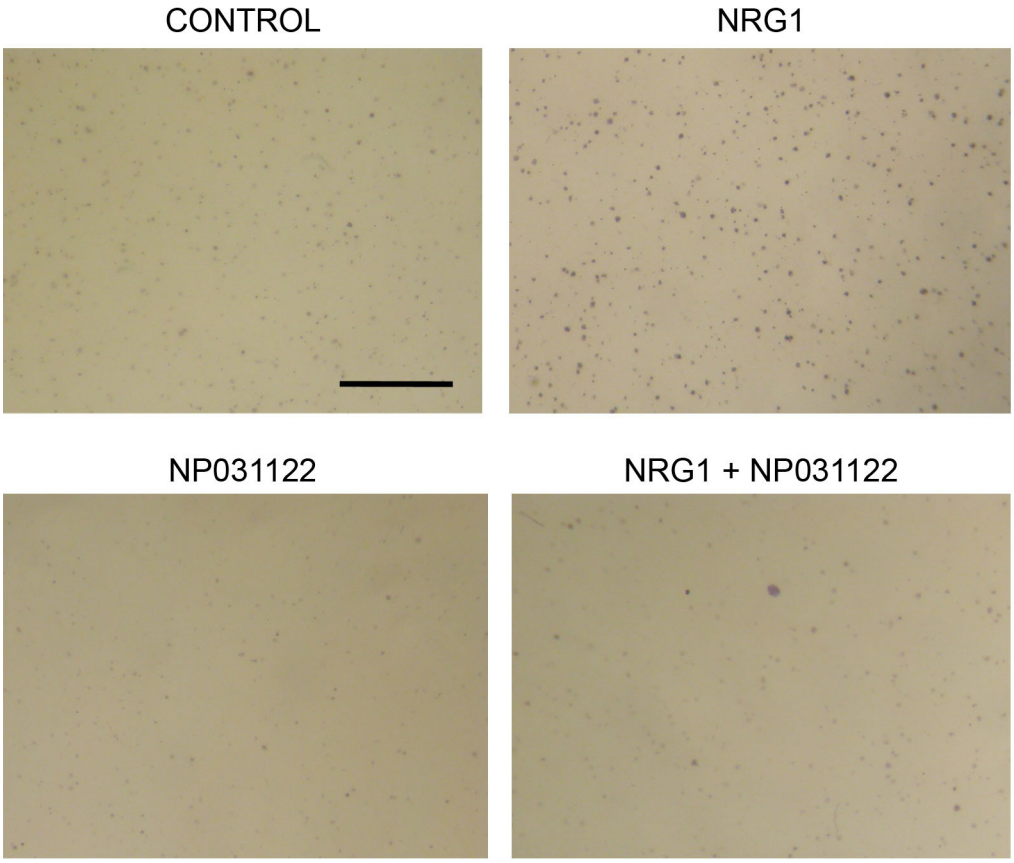

Figure 8. **Effect of NP031122 on clonogenicity of MCF-7 cells.**
Twenty hours after seeding in soft agar, cell were treated with NRG1 to promote growth in the presence or absence of NP031122 (10 μM). After 20 days in culture with periodic feeding and addition of the mentioned treatments, representative images of the resulting colonies were taken. As shown in the images, NP031122 causes a decrease in the number of colonies in comparison to both untreated cultures or cultures treated with NRG1. Scale bar, 0.5 cm.

stimulus due to NRG1 and the number of resulting colonies was even lower to that in control non-treated cells. These results, similar to those exhibited by 15d-PGJ_2 in the same cell type (Pignatelli et al., 2001), indicate that NP031122 can induce a notable decrease in cell growth and abrogate the transforming effects of NRG1 on MCF-7 cell line, reinforcing its potential as therapeutic agent.

Although further study is needed, these results suggest a potential important role of TDZD-8 and NP031122 as therapeutic agents for human breast carcinoma.

2.- 15d-PGJ_2 BLOCKS PROLIFERATION INDUCED BY ACTIVATION OF ErbB RECEPTORS BY MEANS OF INCREASED PHOSPHATASE ACTIVITY.

Previous studies from our laboratory indicate that an important part of the citostatic effects of the PPARγ ligand 15d-PGJ_2 in breast cancer cells are due to its ability to revert the phosphorylation of ErbB2 and ErbB3 induced by NRG1 and NRG2 (Pignatelli et al., 2001). We have further shown that preincubation of the cells with sodium orthovanadate (OVa_4Na_3), an inhibitor of protein tyrosine-phosphatases, impairs this reversion, suggesting that 15d-PGJ_2 promotes dephosphorylation of ErbBs through a mechanism in which a phosphatase (or group of them) could be the main effector. Based on this data, we focused on the identification of this phosphatase.

2.1.- 15d-PGJ_2 does not alter the expression of SHP-1, SHP-2 and BDP1 phosphatases.

We initially analyzed three phosphatases, SHP-1, SHP-2 and BDP1, since they have been previously implicated in ErbB signalling pathways, as commented in the Introduction. First of all, we analyzed the expression levels of these phosphatases over time in MCF-7 cells upon 15d-PGJ_2 treatment to test if 15d-PGJ_2 was upregulating their expression. As it is shown in Figure 9A no change in protein content of any of the phosphatases was observed. The maintenance of expression levels of all three phosphatases was corroborated by quantitative-PCR analysis, that showed no variation in messenger RNA (mRNA) transcription in response to treatment of MCF-7 cells with 15d-PGJ_2 (Fig. 9B). However, a transient shift in the electrophoretic mobility of SHP-1 appeared 12 hours after addition of 15d-PGJ_2.

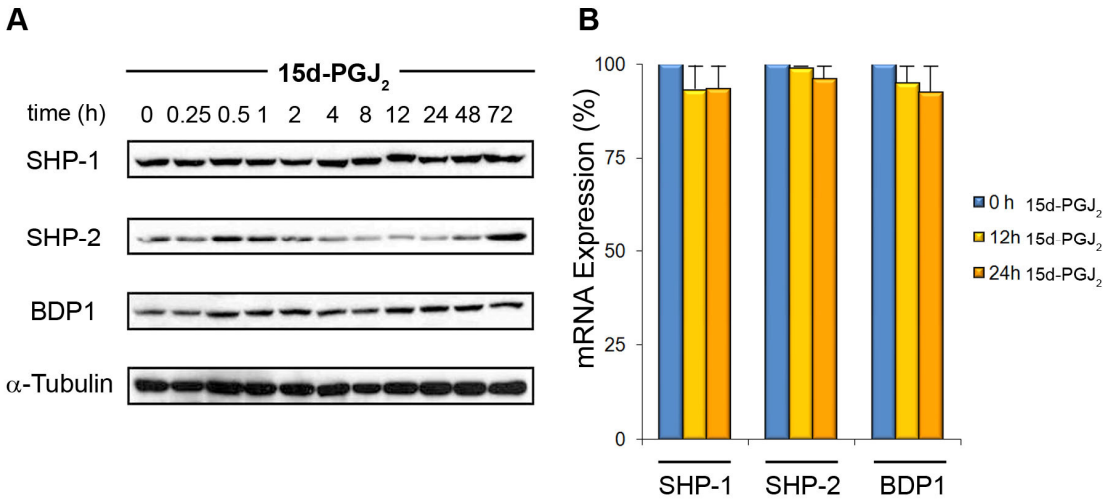

Figure 9. **Changes in the expression levels of protein and mRNA of protein tyrosine phosphatases SHP-1, SHP-2 and BDP-1.**
(A) Western-blot analysis of protein expression of SHP-1, SHP-2 and BDP-1 phosphatases. No changes in protein content were detected upon treatment with 10 μM 15d-PGJ_2. Content in α-tubulin protein is presented as loading control. **(B)** Representation of the transcription levels of mRNA corresponding to the mentioned phosphatases upon treatment with 10 μM 15d-PGJ_2 over time as determined by quantitative-PCR. *, $P < 0.05$; **, $P < 0.01$; *** $P < 0.001$.

2.2.- 15d-PGJ_2 causes redistribution and membrane localization of SHP-1.

We also studied the cellular localization of SHP-1, SHP-2 and BDP1 upon treatment with 15d-PGJ_2. MCF-7 cells were treated with 15d-PGJ_2 for 24 hours and fixed in methanol -20ºC. Immunofluorescence staining with the corresponding antibodies revealed a redistribution of SHP-1 phosphatase in response to treatment with 15d-PGJ_2. In non-treated cells, SHP-1 exhibits a perinuclear localization, whereas in treated cells SHP-1 is located at the membrane and the nucleus (Figure 10). Membrane localization of ErbBs reinforces the possibility of a direct interaction with ErbB receptors.

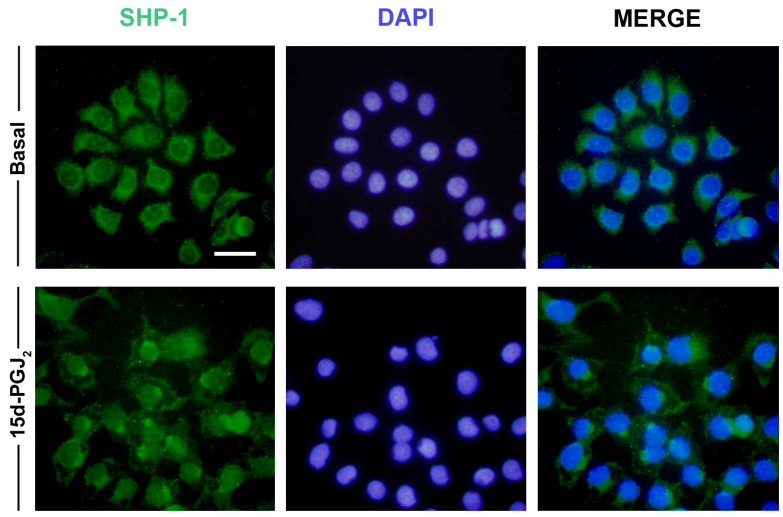

Figure 10. **Redistribution of SHP-1 in response to 15d-PGJ_2 treatment.** Representative images showing localization of SHP-1 in both basal (upper panels) and 15d-PGJ_2–treated cells (lower panels). Addition of 15d-PGJ_2 causes SHP-1 translocation from a perinuclear distribution to membrane localization. Scale bar, 20 μM.

2.3.- 15d-PGJ_2 induces SHP-1 phosphatase activation via its phosphorylation.

Changes in electrophoretic mobility as the ones observed for SHP-1 in the western-blot assay are generally associated to post-transductional protein modifications such as phosphorylation, ubiquitination or sumoylation. With the purpose to verify if this alteration was caused by one of these modifications, MCF-7 cells were treated with 15d-PGJ_2 at different times and immunoprecipitation of SHP-1 within the corresponding lysates was performed. Then, the phosphorylation state of immunoprecipitated SHP-1 was analyzed. As it is shown in Figure 11A, SHP-1 phosphorylation transiently increases after 12 hours of 15d-PGJ_2 treatment; that is, at the same time than the mobility shift is observed. This observation indicates that the 15d-PGJ_2-induced shift is probably due to the phosphorylation of SHP-1.

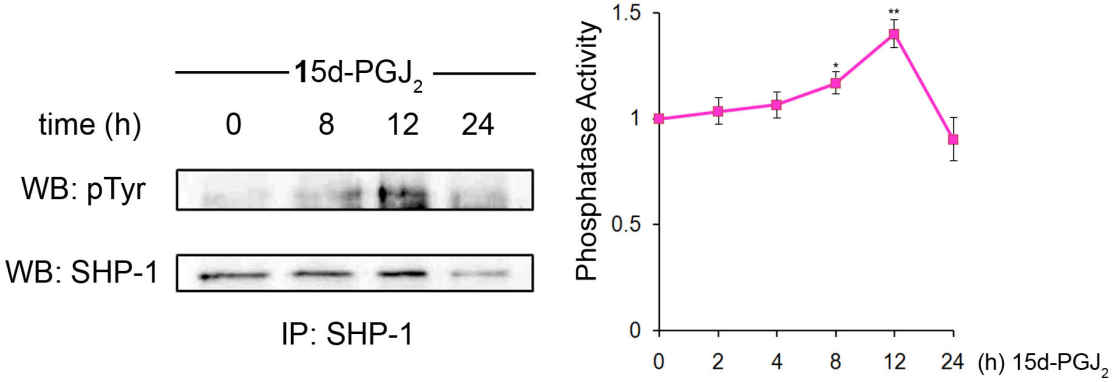

Figure 11. **SHP-1 phosphorylation and activity are transiently increased upon treatment with 15d-PGJ_2.**
(A) MCF-7 cells were treated during different time with 15d-PGJ_2 and SHP-1 phosphatase was immunoprecipiated from the cell lysate. Phosphorylation of immunoprecipitated SHP-1 was determined by western-blot. Transient phosphorylation of SHP-1 is observed 12 hours after treatment with 15d-PGJ_2. **(B)** SHP-1 phosphotyrosine phosphatase activity was assayed in the immunoprecipitates. Colorimetric measurements of activity are expressed in fold increase over basal levels. Values represent the media ± SD of three independent experiments. *, $P < 0.05$; **, $P < 0.01$.

Interestingly, SHP-1 has been described to become active upon phosphorylation in its C-terminal tail (Frank et al., 2004; Uchida et al., 1994). This is an on/off mechanism that facilitates to change the activation state of the phosphatase rapidly and precisely. This fact lead us to analyze whether the modification of SHP-1 phosphorylation state implicated a concomitant change in its phosphatase activity, as this could explain the dephosphorylation observed in ErbBs upon 15d-PGJ_2 addition. Cell lysates were obtained from MCF-7 cells exposed to 15d-PGJ_2 during times varying from 0 to 24 hours. After measuring protein concentration using the Bradford system, equal amounts

of proteins were subjected to SHP-1 immunoprecipitation. Measurements of tyrosine phosphatase activity of the immunoprecipitated SHP-1 phosphatase were perfomed using the Universal Tyrosine Phosphatase assay kit. The results shown in Figure 11B revealed an increase on SHP-1 phosphotyrosine phosphatase activity 12 hours after the addition of 15d-PGJ_2 to the culture medium, the same time than the mobility shift caused by phosphorylation of SHP-1 becomes evident. Thus, 12 hours after its addition, 15d-PGJ_2 induces a transient increase on SHP-1 phosphotyrosine phosphatase activity.

2.4.- Knock-down of SHP-1 expression prevents 15d-PGJ_2-induced ErbB2 dephosphorylation.

In order to assess the implication of SHP-1 in ErbB2 phosphorylation, we carried out transitory transfections of MCF-7 cells with an interference RNA (iRNA) against this phosphatase. As shown in Figure 12 iRNA is efficiently incorporated by most of the cells and interference of SHP-1 is successfully achieved, obtaining a significant reduction in the amount of phosphatase present within the cell.

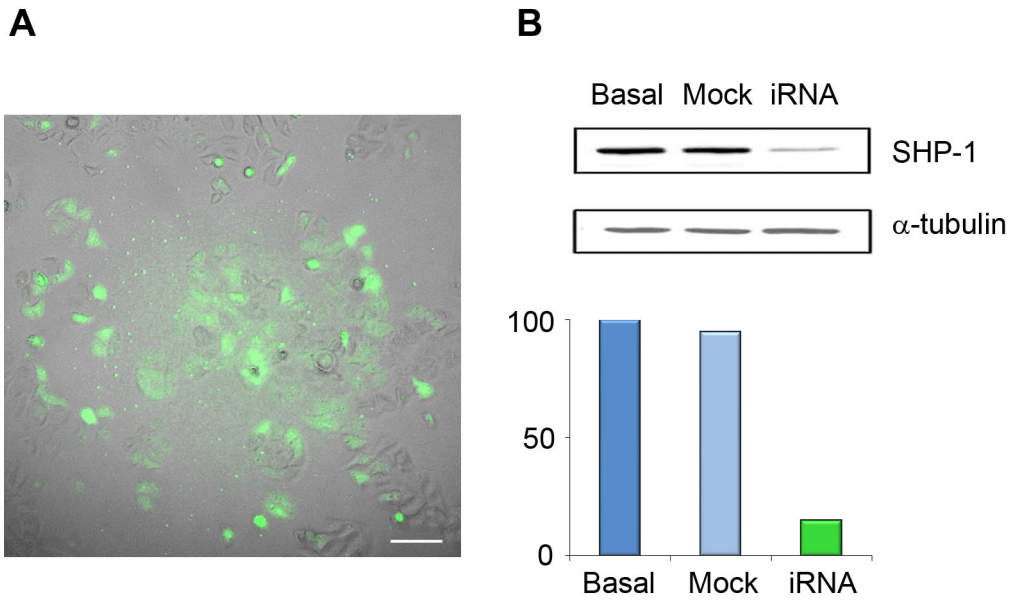

Figure 12. **iRNA significantly reduces SHP-1 protein content within the cell.**
(A) Transfection of MCF-7 with a fluorescent iRNA (siGLO) to assess transfection efficiency. As shown in the photograph, the majority of the cells have successfully incorporated the iRNA 24 hours after transfection. iRNA remained in the cells even 72 hours post-transfection. Scale bar, 20 μM. **(B)** Representative western-blot and its quantification showing SHP-1 protein content in basal cells and in cells transfected with a non-targeting iRNA (Mock) or an iRNA against SHP-1 (iRNA). The image is representative for 3 independent experiments performed 24 and 48 hours after transfection.

Once evaluated the efficiency of transfection and that the iRNA against SHP-1 remained within the cells at long experimental times such as 72 hours, subconfluent MCF-7 cells were then transfected with iRNA and grown during 24 hours in regular medium to allow recovery of the cells and interference of SHP-1. Then, cells were treated with 15d-PGJ_2 for 12 hours and ErbB2 phosphorylation was stimulated afterwards by addition of NRG1 during 5 min. Analysis of ErbB2 phosphorylation state in immunoprecipitates of basal and SHP-1-interfered cells submitted or not to preincubation with NRG1 and/or 15d-PGJ_2 (Fig. 13) reveals an increase in ErbB2 phosphorylation when the expression levels of SHP-1 are decreased. Similarly, depletion of SHP-1 causes 15d-PGJ_2-induced ErbB2 dephosphorylation to be milder than when SHP-1 is present.

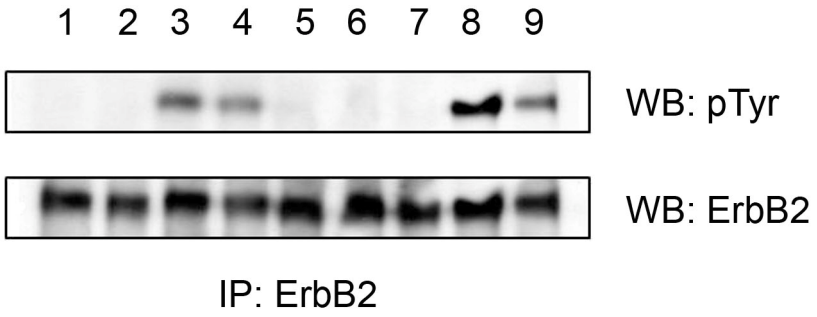

Figure 13. **Effect of SHP-1 knock-down in 15d-PGJ_2-induced ErbB2 dephosphorylation.** MCF-7 cells were allowed to grow in regular medium (lanes 1-4), transfected with a non-targeting iRNA (lane 5) or with an iRNA against SHP-1 phosphatase (lanes 6-9). Twenty four hours post-transfection, cells were treated with 10 μM 15d-PGJ_2 (lanes 2, 4, 7 and 9) for 12 hours before stimulation of ErbB2 phosphorylation by addition of NRG1 (lane 3, 4, 8, 9) during 5 min. Then, cells were harvested and ErbB2 was immunoprecipitated. Image shows a representative western-blot of the phosphorylation levels of ErbB2. An increase in ErbB2 phosphorylation is observed in NRG1-treated cells when the expression levels of SHP-1 are decreased (lane 8) in comparison to normal SHP-1 levels (lane 3). Moreover, the reversion of this phosphorylation in cells treated with 15d-PGJ_2 and NRG1 is lower in the SHP-1 knock-out (lane 9) than in presence of SHP-1 (lanes 4).

Altogether, these results suggest that activation of SHP-1 by 15d-PGJ_2 would be responsible, at least in part, for the observed dephosphorylation effect of this prostaglandin on ErbB2 receptor.

3.- 15d-PGJ$_2$ INDUCES MITOTIC ARREST AS A RESULT OF MICROTUBULE DISRUPTION VIA TUBULIN BINDING.

Previous studies performed in our laboratory on the induction of apoptosis in breast cancer cells by 15d-PGJ$_2$ indicated that treatment with this prostaglandin promoted severe changes in the morphology of the mitochondria. Under basal conditions, mitochondria show an elongated shape with a form similar to that of a stick. However, shortly after addition of 15d-PGJ$_2$ mitochondria become smaller and rounder, and their localization becomes mainly perinuclear. As it is well-known that the characteristic shape of mitochondria is due to its association to microtubules (Ball and Singer, 1982), we decided to analyze whether 15d-PGJ$_2$ was responsible for inducing a disruption in microtubule architecture.

First, we wanted to confirm the effects of 15d-PGJ$_2$ on mitochondrial morphology. To this end, MCF-7 cells growing in glass coverslips in 24-well culture plates were treated with for 24 hours after which 20 nM Mitotracker Red CMXRos (Molecular Probes, Leiden, The Netherlands) was added for 45 min. As it is shown in Figure 14, confocal microscopy reveals morphological alterations in mitochondria, that acquire circular shape following treatment.

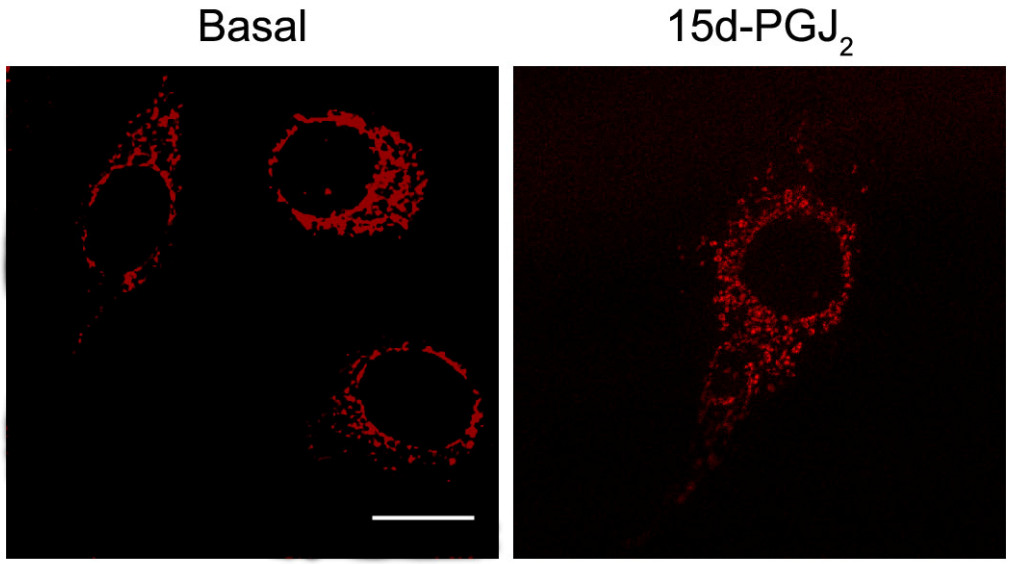

Figure 14. **15d-PGJ$_2$ induces alterations in mitochondrial morphology.**
Images show mitochondrial distribution and morphology in control cells and in cells treated for 24 hours with 10 μM 15d-PGJ$_2$. Scale bar, 20 μM.

Addition of 15d-PGJ_2 also originated morphological changes in the microtubule network. Microtubules (MT) are intracellular, filamentous, polymeric structures composed of two structurally similar protein subunits, namely, α- and β-tubulin (molecular weight, 50 kDa each). They constitute the principal component of the cytoskeleton network of eukaryotic cells and have been shown to be deeply involved in cell division, cytokinesis, maintenance of cell morphology, and signal transduction (Jordan and Wilson, 2004). During mitosis, microtubules undergo rapid polymerization and depolymerization to enable movement of chromosomes. As cell division approaches metaphase, microtubules are disrupted and form a spindle surrounding the centrosome, thereby facilitating chromosomal alignment on the metaphase plate. In this process, tubulin subunits freely exchange on the microtubules. If such free exchange of tubulin subunits is disrupted, the mitotic spindle is compromised and the cell cannot divide. Thus, drugs such as nocodazole that affect microtubule organization by binding to tubulin and preventing its incorporation into growing microtubules impair cell division and constitute therefore an important class of antineoplastic compounds.

3.1.- 15d-PGJ_2 arrests the cell cycle at G_2/M phase.

Based on the commented mitochondrial alterations observed in response to treatment of MCF-7 cells with 15d-PGJ_2, we reasoned that 15d-PGJ_2 could be causing disruption of the microtubule network. It is well documented that MT inhibitors arrest cells in G_2/M phase and induce therefore cell death. Thus, if 15d-PGJ_2 provokes significant microtubule disorganization, a concomitant effect on cell cycle should be appreciated.

To determine the effect of 15d-PGJ_2 on cell cycle, exponentially growing MCF-7 cells were treated with 15d-PGJ_2 for 24 hours and their cell cycle progression was followed by fluorescence activated cell sorting analysis. Figure 15 demonstrates that treatment with 15d-PGJ_2 led to significant accumulation of cells in the G_2/M compartment of the cell cycle, compared with non-treated control cells. On the contrary, the percentage of cells in the G_2/M cell cycle state did not differ markedly between control and MCF-7 cells treated with rosiglitazone. Nocodazole, a potent anti-microtubule agent capable of rapidly depolymerizing the MT network, was used as control. Nocodazole is known to cause microtubule disruption by binding to β-tubulin, impairing thus its incorporation in the microtubule.

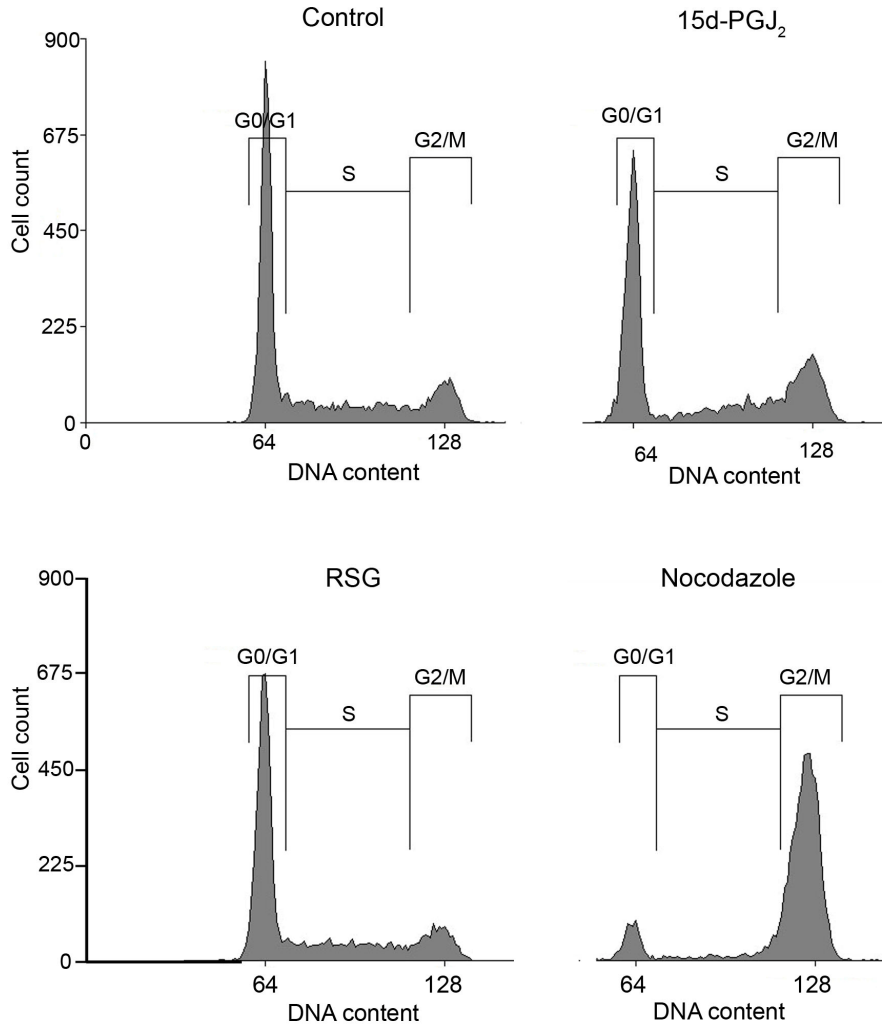

	G0/G1	S	G2/M
Control	50.33 ± 4.93	29.33 ± 0.89	18.67 ± 2.08
15d-PGJ_2	50.00 ± 6.56	14.20 ± 4.13 *	34.33 ± 4.73 *
RSG	59.76 ± 4.85	21.14 ± 3.16 *	19.66 ± 5.50
Nocodazole	6.23 ± 3.61 ***	12.26 ± 1.65 *	79.44 ± 1.81 ***

Figure 15. **Effects on cell cycle of treatment with 15d-PGJ_2 and rosiglitazone.**
Effect of 15d-PGJ_2 and rosiglitazone on cell cycle distribution of exponentially dividing MCF-7 cells. Cells were exposed to 10 μM 15d-PGJ_2, 30 μM rosiglitazone (RSG) or 1 μM nocodazole for 24 hours and analyzed by FACS. Nocodazole was used as positive control of microtubule depolymerization The numbers in the table indicate the percentage ± SD of cells in each phase of the cell cycle. Data are representative of three independent experiments. *, $P < 0.05$; *** $P < 0.001$.

3.2.- 15d-PGJ_2 disrupts the cytoskeleton network by depolymerizing microtubules.

Once verified that 15d-PGJ_2 promotes similar effects on cell cycle to those of MT inhibitors, causing arrest at G_2/M phase, we had to confirm that 15d-PGJ_2 was a real microtubule disruptor. To test this, we first examined whether 15d-PGJ_2 could directly affect the organization of the MT network of MCF-7 cells in interphase. MCF-7 cells were treated with 15d-PGJ_2, rosiglitazone, or nocodazole and the MT network was visualized by immunofluorescence after 12 hours of incubation. In control cells, the MT network exhibited normal arrangement with MT seen to traverse intricately throughout the cell and a normal compact rounded nucleus (Fig.16). In contrast, 15d-PGJ_2 treatment caused a dramatic disruption of the MCF-7 cytoskeleton, producing a diffuse MT network. These effects, which are similar to those exerted by nocodazole, were not observed after rosiglitazone treatment. The multiple-dot pericentrin pattern obtained is characteristic of certain breast cancer cell lines (Schneeweiss et al., 2003) and was corroborated by γ-tubulin staining.

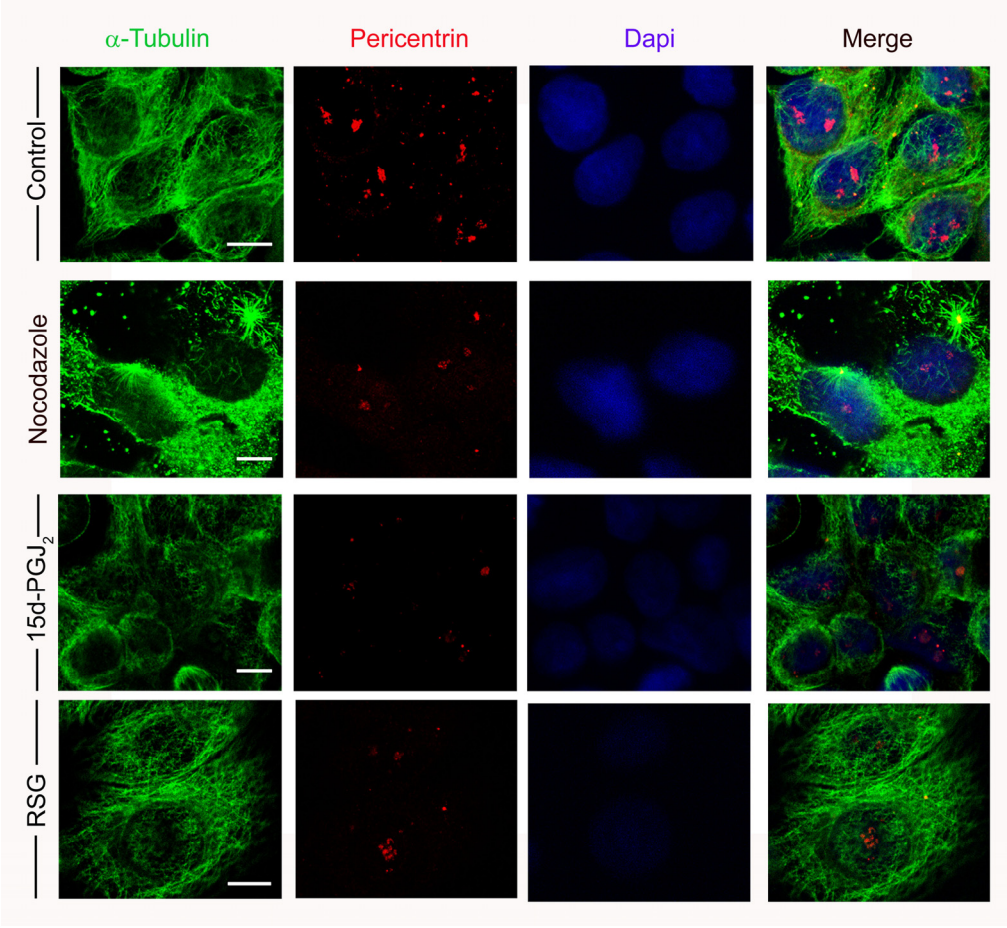

Figure 16. **Disruption of microtubules in 15d-PGJ_2-treated MCF-7 cells.**
Cells were treated for with 1 μM nocodazole, 10 μM 15d-PGJ_2 or 30 μM rosiglitazone (RSG) and stained with anti-α-tubulin and anti-pericentrin. DNA was stained with DAPI. Scale bar, 10 μm.

To further demonstrate that 15d-PGJ_2 could promote MT depolymerization *in vivo*, we assessed the fraction of free and polymerized α-tubulin in control and 15d-PGJ_2-treated MCF-7 cells, by harvesting the cells in a MT-stabilizing buffer and performing differential sedimentation. The amount of polymerized α-tubulin in the pellet fraction was significantly decreased 12 hours after treatment with 15d-PGJ_2, when compared with basal cultures (Fig. 17). In contrast, we could not observe any decrease in polymerized tubulin after treatment with rosiglitazone, in comparison with control cells.

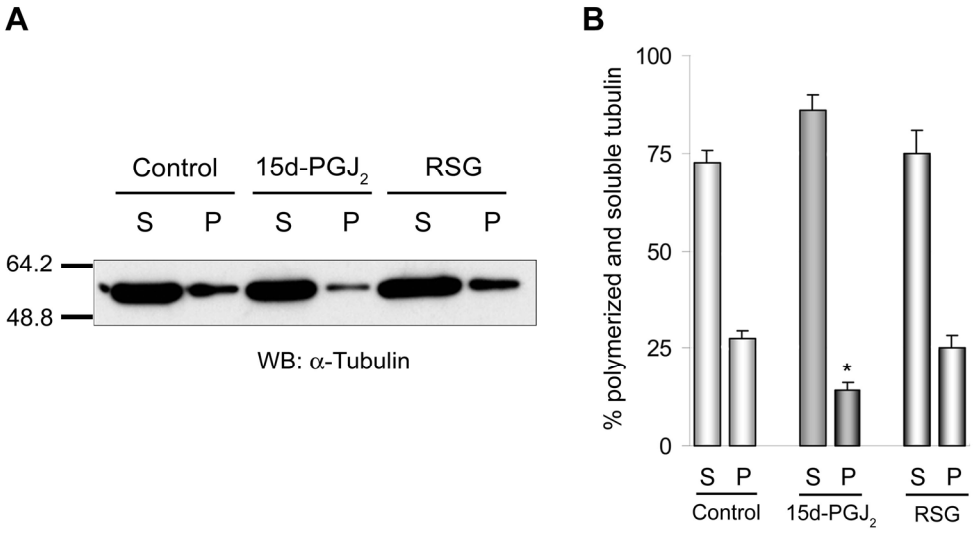

Figure 17. **Assessment of the ratio soluble/polymerized**
(A) Polymerized tubulin (P) was differentially extracted from soluble (S) tubulin in control, rosiglitazone (RSG), and 15d-PGJ_2-treated MCF-7 cell lysates prepared in a microtubule-stabilizing buffer. Soluble and polymerized tubulin fractions were then analyzed by blotting for α-tubulin. **(B)** Tubulin bands were quantified by densitometric analysis and expressed as a percentage of total tubulin levels. *, $P < 0.05$.

3.3.- Microtubule disorganization after 15d-PGJ_2 treatment results in mitotic abnormalities.

MT targeting agents arrest the cell cycle in early mitosis i.e. prometaphase/metaphase. Therefore, we investigated the effect of 15d-PGJ_2 on MCF-7 cell division by examining mitotic figures in MCF-7 cells treated or not with 15d-PGJ_2 for 24 hours, fixed and co-stained with 4,6-diamidino-2-phenylindole (DAPI) and anti-α-tubulin and anti-pericentrin antibodies to monitor DNA, mitotic spindle, and centrosomes, respectively. Cell morphology and percentage of cells at different stages of mitosis and cytokinesis were determined using confocal microscopy. Untreated cells rounded up at the beginning of mitosis and split into two symmetrical daughter cells as expected (Fig. 18).

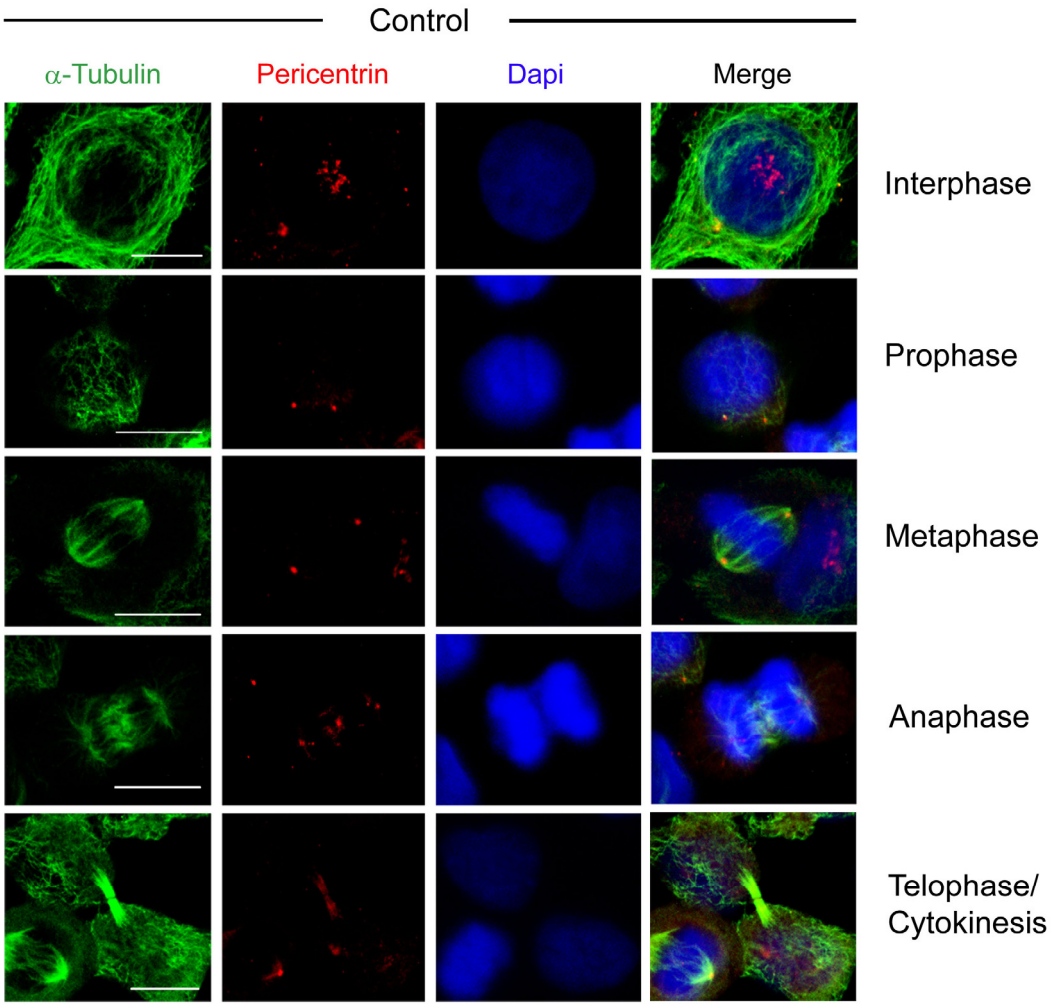

Figure 18. **Non-treated MCF-7 progression through the cell cycle.**
Shown are representative confocal images of MCF-7 cells mitotic progression. Control cells were fixed and stained with anti-α-tubulin and anti-pericentrin. DNA was stained with DAPI. Scale bar, 10 μm.

In contrast, although 15d-PGJ_2-treated cells developed spindle-like structures (Fig. 19), the MT fibers generally lack the organization observed in control cells. Also, in the cultures treated with 15d-PGJ_2, we could not detect any cell proceeding to either anaphase or telophase/cytokinesis and these cells displayed distinct signs of arrest in the metaphase stage of mitosis as the nuclear membrane has disappeared and the chromatin was condensed. The major changes, however, were the complete absence of anaphase and telophase cells and the large increase in the percentage of metaphase cells exhibiting metaphase plates with incomplete chromosome alignment, following 15d-PGJ_2 treatment. Cells with such characteristics were unable to undergo cytokinesis.

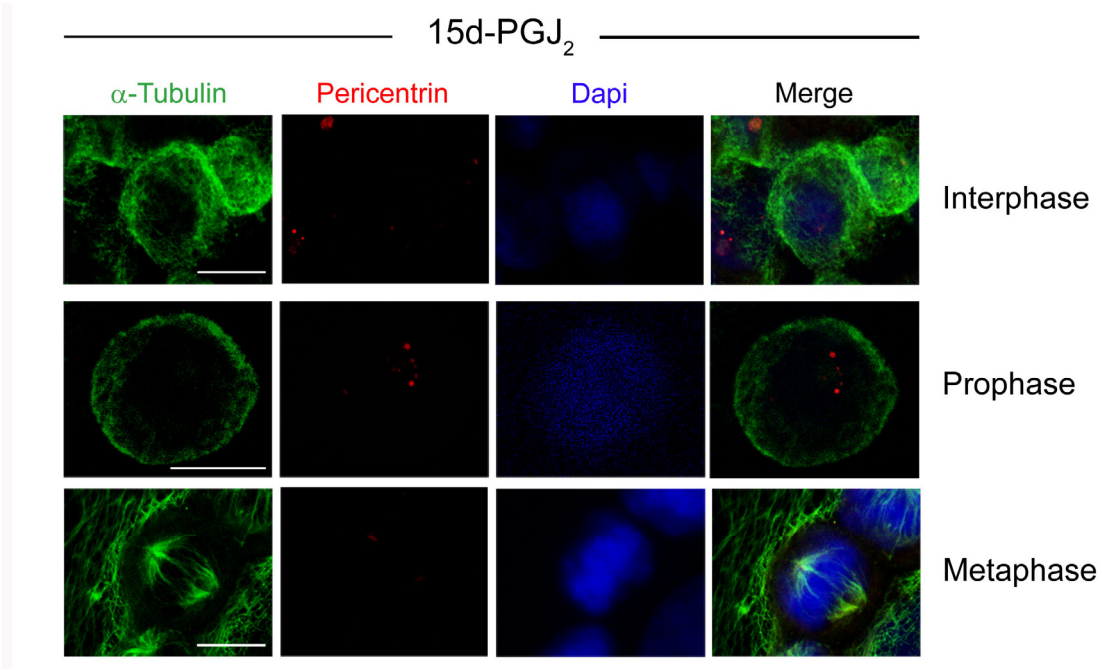

Figure 19. **Treatment of MCF-7 cells with 15d-PGJ$_2$ perturbs mitotic progression.**
Cells treated for 24 hours with 15d-PGJ$_2$ were fixed and stained with anti-α-tubulin and anti-pericentrin. DNA was stained with DAPI. Shown are representative confocal images of the mitotic progression of 15d-PGJ$_2$-treated MCF-7 cells. Scale bar, 10 μm.

The stage of mitosis at which the block occurred was further determined by counting the number of cells at each stage of mitosis. As shown in Figure 20, in the 15d-PGJ$_2$-treated MCF-7 cells, the number of cells in anaphase and telophase/cytokinesis decreased to zero, indicating a block specifically at the transition from metaphase to anaphase. These results suggest that 15d-PGJ$_2$ acts as a mitotic inhibitor, causing failure to form a stable metaphase plate, incapacity to progress through anaphase, and failure to complete cytokinesis.

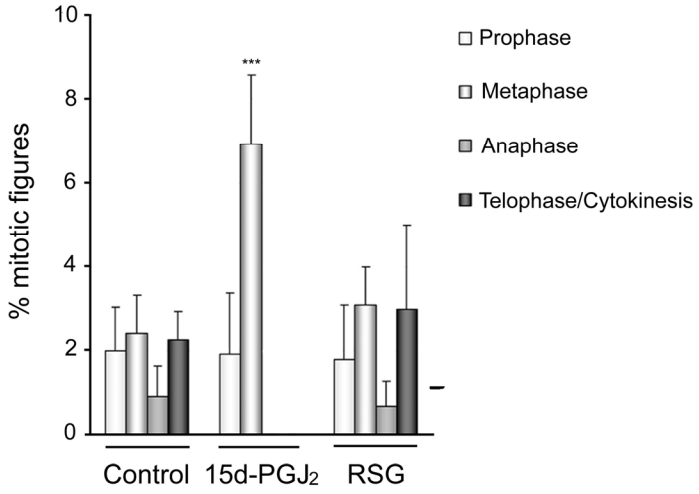

Figure 20. **Cell distribution in the different phases of the cell cycle.**
Frequency of mitotic stages in control and 15d-PGJ$_2$-treated MCF-7 cells was quantified and expressed as a percentage of total cells. ***, $P < 0.001$.

Time-lapse microscopy was utilized to characterize the fate of MCF-7 cells treated with 15d-PGJ_2 and rosiglitazone (Fig. 21 and Supplementary Videos 1-3). We have found that the majority of control non-treated cells undergo cell division within 80 to 90 min (Fig. 21 and Supplementary Video 1). Non-treated cells segregate chromosomes, proceed through anaphase, initiate furrow formation and elongate the midbodies. Eventually the cells segregate and flatten out. However, the majority of 15d-PGJ_2-treated cells took 3 hours or longer for a significant number of cells to proceed to metaphase. During that time, cells could go through the nuclear envelope breakdown but they were unable to form a stable metaphase plate with all the chromosomes aligned to it and eventually proceed to anaphase. The single prominent phenotype associated with 15d-PGJ_2 treatment was failure to complete cytokinesis. After more than 7 hours in 'metaphase-like' stage, cells shriveled and died (Fig. 21, Supplementary Video 2).

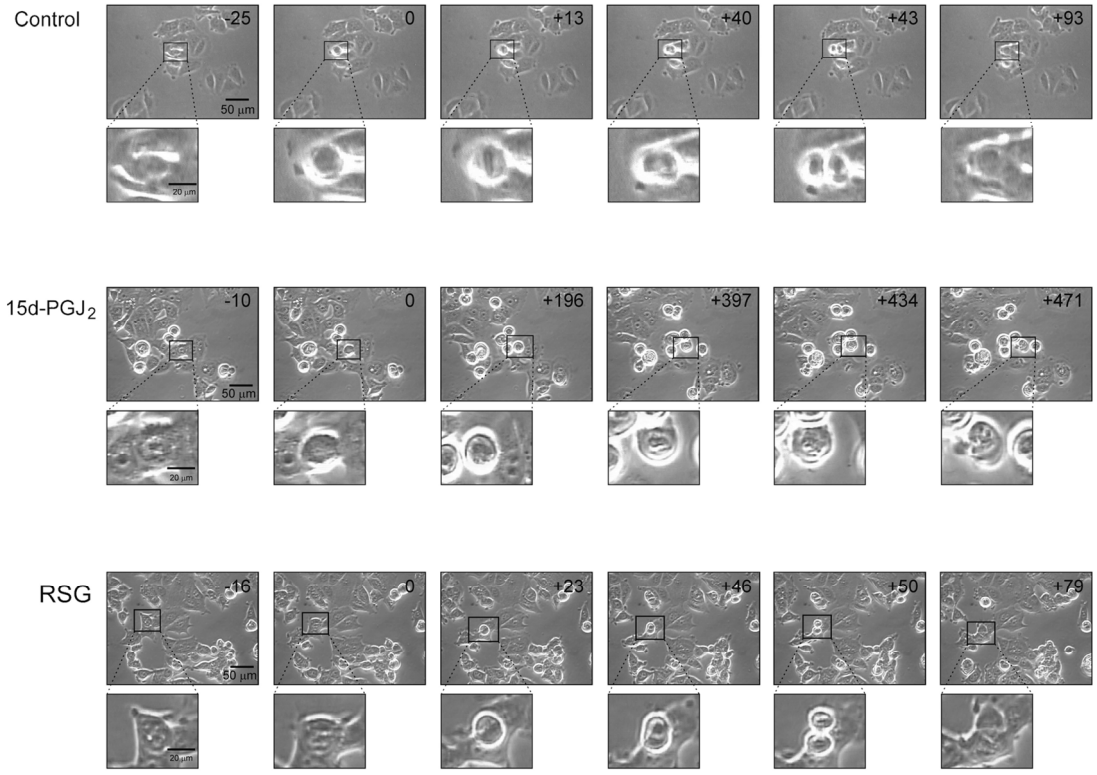

Figure 21. **Analysis of mitosis in live MCF-7 cells.**
Representative images from time-lapse analysis of live cells showing the different phases of mitosis. Time zero, shown in minutes, is the time point at which the nuclear envelope is broken down and chromatin condensation is evident, just at prophase onset. Cultures were incubated with 10 μM 15d-PGJ_2 or 30 μM rosiglitazone (RSG) and areas were subsequently followed by time-lapse microscopy. Cells treated with 15d-PGJ_2 remained in metaphase for more than 8 hours afterward they die. In contrast, non-treated and rosiglitazone-treated cells escaped mitosis after ~ 1 hour. Scale bars, 50 (lower magnification) and 10 (higher magnification) μm. Time-lapse movies for the sequential images shown in this Figure can be found in the accompanying CD.

When MCF-7 cells were treated with rosiglitazone, no significant differences in the process of mitosis were observed (Fig. 21 and Supplementary Video 3). Cells treated with rosiglitazone were able to complete mitosis within a period of time similar to the one observed for control non-treated cells. When taken together with the images shown in Figure 19, these results provide compelling evidence that treatment of MCF-7 cells with 15d-PGJ_2 results in failure of cell division through arrested metaphase.

3.4.- 15d-PGJ_2 causes microtubule depolymerization through direct binding to tubulin.

Because 15d-PGJ_2 markedly disrupted the cellular MT network, we tested whether 15d-PGJ_2 could directly affect tubulin, the main component of this network. An *in vitro* biochemical tubulin polymerization assay was carried out to investigate the activity of 15d-PGJ_2 on MT function. Results presented in Figure 22 show that 15d-PGJ_2 significantly inhibited the polymerization of tubulin, similar to the effect elicited by nocodazole, a well-known MT destabilizer. On the contrary, the addition of paclitaxel, in agreement with previous reports, favours tubulin polymerization. In contrast, rosiglitazone was found to have a negligible effect upon the polymerization of *tubulin in vitro*, relative to the vehicle control (data not shown), in agreement with its lack of effect upon the cellular MT network. This again, distinguishes the mechanism of action of both PPARγ ligands and suggests that the effects of 15d-PGJ_2 are independent of PPARγ activation. These data suggest that 15d-PGJ_2 could bind directly to tubulin and thereby prevent its polymerization and identify tubulin as a molecular target of 15d-PGJ_2.

The possibility that 15d-PGJ_2 could directly bind to, both α- and β-tubulin *in vivo* was investigated by using a biotinylated 15d-PGJ_2 derivative. To this end, we first analyzed the incorporation of biotinylated 15d-PGJ_2 into α- and β-tubulin by Neutravidin-gel pull down followed by Western blot with anti-α-tubulin or anti-β-tubulin antibodies. Figure 23 shows that α- and β-tubulin present in lysates from biotinylated 15d-PGJ_2-treated MCF-7 cells were retained on Neutravidin beads, suggesting that 15d-PGJ_2 is able to react with endogenous α- and β-tubulin in intact MCF-7 cells.

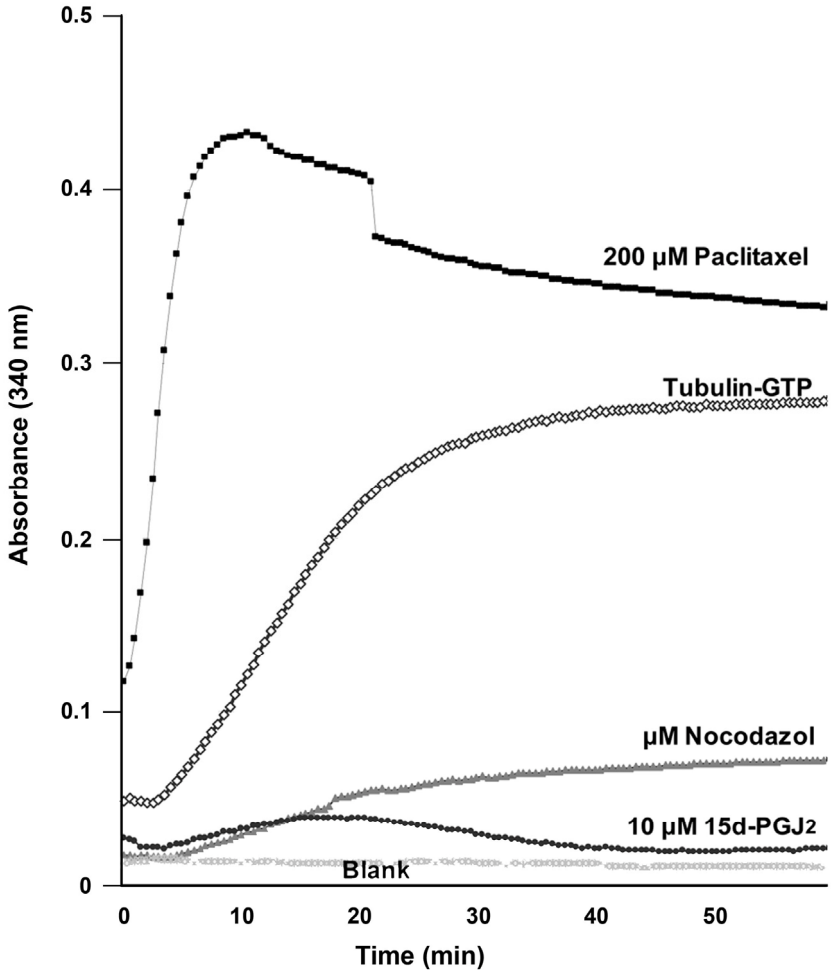

Figure 22. **Effect of 15d-PGJ$_2$ on tubulin polymerization in vitro.**
Purified bovine brain tubulin was incubated in the presence of buffer (blank), 1 µM nocodazole, 10 µM 15d-PGJ$_2$, or 200 µM paclitaxel at 37ºC, and absorbance readings were recorded at 340 nm each 30 seconds for 1 hour. Data are representative of two independent experiments performed in triplicate.

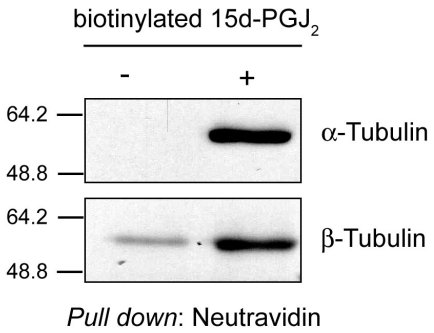

Figure 23. **Binding of biotinilated 15d-PGJ$_2$ to α- and β-tubulin *in vivo*.**
MCF-7 cells were incubated or not with biotinilated 15d-PGJ$_2$ for 2 hours and cell lysates were subjected to pull-down assays with Neutravidin-gel beads. The presence of α- and β-tubulin was assessed by Western blot analysis with specific antibodies.

To further analyze the *in vivo* association between tubulin and 15d-PGJ_2 in the living cell, we performed confocal microscopy analysis of MCF-7 cells treated or not with biotinylated 15d-PGJ_2 for 2 hours and stained with anti-α- or anti-β-tubulin. As shown in Figure 24A, a biotinylated 15d-PGJ_2 network, which colocalized with the endogenous tubulin network was clearly seen. This colocalization is also observed as the cell progresses into the cell cycle (Fig. 24B). These results further suggest a direct binding between 15d-PGJ_2 and the MT network.

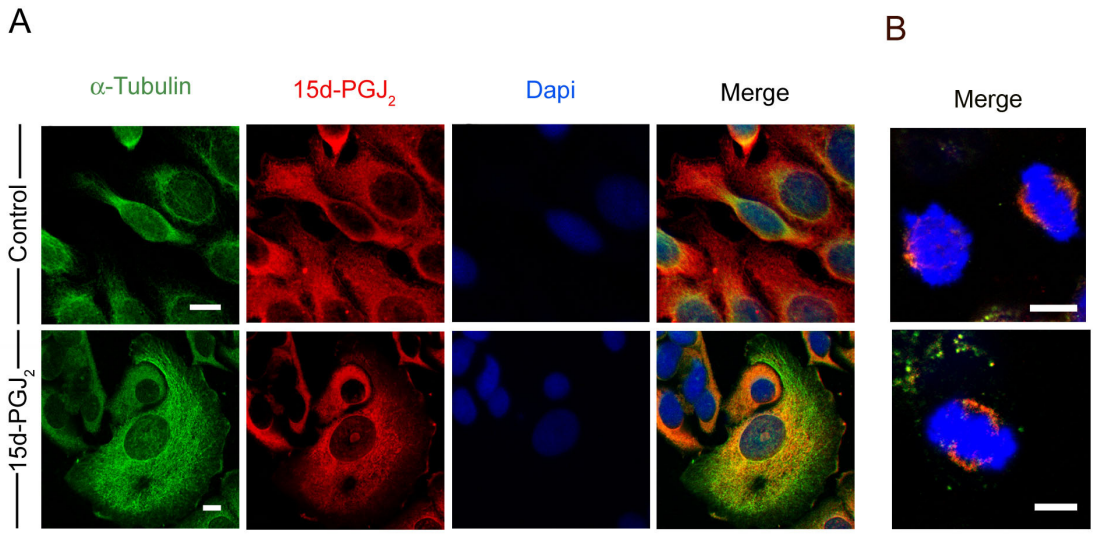

Figure 24. **Binding of biotinilated 15d-PGJ_2 to α- and β-tubulin *in vivo*.**
(A) Evaluation by confocal microscopy of binding of biotinylated 15d-PGJ_2 to MCF-7 cells. MCF-7 cells were untreated (upper panels) or treated with 15d-PGJ_2 (lower panels) for 2 hours. Scale bar, 10 μm. **(B)** Same staining as in B, showing colocalization of biotinylated 15d-PG_2 in mitotic cells. Scale bar, 20 μm.

The above results indicate that 15d-PGJ_2 binds to both α- and β-tubulin. Therefore, we next analyzed untreated and 15d-PGJ_2-treated microtubules samples by mass spectrometry (MS) to characterize the binding site(s) of 15d-PGJ_2 within tubulin. We used a recently reported approach based on hybrid triple-quadrupole mass spectrometry to find the 15d-PGJ_2-binding site(s) (Buey et al., 2007). We first made the characterization of 15d-PGJ_2 molecule by off line mass spectrometric analysis, and an ion at m/z 317.4 Da, corresponding to the monoisotopic, protonated 15d-PGJ_2 molecule, was observed (Fig. 25A). In order to find the main fragments corresponding to single or multiple cleavage sites within the 15d-PGJ_2 molecule, an enhanced product ion experiment was performed (Fig. 25B).

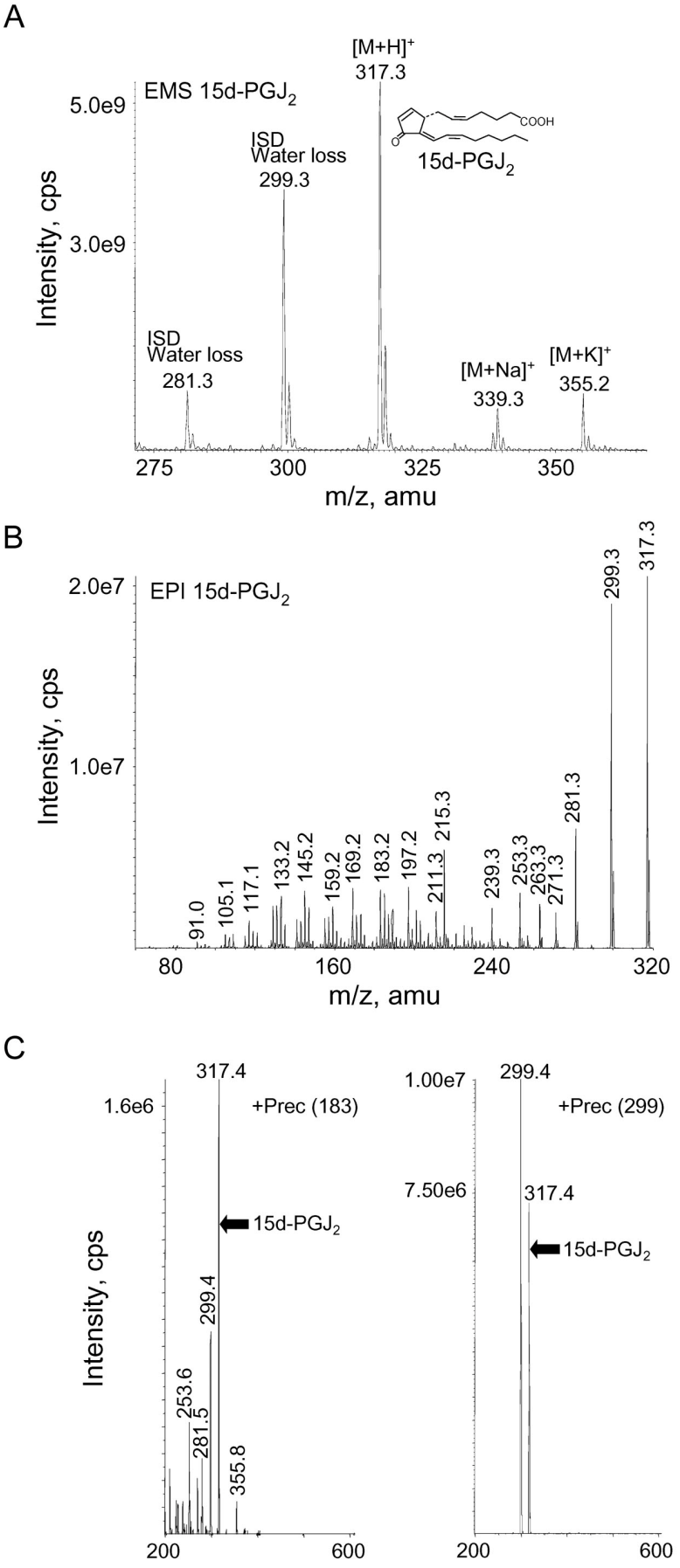

Figure 25. ***Off line*** **nanospray characterization of 15d-PGJ2 by triple quadrupole MS.**
An ion at m/z 317.3 Da, corresponding to the monoisotopic, protonated 15d-PGJ_2 molecule, was observed **(A)**. In order to find the main fragments corresponding to single or multiple cleavage sites within the 15d-PGJ_2 molecule, an enhanced product ion experiment was performed. The ion at m/z 317.3 Da was isolated and fragmented **(B)**. The most intense fragment ions were selected as potential markers for later precursor ion scanning experiments in order to find the best marker mass to select precursor ions for filtration of peptides that were tagged with 15d-PGJ_2. The fragment ion at m/z 299.4 Da was the signal of choice for precursor ion filtering experiments **(C)**. The efficiency of precursor ion scanning experiments was lower when using other fragment ions present in the MS/MS spectrum from the 15d-PGJ_2 molecule (black arrows) **(C)**.

The most intense fragment ions were selected as potential markers for later precursor ion scanning experiments. The fragment ion at m/z 299.4 Da, out of the seven tested (145.2, 169.2, 183.2, 197.2, 215.4, 281.4, and 299.4), was the signal of choice for precursor ion filtering experiments (Fig. 20C). The efficiency of precursor ion scanning experiments was lower when using the other seven fragment ions present in the MS/MS spectrum from the 15d-PGJ_2 molecule (Fig. 20C). Precursor ion scanning-MS chromatograms of trypsin-digested microtulules from untreated (Fig. 26, upper panel) or 15d-PGJ_2-treated (Fig. 26, lower panel) samples were analyzed.

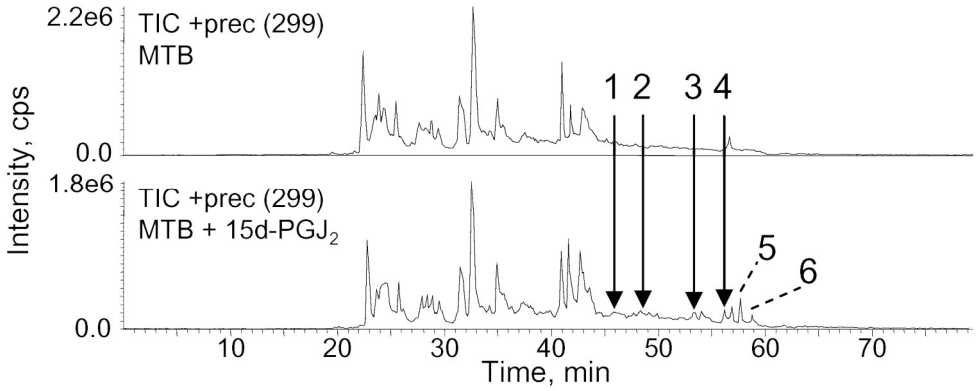

Figure 26. **MS analyses of 15d-PGJ_2 binding to microtubules.**
Total ion chromatogram (TIC) of the precursor ion scanning of fragment at m/z 299.4 from control (upper panel) or 15d-PGJ_2-treated (lower panel) microtubules samples, digested with trypsin. Arrows labelled as 1-4 indicate retention times corresponding to different peptide mass composition between control and 15d-PGJ_2-treated microtubules samples.

Although no differential, intense chromatographic peaks were found, an exhaustive mass composition chromatographic analysis revealed six time positions (1-6 in Fig. 26) along the chromatograms corresponding to differential signals producing the 15d-PGJ_2-derived fragment ion at m/z 299.4 Da. These time positions marked the elution time for differential signals tagged with 15d-PGJ_2 (Fig. 27), which were only present in the 15d-PGJ_2-treated sample, as indicated by the asterisks (Fig. 27).

MS/MS-based peptide sequencing of differential masses 1, 2, and 4 (Fig. 28) demonstrated that these sequences (353-TAVC^{PG}DIPPR-361, 300-NMMAAC^{PG}DPR-308, and 219-LTTPTYGDLNHLVSATMSGVTTC^{PG}LR-243, respectively) mapped into β-tubulin, while the sequences from differential masses 3 (312-YMACC^{PG}LLYR-320), and 5 (309-HGKYMACC^{PG}LLYR-320; one missed cleavage at K311; not shown) corresponded to α-tubulin-derived peptides (Fig. 28). A comprehensive study of the

fragmentation spectra from the parent ions corresponding to masses 1-5 revealed that in all cases the cysteine within the sequence was the 15d-PGJ_2-binding residue (superscripted PG-cysteine in text and Fig. 28). For peptides 3 and 5, only one of the two cysteine residues was modified by 15d-PGJ_2. Differential mass 6 corresponded to the unbound 15d-PGJ_2 dimer, appearing later on the chromatogram due to the highly hydrophobic nature of the molecule. In conclusion, 15d-PGJ_2 binds to tubulin through the formation of a covalent adduct with at least four cysteine residues, one in α-(cysteine 316) and three in β-tubulin (cysteine 241, 305 and 356).

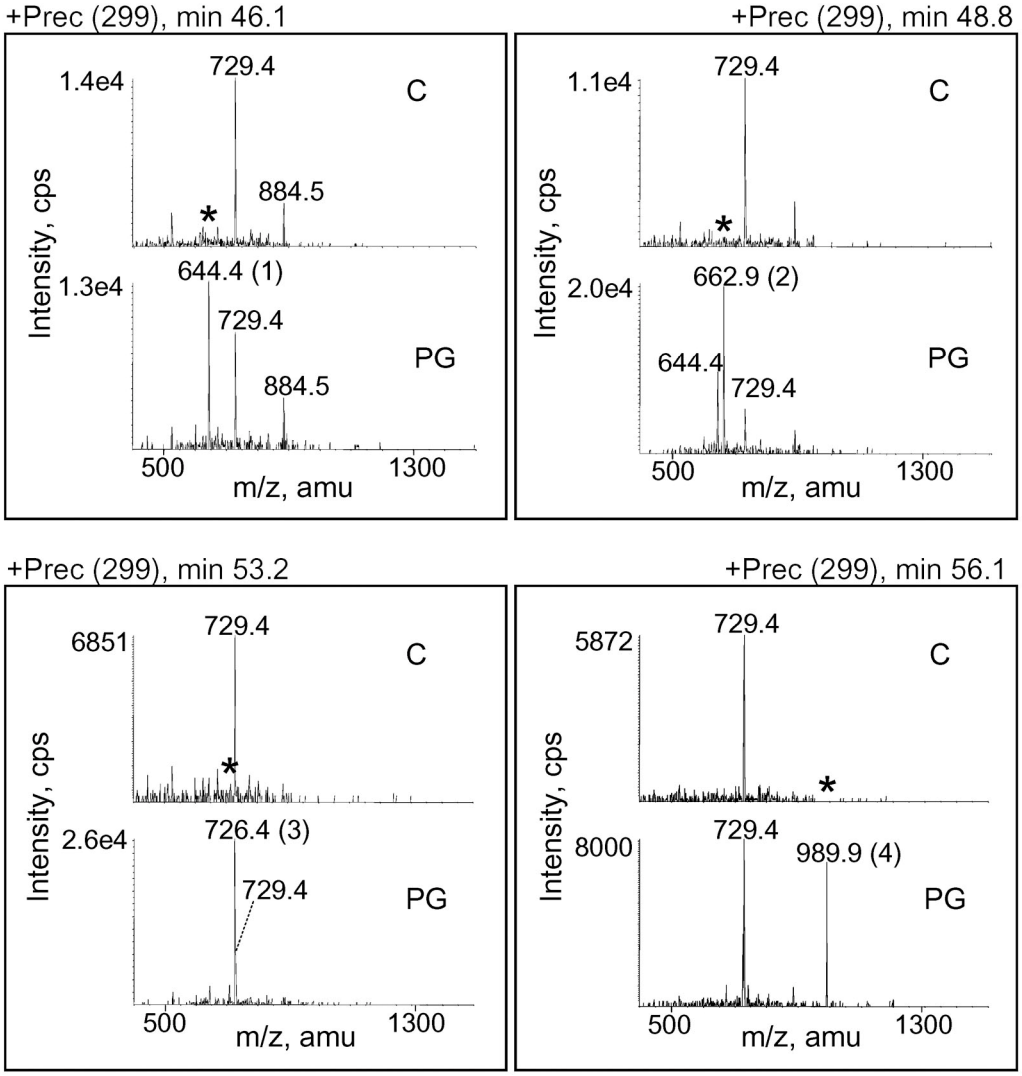

Figure 27. **Analysis of differential mass composition.**
Labels 1-4 indicate the 15d-PGJ_2-modified sequences. C means control-, and PG means 15d-PGJ_2-treated microtubules samples. Differential masses absent in the control mass spectrum are labelled as an (*). Peaks 5 and 6 correspond to differential chromatographic peaks. Peak 5 contains the peptide with sequence 309-HGKYMACC^{PG}LLYR-320 (one missed cleavage at K311). Peak 6 corresponds to the 15d-PGJ_2 dimer.

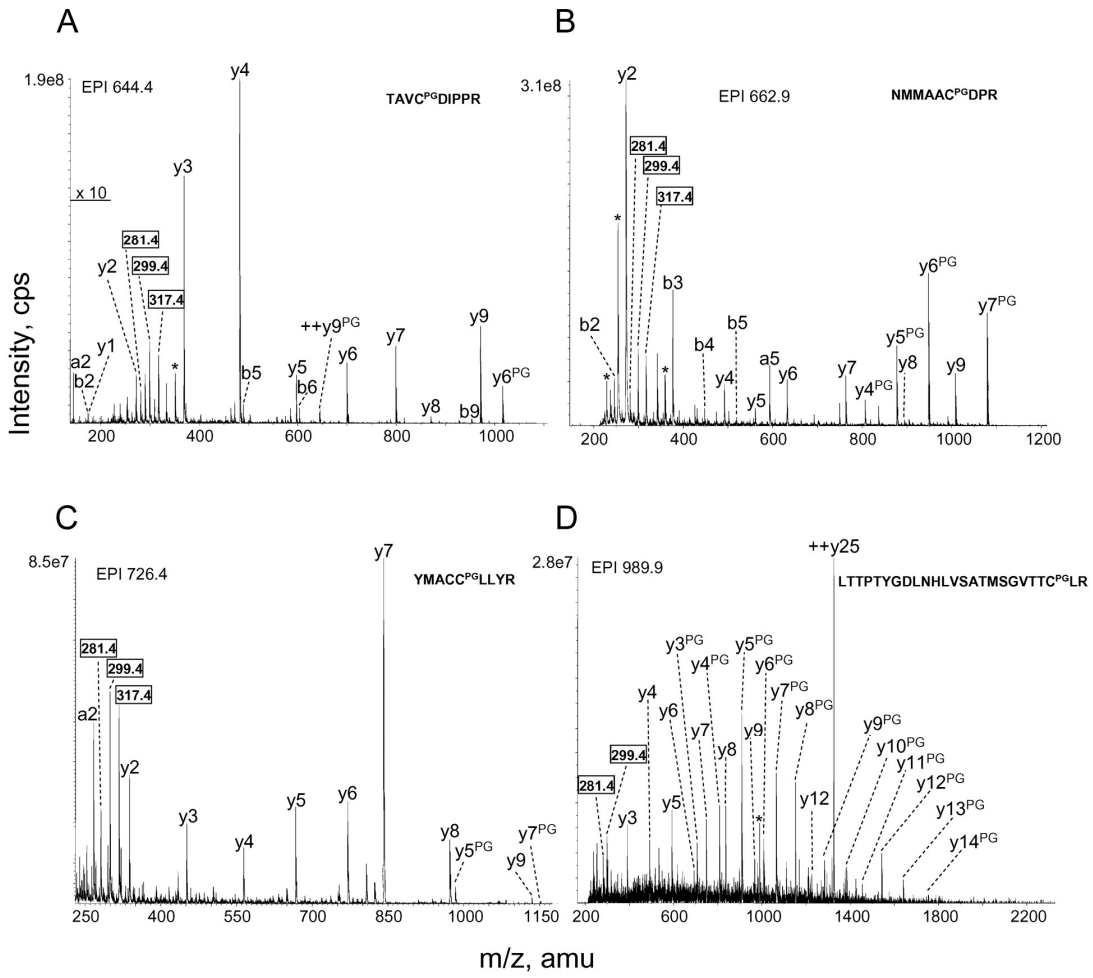

Figure 28. **Characterization of 15d-PGJ$_2$ binding site by triple quadrupole MS.**
The figure displays the main fragmentation series (carboxy, y, and amino, b, series) for the doubly-charged parent ions from peak 1-3 **(A-C, respectively)**, and for the triply-charged parent ion from peak 4 **(D)**. On each panel the corresponding peptide sequence is shown, as well as fragments containing the 15d-PGJ$_2$ (superscripted PG). Numbers in boxes (including the filtering mass at m/z 299.4 Da for the precursor ion scanning experiments) indicate masses resulting from fragmentation of the 15d-PGJ$_2$ molecule. Water loss of some fragments are marked with an (*), and some secondary fragmentation series peptides (a series) are also indicated.

These results were verified by Multiple Reaction Monitoring (MRM) experiments (Fig. 29). Ions at m/z 644.4, 662.9, 726.4, and 989.9 (corresponding to differential masses 1, 2, 3, and 4, respectively) were isolated and fragmented in untreated and 15d-PGJ$_2$-treated microtubules samples. As can be observed, only in the 15d-PGJ$_2$-treated chromatogram, the four differential, intense chromatographic peaks were detected (Fig. 29).

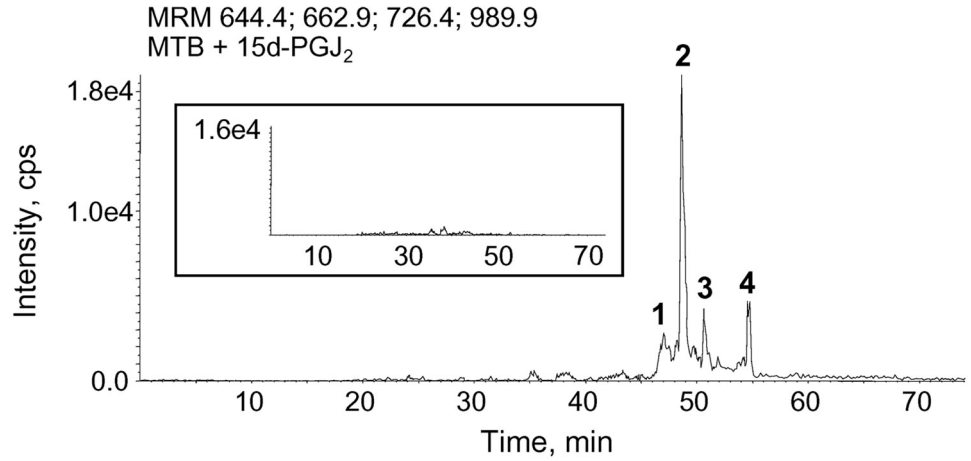

Figure 29. **MRM experiments with control and 15d-PGJ$_2$-treated microtubules samples.** MRM experiments from tryptic, 15d-PGJ$_2$-modified peptides 1-4. The inset shows the MRM results for the corresponding control microtubules sample.

4.- PPARγ LIGANDS EFFICIENTLY REDUCE HUMAN BREAST CANCER STEM CELL POPULATION.

To be considered an antitumorigenic drug, a compound must be capable of causing tumour shrinkage, an effect that is usually achieved by inhibiting tumour growth and promoting cell death processes such as apoptosis. However, the assumption of the cancer stem model has included an additional premise for a compound to be considered potently antitumorigenic: the compound must be capable of eradicating cancer stem cells. Otherwise, as these cells are able to reconstitute the whole tumour, tumour will relapse even in the case that only a single cancer stem cell survives therapy. Thus, cell death must not only be assessed in the bulk of the tumour but also in the subset of cells that constitute its stem cell population.

Ligands for PPARγ have a potent antitumorigenic capacity, as this work and others prove. However, their effect on cancer stem cells has not been tested so far. In order to evaluate the antiproliferative and proapoptotic potential on human breast cancer stem cells, we have performed an in-depth study on the outcome of the treatment of these cells with different PPARγ ligands.

4.1.- Human breast cancer cell lines contain cancer stem cells.

To this end, we first cultured human breast cancer cell lines SKBR3, MDA-MB-231, MCF-7 and T47D under non-adherent conditions in DMEM/HAM'S F12 medium supplemented with 20 ng/mL epidermal growth factor (EGF), 20 ng/mL basic fibroblast growth factor (bFGF), and B27 supplement. Under these conditions only cancer stem cells survive, whereas non-stem cells undergo a process of anoikis which results in death (Dontu et al., 2003). While cultured in this medium, cancer stem cells grow and divide, originating globular structures in the form of a condensed sphere which are commonly known as primary mammospheres and which are supposed to be enriched in progenitor cells. As Figure 30 reveals, all the cell lines tested contain cancer stem cells, as they are able to generate mammospheres. Spheres formed by MCF-7 and T47D cells are circular and condensed, whereas MDA-MB-231-derived spheres had a more irregular and less condensed morphology. SKBR3 showed a great ability to adhere to the culture dish, although cultured in ultra-low adherence-plates.

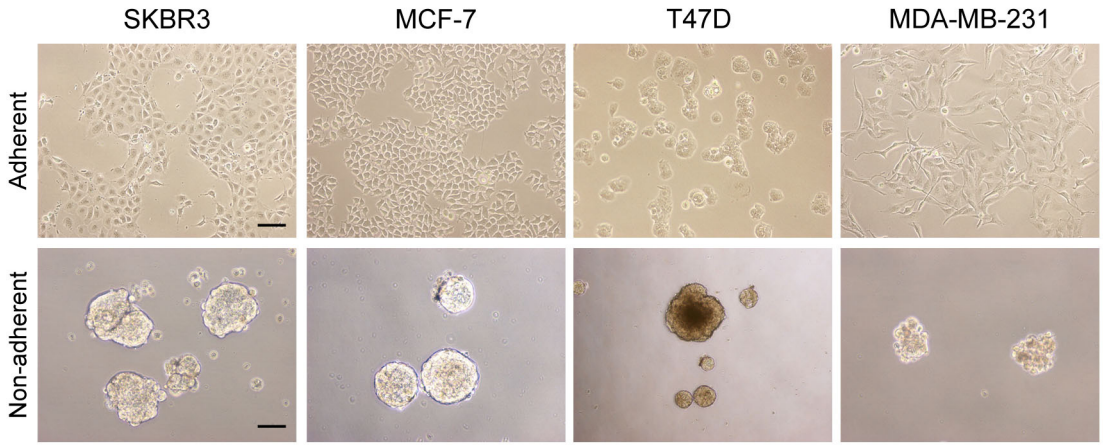

Figure 30. C**ultures of breast cancer cell lines.**
Shown are representative images of SKBR3, MCF-7, T47D and MDA-MB-231 cell lines cultured under adherent conditions (upper panels) and under non-adherent conditions as mammospheres (lower panels). Scale bar, 25 μM.

To evaluate the mammosphere formation frequency of each cell line, 2,000 cels/mL were seeded onto low-adherence plates and the number of spheres originated was estimated (Fig. 31). Differences in the frequency of mammosphere formation were appreciated, with ~1% of the initial MCF-7 and T47D cells originating spheres and lower percentages (~0.5%) for SKBR3 and MDA-MB-231 cell lines. This observation suggests that cancer stem cells are present in a different proportion in each cell line.

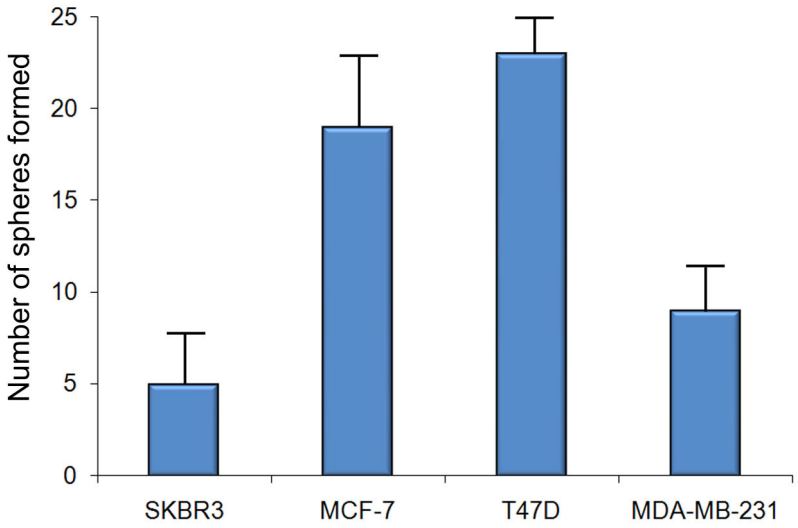

Figure 31. **Mammosphere forming-frequency in breast cancer cells.**
Two thousand viable cells from each cell line were seeded under non-adherent conditions, and the number of mammospheres formed after 5 days was counted. Results represent the mean ± SD of three independent experiments.

4.2.- PPARγ ligands dramatically reduce primary mammosphere number and size.

To directly assess the effect of PPARγ ligands in breast cancer stem cells without interferences from cells of the bulk of the tumour equal amounts of primary mammospheres originated from MCF-7 cells were treated along 12 days with 10 μM 15d-PGJ_2, 30 μM rosiglitazone and 10 μM pioglitazone respectively. As it can be observed in Figure 32, all PPARγ ligands tested caused a dramatic reduction in sphere number and size, with 15d-PGJ_2 and rosiglitazone inducing complete dissociation of the sphere and death of the cells that were forming it. A similar but milder effect is observed upon pioglitazone treatment.

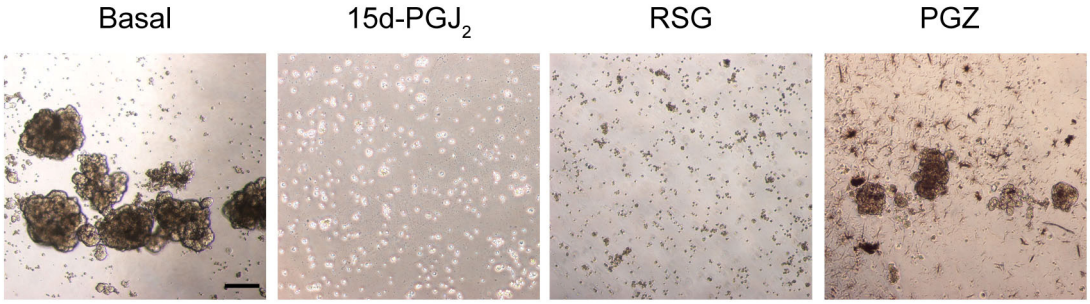

Figure 32. **Effect of PPARγ ligands on mammosphere growth.**
MCF-7-derived mammospheres were cultured for 12 days in presence or absence of 10 μM 15d-PGJ_2, 30 μM rosiglitazone (RSG) and 10 μM pioglitazone (PGZ). Images show the decrease of both mammosphere number and size in response to the different treatments. Scale bar, 200 μM.

4.3.- Treatment with PPARγ ligands impairs mammosphere self-renewal.

As commented above, antitumorigenic drugs must guarantee elimination of every cancer stem cell to avoid tumour relapse. One of the characteristics that defines cancer stem cells is their ability to self-renew, that is, to undergo asymmetric divisions that generate an identical daughter cell which is therefore a cancer stem cell, and a second more differentiated daughter cell that will form part of the bulk of the tumour. Thus, evaluation of self-renewal capacity after treatment with an antitumorigenic drug is fundamental to define its potential.

The ability of cells that constitute a primary sphere to originate a secondary mammosphere after dissociation of the former is a trait of self-renewal capacity. We used this property to assess the self-renewal capacity of mammospheres after treatment with PPARγ ligands. Mammospheres derived from MCF-7 cells were grown during 5 days in regular medium. Then, spheres were maintained in regular medium or treated with 15d-PGJ_2, RSG or PGZ for 5 days (days 6-10). A decrease in mammosphere number and size proportionally similar to that stated in the previous section was observable after 5 days of treatment (day 10). Then, medium was shifted and treatment

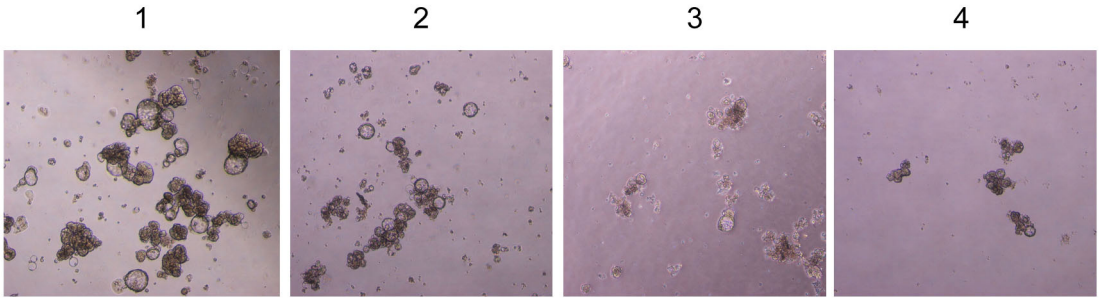

Figure 33. **Assessment of self-renewal capacity.**
Self renewal capacity mammospheres derived from MCF-7 cells grown under basal conditions (1) or treated with 10 μM pioglitazone (3). In the case of (2), spheres were cultured under basal conditions for 5 days and treated with pioglitazone during the next 5 days. Conversely was done in (4), cells were treated during the first 5 days and not treated in the following 5 days. Growth factor supplementation was performed every 2.5 days. Scale bar, 250 μM.

was added to half of the basal cultures, while treatment was maintained in half of the previously treated cultures and arrested in the other half. Spheres were allowed to grow for 5 additional days (day 10-15). Like this, we obtained cultures grown under basal conditions, cultures that had been treated only during the initial or the final period and cultures that had been treated during all the process. Figure 33 illustrates the results

obtained for spheres treated with PGZ. Images from cultures with 15d-PGJ_2 and RSG are not presented as treatment with these agents causes such a dramatic effect that no viable cell is detected after 5 days of treatment with any of these drugs. As it can be observed in the images, treatment with PGZ causes a decrease in mammosphere number and size which is dependent on the exposure time, and, more importantly, spheres treated with PGZ only during the first period are not able to self-renew and originate *de novo* more spheres than the ones which are already present.

4.4.- $CD44^{+}/CD24^{-/low}$ expression profile is a marker for basal origin but not 'stemness'.

Because recent studies have performed a parallel identification of human breast cancer stem cells and concluded that these cells can be identified by analysis of the membrane antigens CD44 and CD24, we analyzed the presence in our cultures of cells with the $CD44^{+}/CD24^{-/low}$ expression profile that had been proposed as marker of 'stemness'. Adherent cultures of SKBR3, MDA-MB-231, MCF-7 and T47D cells were stained with fluorescent antibodies recognizing human CD44 and CD24 and phenotype distribution was analyzed by flow cytometry, as it is shown in Figure 34.

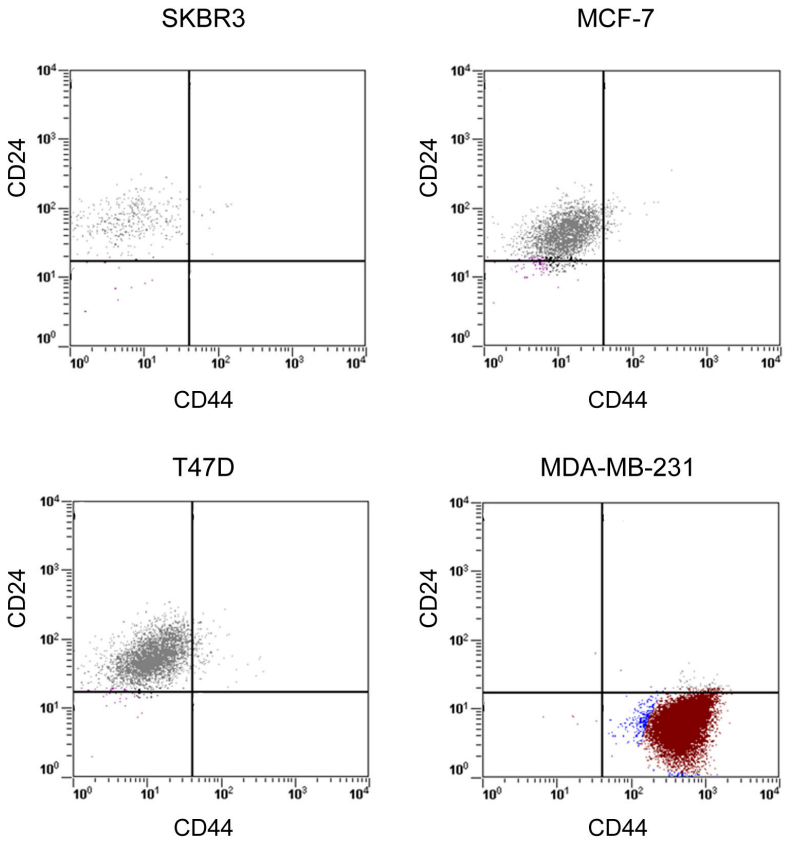

Figure 34. **Flow cytometry analysis of CD44 and CD24 expression in adherent human breast cancer cell lines.** Detection of CD44 and CD24 membrane antigens in MCF-7, SKBR3, T47D and MDA-MB-231 cell lines. Representative graphs indicative of the distribution of both markers in 4 independent experiments are shown.

As it can be observed in the table showing the phenotype distribution (Figure 35, upper panel), cells from luminal origin (MCF-7, SKBR3 and T47D) are depleted of $CD44^{+}/CD24^{-/low}$ cells, whereas cell lines from basal origin (MDA-MB-231) are almost 100% $CD44^{+}/CD24^{-/low}$. These results, together with the fact that mammosphere-forming assays had already shown that MCF-7, SKBR3 and T47D cell lines contain cancer stem cells, lead us to think that $CD44^{+}/CD24^{-/low}$ phenotype identifies cells from basal origin, instead of cells with stem properties.

ADHERENT CULTURES

(% ± SD)	SKBR3	MCF-7	T47D	MDA-MB-231
CD44-/CD24+	94.20 ± 0.16	94.88 ± 0.55	96.83 ± 0.70	0.00
CD44+/CD24+	2.67 ± 0.21	2.38 ± 0.07	2.45 ± 0.13	0.75 ± 0.55
CD44-/CD24-	3.13 ± 0.37	2.51 ± 0.25	0.71 ± 0.79	0.03 ± 0.02
CD44+/CD24-	**0.00**	**0.00**	**0.00**	**99.22 ± 0.575**

MAMMOSPHERES

(% ± SD)	SKBR3	MCF-7	T47D	MDA-MB-231
CD44-/CD24+	93.46 ± 0.47	94.93 ± 0.47	97.13 ± 0.61	0.03 ± 0.026
CD44+/CD24+	2.67 ± 0.21	2.45 ± 0.07	2.32 ± 0.31	0.70 ± 0.54
CD44-/CD24-	3.86 ± 0.33	2.60 ± 0.40	0.54 ± 0.52	0.01 ± 0.02
CD44+/CD24-	**0.00**	**0.00**	**0.00**	**99.27 ± 0.56**

Figure 35. **Frequency of $CD44^{+}/CD24^{-/low}$ population in adherent cultures and mammospheres.** Percentages of the resulting phenotypes after screening for CD44 and CD24 expression. Upper table indicates the percentages observed in adherent cultures whereas lower table refers to cultures of mammospheres. Shown are means of 3 independent experiments ± SD.

In addition, similar studies were performed in primary mammospheres derived from each of the previously mentioned cell lines. It is widely accepted that mammospheres are enriched in progenitor cells, and consequently, if breast cancer stem cells are represented by the $CD44^{+}/CD24^{-/low}$ phenotype, the proportion of cells showing this phenotype should be higher in mammospheres in comparison with adherent cultures. However, when analysis of CD44 and CD24 expression is performed in mammospheres, exactly similar phenotype distribution than in normal cultures is obtained (Figure 35, lower panel). This findings corroborate our findings that $CD44^{+}/CD24^{-/low}$ phenotype is not a marker for human breast cancer stem cells but for basal origin.

4.5.- Identification of the Side population in MCF-7 cell line.

The lack of markers to directly identify breast cancer stem cells within a cell population limits the studies of the effects of potential therapeutic agents on cancer stem cells to indirect methods such as the previously commented mammosphere culture. Nonetheless, some authors consider cells in the side population (SP) as a model for cancer stem cells, since some studies have reported higher colony-formation capacity and greater tumorigenicity *in vivo* for SP cells than for non-SP cells (Engelmann et al., 2008; Zhou et al., 2007).

In order to evaluate the effect of PPARγ ligands on the SP we first performed flow cytometry studies to detect this population. The SP is a subset of cells with the property to differentially efflux the vital dye Hoechst 33342, which exits the cell through the drug resistance transporter ABCG2. When blue and red fluorescence of Hoechst 33342 are plotted one against each other, SP appears as a tail-like structure. We used this approach to identify the SP in MCF-7 cells (Fig. 36). To ensure that this population corresponded to SP cells, a control treated with the specific inhibitor of ABCG2 fumitremorgin C (FTC) was included.

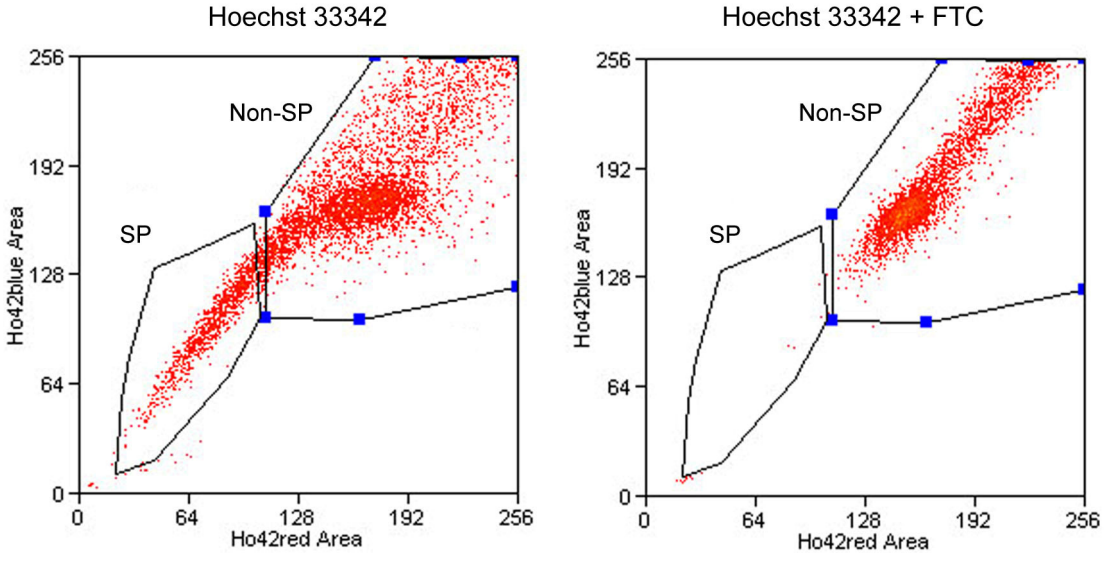

Figure 36. **Detection by flow cytometry of Side Population in MCF-7 cells.**
MCF-7 cells were stained with 5 µg/mL Hoechst 33342. SP cells differentially efflux the dye through their ABCG2 transporter and appear as a tail-like structure when Hoechst-red signal is displayed vs. Hoechst-blue signal. Control samples were added 10 µmol/mL of the ABCG2 inhibitor Fumitremorgin C (FTC).

4.6.- Side population remains unaltered upon treatment with PPARγ ligands.

Once identified the SP in MCF-7 cells we sought to evaluate alterations in this population following treatment with PPARγ ligands. MCF-7 cells were shifted to RPMI medium containing 5% stripped FBS and allowed to grow for 24 hours before addition of 10 μM 15d-PGJ_2 or 30 μM rosiglitazone. After 24 hours exposed to treatment, cells were trypsinized and incubated with 5 μg/mL Hoechst 33342 during 90 min at 37ºC previously to analysis in a MoFlo cytometre. The percentage of cells in the SP relative to the total population was determined for both basal and treated cells. As shown in Figure 37, the proportion of cells comprising the SP subpopulation remains constant upon treatment with 15d-PGJ_2 and rosiglitazone.

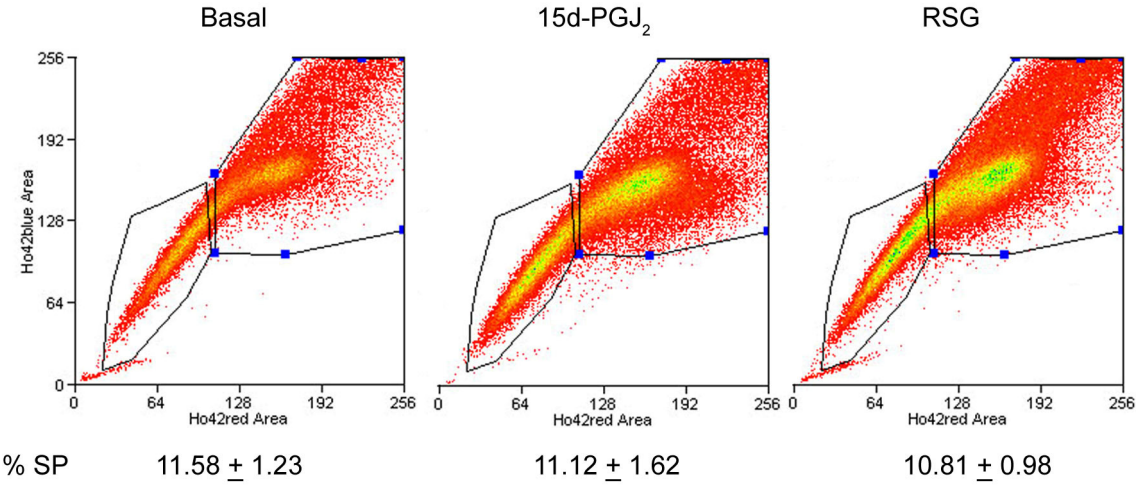

Figure 37. **Determination of changes in SP upon treatment with PPARγ ligands.**
MCF-7 cells cultured in basal conditions or treated for 24 hours with 10 μM 15d-PGJ_2 or 30 μM rosiglitazone (RSG) were subjected to flow cytometry analysis of their SP. Results indicate non-significant variability of the percentage of cells that comprise the SP in response to the different treatments.

4.7.- SP and non-SP cells show similar colony-formation efficiency *in vitro* and tumorigenicity *in vivo*.

To verify that SP fraction is enriched in cells with stem properties, we isolated the SP in MCF-7 cells as previously described. Isolation was performed in a FACS Aria SORP cytometre. Cells within the SP fraction were sorted to a low-adherent multi-well plate at the same time that a subset of cells showing a distribution distant from the SP region were isolated to be used as control non-SP cells.

Immediately after cell sorting the cells were divided in two groups. With one group colony-formation efficiency was evaluated. Both SP and non-SP cells were plated separately in low-adherent 96-well culture plates containing DMEM:Ham's F-12 medium supplemented with B27 and 20 ng/mL EGF and bFGF. Cells were plated at a density of 50 cells/well and allowed to growth indefinitely with medium and supplement refreshment each 2.5 days. As it is shown in Figure 38, both SP and non-SP cells give rise to mammospheres. In fact, the number of mammospheres originated from non-SP cells was similar to that derived from SP cells, indicating thus that SP fraction in MCF-7 cells is not enriched in cells with stem properties.

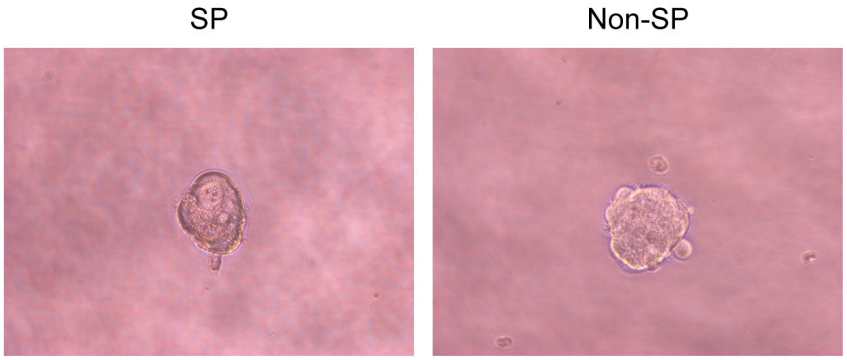

Figure 38. **Mammosphere-forming potential of SP and Non-SP cells.**
MCF-7 cells stained with Hoechst 33342 were analyzed by flow cytometry to determine the SP region. Both cells in the SP region and cells in a non-SP region were sorted and seeded in non-adherent plates at a density of 50 cells/well. Mammosphere formation was evaluated by direct observation. Non-SP cells, as well as SP cells, formed spheres. Images were taken 10 days after cell sorting. Scale bar, 200 μM

The second group of cells was used to assess tumorigenicity in an *in vivo* orthotopic model of breast cancer. With this aim, 200 SP or non-SP cells were injected into the fourth mammary fat pad of 6-week-old virgin nu/nu female mice (n=6) that had received oestrogen implementation before. Tumour apparition was checked daily by palpation and tumour volume was measured with a caliper thrice a week. As it can be observed in Figure 39 both SP and non-SP cells gave rise to detectable tumours at approximately 15 days after inoculation, and tumour burden followed a similar progression in both groups, indicating similar tumorigenicity *in vivo* for SP and non-SP cells.

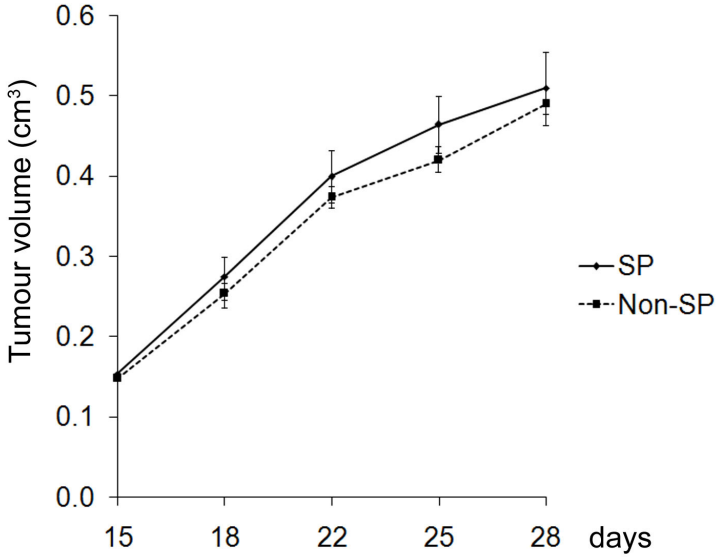

Figure 39. ***In vivo* tumorigenicity of SP and non-SP cells.**
Measurement of tumour burden in nu/nu female mice inoculated orthotopically with SP or non-SP human breast cancer cells. Results show means value ± SD.

Altogether, these results indicate that PPARγ ligands significantly reduce growth and self-renewal of breast cancer stem cells. At the same time our findings disqualify screening for the $CD44^{+}/CD24^{-/low}$ phenotype and SP sorting as methods for direct isolation of cancer stem cells, at least in the cell lines analyzed in this study.

DISCUSSION

DISCUSSION

Cancer is a multifactorial disease resulting from deregulation of cell proliferation and cell death; two processes strictly regulated as they constitute the basis for the correct tissue architecture and physiology, and, therefore, for the adequate performance of an organism. Under normal circumstances this balance is maintained by processes of opposing outcome, such as proliferation, differentiation and programmed cell death. However, when cells escape the control of mitogenic signals and become capable of growing independently, are incapable of evolving towards a differentiated phenotype or avoid apoptotic processes, the equilibrium is disrupted and the cell behaves no more as part of an organism but as an individual, giving rise to the apparition of a tumour.

Currently, cancer is the second leading cause of death after cardiovascular disease. Thus, the discover of therapies that efficiently suppress tumour growth or cause its complete involution is a main objective in the actual medical horizon. During the last years PPARγ ligands have been shown not only to be effective in the treatment of type II diabetes or inflammation, but also to have a potent anti-tumorigenic effect in several types of carcinomas. Nowadays, it is widely accepted that activation of the receptor PPARγ inhibits tumour cell growth, promotes differentiation and induces apoptosis. The anti-tumoral effects of PPARγ ligands are exerted not only through activation of this receptor but also as a result of interactions with other proteins within the cell.

Our work has focused on the elucidation of the antitumorigenic effects and mechanism of action of PPARγ ligands in human breast cancer cells, both in the bulk population of the tumour and in the cancer stem cell subset.

1.- EFFECT OF PPARγ LIGANDS ON THE GROWTH OF HUMAN MAMMARY CANCER CELLS.

Previous studies from our lab indicated that PPARγ ligands exert antiproliferative and proapoptotic effects on human breast cancer cells (Pignatelli et al., 2003; Pignatelli et al., 2001; Pignatelli et al., 2005). To further corroborate this we have performed a complete study on cell viability, proliferation and apoptosis with three PPARγ ligands of known antineoplastic capacity: 15-deoxi-$\Delta^{12,14}$-PGJ_2 (15d-PGJ_2), rosiglitazone (RSG) and pioglitazone (PGZ).

In agreement with previous data, 15d-PGJ_2, rosiglitazone and pioglitazone cause a reduction in viability of SKBR3, MCF-7, T47D and MDA-MB-231 cells. However, the extent of the effect on cell viability varies along these PPARγ ligands. Thus, 15d-PGJ_2 provokes drastic levels of cell death rapidly, whereas the effects of rosiglitazone and pioglitazone, although significant, are not so pronounced at short times. This raises the possibility that each agonist is acting through different mechanisms. In fact, 15d-PGJ_2 has been reported to induce cell death through pleiotropic mechanisms (Pignatelli et al., 2005), in which PPARγ activation is not a compulsory requirement (Clay et al., 2002). In addition, reduced cell viability after treatment with PPARγ ligands is accompanied by decreased cell proliferation and increased apoptosis of breast cancer cells. Similar effects have been reported after treatment with this compounds in a wide range of cell types, including prostate carcinoma, colon carcinoma, lung cancer and glioma (Grommes et al., 2004).

Moreover, our work identifies members of the thiadiazolidinones (TDZDs) family of compounds, such as TDZD-8 and NP031122 as compounds with antitumorigenic activity in breast cancer cells. Treatment of human breast cancer cells with these agents caused a reduction in cell proliferation, viability and clonogenicity. Moreover, our data suggest that these effects could be mediated by PPARγ activation, since our results demonstrate that TDZD-8 efficiently activates transcription of a PPARγ-response construct. This is in agreement with previous data from our laboratory indicating that TDZDs effects are mediated by PPARγ (Luna-Medina et al., 2005; Luna-Medina et al., 2007). Interestingly, several members of the TDZD family had been reported to date to exert cytoprotective effects in brain tissue, and thus our findings indicate that these compounds exert different effects in normal and cancer cells. Accordingly, recent evidence indicate that TDZD-8 is a potent inductor of cell death in leukaemia stem cells, with significant cell death observed as soon as 2 hours after addition of TDZD-8. Taking into account that these compounds are known inhibitors of GSK-3β, our findings open the possibility of an alternative mechanism of action of the members of the family of the TDZDs mediated by PPARγ instead of, or in cooperation with, inhibition of GSK-3β.

2.- BLOCKADE OF PROLIFERATIVE SIGNAL TRANSDUCTION PATHWAYS TRIGGERED BY ErbB RECEPTORS.

Our work identifies SHP-1 phosphatase as an effector of ErbB receptors dephosphorylation in response to 15d-PGJ_2 treatment in breast cancer cells. Previous studies of our laboratory indicate that dephosphorylation of ErbB2 and ErbB3 causes their inactivation and subsequent blockade of MAPK and PI3K pathways, leading to a reduction in cell survival and proliferation (Pignatelli et al., 2001). In agreement with this, SHP-1 has been shown to have a negative role in regulating proliferation of several types of cancers. Thus, knock-out mice lacking expression of SHP-1 show hyperproliferation of hematopoietic cells in response to growth factor stimulation. Moreover, SHP1 protein is decreased in most of the highly aggressive lymphoma and leukaemia cell lines (Oka et al., 2001). Together, these findings strongly suggest a negative regulatory role for SHP-1 in cell proliferation induced by growth factors.

Moreover, SHP-1 has been previously implicated as a negative mediator in receptor tyrosine kinase signalling pathways. Among others, SHP-1 has been previously reported to negatively regulate C-kit (Paulson et al., 1996), colony-stimulating factor-1 receptor (Chen et al., 1996) and Lck (Lorenz et al., 1996) and cytokine receptors such as erythropoietin receptor (Klingmuller et al., 1995) and interleukin-3-receptor (Yi et al., 1993). In fact, SHP-1 is known to interact and dephosphorylate EGFR signalling pathway in several cancer cell lines, including MCF-7 cells (Tomic et al., 1995). SHP-1 binds EGFR via its two SH2 domains and dephosphorylates the receptor (Tenev et al., 1997). EGFR, in turn, is capable of phosphorylating SHP-1 increasing its activity and promoting its recruitment to the receptor (Keilhack et al., 1998). Interestingly, although SHP-1 has been reported to interact with EGFR in MCF-7 cells and results from other groups point to a close relationship between EGFR and SHP-1, no changes in EGFR phosphorylation were observable upon treatment with 15d-PGJ_2 (Pignatelli et al., 2001). However, EGFR is not the only member of the ErbB family that has been related with SHP-1. SHP-1 has also been found to be capable of binding to a chimeric ErbB2 receptor *in vitro* (Vogel et al., 1993). Moreover, SHP-1 dephosphorylates the chimeric ErbB2. With regard to this, our data indicate association of SHP-1 with both ErbB2 and ErbB3, although immunoprecipitation studies indicate that the amount of phosphatase bound to each receptor remains unaltered after 15d-PGJ_2 treatment.

Although no changes in total SHP-1 protein or mRNA content were observable upon 15d-PGJ_2 treatment, a shift in the electrophoretic mobility of the protein occurred. This shift was confirmed by immunoprecipitation studies to be caused by phosphorylation of the phosphatase. SHP-1 becomes active upon tyrosine phosphorylation by several receptors. The insulin receptor, for example, phosphorylates SHP-1 on Tyr536 (Uchida et al., 1994) and nerve growth factor receptor, Lck and Src are also able to phosphorylate SHP-1, leading to an increase in its activity *in vitro* (Frank et al., 2004; Vambutas et al., 1995). SHP-1 exists in a closed, autoinhibited conformation with the N-terminal SH2 domain occupying the catalytic region of the phosphase. Binding of the C-terminal SH2 domain to a phosphotyrosine residue in the target protein together with phosphoylation of the phosphatase induces a conformational change in SHP-1 that results in the release of the autoinhibition (Yang et al., 2003). Two major phosphorylation sites at tyrosines 536 and 554 have been reported to cause SHP-1 activation. Accordingly, our data show that phosphorylation of SHP-1 in response to 15d-PGJ_2 is correlated with an increase in its phosphatase activity, that would be responsible for dephosphorylating ErbB2 and ErbB3. This statement is further supported by the fact that overexpression of SHP-1 in MCF-7 cells partially reverts ErbB2 and ErbB3 NRG-induced phosphorylation. Moreover, we report that dephosphorylation of ErbB2 in response to 15d-PGJ_2 is not completely abolished by reduction of SHP-1 protein. As we were not able to completely knock-out SHP-1 by iRNA strategy, we do not know whether this finding is due to either the activity of the remaining SHP-1 or additional tyrosine phosphatases, which could contribute to dephosphorylate ErbB2/3 in 15d-PGJ_2-treated breast cancer cells.

Interestingly, the observed increase in SHP-1 activity is not sustained in time but transient. Short-lasting signals are common regulatory mechanisms of cell signalling cascades, especially in the case of switch-on/off regulation. By being transiently activated during a short period of time, the cell obtains an on/off mechanism that allows a fast and sharp regulation of cell signaling processes. In line with this, SHP-1 is known to possess the capacity to autodephosphorylate, loosing then its activity. This could explain the limited duration of the observed increase in SHP-1 phosphorylation and activity reported in our work.

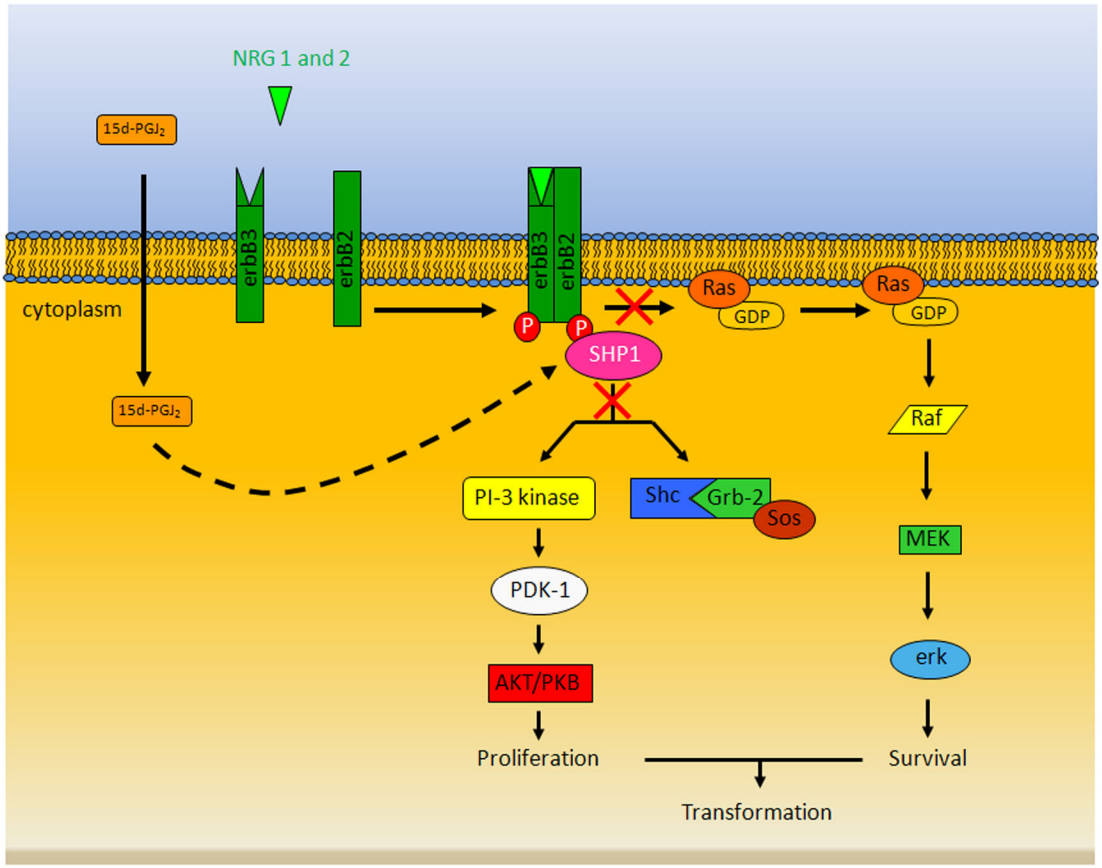

Figure 1. **Proposed action of SHP-1 on ErbB2/ErbB3 signalling pathway.**

Our data do not clarify the biochemical mechanism by which, upon treatment with 15d-PGJ_2, SHP-1 causes dephosphorylation of ErbB2/ErbB3. Although we do not know yet whether this effect is direct or indirect via adapter proteins, studies are now in progress to specifically address this issue. Nonetheless, identification of SHP-1 as the mediator of ErbB2 and ErbB3 dephosphorylation gives a new insight in the regulation of ErbB signalling and serves as basis for an interesting discussion on ErbB signalling network. Recent studies suggest that SHP-2 could play a role in ErbB2 signalling regulation antagonizing the one we propose for SHP-1. According to these studies, SHP-2 inhibition in ErbB2-containing breast cancer cell lines abolishes mitogenic and pro-survival signalling cascades at the same time that reverts transformation (Zhou and Agazie, 2008). This would be due to active SHP-2 promoting Ras activation by blockade of its down-regulator Ras-GTPase activating protein (Ras-GAP). This opens the possibility of a possible countermeasure mechanism between SHP-1 and SHP-2 *in vivo* that would regulate the proliferative output of the cell.

These data demonstrate that responsiveness to 15d-PGJ_2 in breast cancer cells is partially mediated by SHP-1 phosphatase activity. Therefore, the effects of this prostanoid on cell proliferation and survival are dependent on SHP-1 activation status, since this determines ErbB2/ErbB3 phosphorylation and subsequent activation of PI3K and MAPK signalling pathways.

3.- INDUCTION OF MITOTIC ARREST AND CYTOSKELETON DYSRUPTION.

In this work, we also present evidence of other possible mechanism through which 15d-PGJ_2 could affect proliferation and cell death of breast cancer cells. We show that cell death induced by 15d-PGJ_2 in human MCF-7 cells is preceded by a marked G_2/M arrest. The cells also displayed morphological features that identified a mitotic arrest, specifically in metaphase. Our studies also show that 15d-PGJ_2 binds to microtubules, forming a covalent bond with several cysteine residues in α- and β-tubulin. Overall these results point to a role of 15d-PGJ_2 in breast cancer cells independent of PPARγ activation and involving a direct binding to tubulin and posterior disruption of microtubules. This idea is further substantiated by the fact that these effects are not observed in rosiglitazone-treated MCF-7 cells.

We have previously demonstrated that 15d-PGJ_2 inhibits proliferation and induces cellular differentiation and apoptosis in the breast cancer cell line MCF-7, in part by blocking the ErbB receptor signalling pathway (Pignatelli et al., 2001) and by inducing early mitochondrial alterations (Pignatelli et al., 2005). Our results suggest that the effects of 15d-PGJ_2 can be both dependent and independent of PPARγ activation (Martinez et al., 2005; Pignatelli et al., 2003; Pignatelli et al., 2005). This is in accordance with the description by other groups of PPARγ-independent pleiotropic effects of 15d-PGJ_2 responsible for its antiproliferative activity (Chaffer et al., 2006; Kim et al., 2008). Although 15d-PGJ_2 is a potent PPARγ activator, an important part of the effects exerted by this compound have been proved to be independent of the activation of PPARγ. Thus, 15d-PGJ_2 has been shown, for example, to induce apoptosis of breast cancer cells (Clay et al., 2002) and inhibit microglial activation (Phulwani et al., 2006) independently of PPARγ. Our data also indicated a possible involvement of the cytoskeleton in the antiproliferative effect of 15d-PGJ_2 (Pignatelli et al., 2005).

Consistent with this idea, in this study we demonstrate that 15d-PGJ_2 treatment of MCF-7 cells causes extensive microtubule (MT) depolymerization and disruption of the MT network in interphase cells, similar to the one observed in cells treated with nocodazole. This effect is probably due to the observed *in vitro* and *in vivo* binding of 15d-PGJ_2 to, both α- and β-tubulin subunits.

Our work reveals that 15d-PGJ_2 profoundly affects cell division, since treatment with this prostanoid alters the centrosome pattern of MCF-7 cells. Centrosomes abnormalities are hallmarks of various cancers and are found in essentially all high-grade cancers and in cell lines derived from tumors (Badano et al., 2005; Pihan et al., 1998; Pihan et al., 2001; Sankaran and Parvin, 2006; Schneeweiss et al., 2003; Srsen and Merdes, 2006). These anomalies are usually associated with an increase in pericentrin staining and the appearance of clusters of pericentrin staining material, which may represent multiple centrosomes clumped together at a single pole or an inappropriate accumulation of pericentrin. On the contrary, non-tumor tissues present a low level of diffuse staining, probably reflecting the modest level of cytoplasmic pericentrin present in normal cells, or a single discrete focus of pericentrin (Pihan et al., 1998). Our results show that, in the presence of 15d-PGJ_2, MCF-7 cells exhibited fewer pericentrin foci and pericentrin staining was considerable lower than in non-treated cells. Also, the abnormal large aggregates of pericentrin seen in control MCF-7 cells, were not observed in 15d-PGJ_2-treated cells, indicative of a less transformed phenotype.

Our findings also show arrest of 15d-PGJ_2-treated MCF-7 cells in G_2/M phase of the cell cycle. This ability of 15d-PGJ_2 to block MCF-7 cells in G_2/M phase is consistent with a disruption of cytoskeleton via binding to tubulin (Schneider et al., 2003). Among novel drugs for the treatment of breast cancer are those that target microtubules. These drugs suppress MT dynamics and trigger mitotic arrest at the metaphase/anaphase transition (Jordan, 2002; Wilson and Jordan, 1995). In the presence of these drugs, spindle form and mitosis can progress as far as the metaphase/anaphase transition. However, the spindles are unable to pass the mitotic checkpoint and to initiate anaphase, or do so only after a long period of mitotic arrest. In agreement with this, our results show that 15d-PGJ_2 completely blocks the transition to anaphase. Only a few cells appear to enter the anaphase state but they are unable to complete the segregation of the chromosomes and eventually return to a "metaphase-like" stage afterward they die.

Regarding this point, there is compelling evidence indicating that mitotic arrest caused by tubulin-binding agents such as paclitaxel and the *vinca* alkaloids is frequently found to precede apoptosis of cancer cells (Jordan, 2002; Lin et al., 1998). Thus, the hypothesis that arrest of the cell cycle at mitosis is the primary stimulus for apoptosis has been widely accepted. For example, apoptosis induced by paclitaxel was found to occur directly after a mitotic arrest or after an aberrant mitotic exit (Jordan et al., 1996; Woods et al., 1995). Nevertheless, some investigators have provided evidence against the involvement of mitotic arrest in apoptosis induction by microtubule-binding agents by demonstrating apoptotic events in other phases of the cell cycle (Huang et al., 2000; Miller et al., 1999). Apoptosis is not the only mechanism by which cells die following a failed mitosis. Many studies have described a form of cell death called mitotic catastrophe. This form of cell death does not require caspase 9 or 3 and can still occur in the presence of caspase inhibitors such as z-VAD-fmk. In this regard, previous work from our laboratory have shown that the cell death induced by 15d-PGJ_2 in breast cancer cells cannot be completely inhibited by treatment with this caspase inhibitor, albeit caspases are activated in MCF-7 cells treated with this prostaglandin (Pignatelli et al., 2005). On the other hand, we could not observe any of the common features attributed to mitotic catastrophe, such as giant non-viable multinucleated cells. 15d-PGJ_2-arrested mitotic MCF-7 cells appear to remain arrested in metaphase from which they subsequently entered a cell death pathway without exiting mitosis. This phenomenon has been previously shown in endothelial cells treated with the tubulin-binding agent combretastin A-4-phosphate (Kanthou et al., 2004; Nabha et al., 2002). These authors have shown that combretastin A-4-phosphate damages mitotic spindles, arrests cells at metaphase, and leads to the death of endothelial mitotic cells with characteristic G_2/M DNA content.

Furthermore, our results obtained from mass spectrometry (MS) analyses demonstrated that 15d-PGJ_2 binds covalently to tubulin and that this binding is the cause of microtubule depolymerization in 15d-PGJ_2-treated MCF-7 cells. Our findings show that 15d-PGJ_2 binds covalently to at least, four cysteine residues into the α- and β-tubulin moieties, as detected by MS. 15d-PGJ_2 is characterized by the presence of a cyclopentenone ring containing an electrophilic carbon (C9), and an electrophilic unsaturated carbonyl group (C13) next to the cyclopentenone ring. These two reactive

centers can react covalently by means of Michael's addition reaction with nucleophiles, such as the cysteinyl thiol groups in proteins, to form a covalent adduct which is thought to be irreversible under physiological conditions. Some examples of 15d-PGJ_2 Michael's addition to cysteine residues include PPARγ (reactive carbon at position 13) and NF-κB (reactive carbon at position 9) proteins (Kim and Surh, 2006).

Tubulin is a heterodimeric protein containing 20 cysteine residues, of which twelve are in the α subunit and eight in the β subunit. Five of these cysteines have been characterized as highly reactive (Britto et al., 2002). We have shown here that, at least four of them react with 15d-PGJ_2. Cysteine 305 from β-tubulin is located on the surface of the MT near the pore, and probably does not have any effect on MT stability. In contrast, cysteines 241 and 356 are located at the inner face, between the GTP and the taxol binding sites, and the binding of 15d-PGJ_2 to these residues could alter the normal curvature of the heterodimer, inducing MT depolymerization. In addition, cysteine 316 from α-tubulin is located in the interphase between an α-subunit and a β-subunit, and, consequently, it is very likely that 15d-PGJ_2-binding to this residue could also interfere in the microtubule assembly. Thus, covalent binding of 15d-PGJ_2 to cysteine residues in microtubules is probably the cause of the observed microtubules depolymerization.

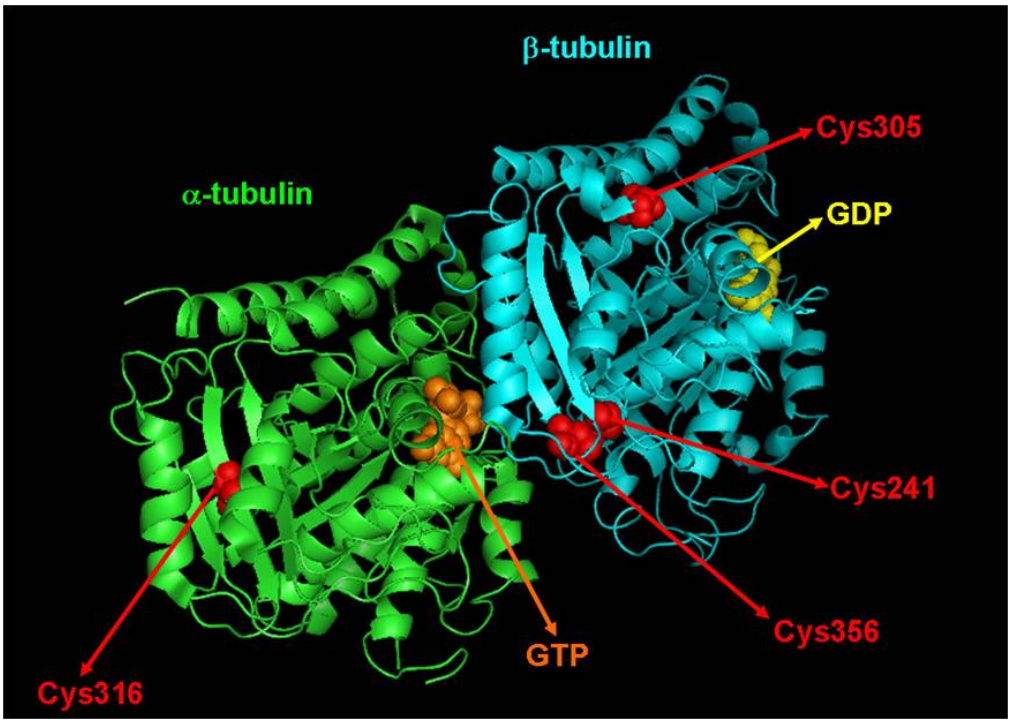

Figure 2. **Identified binding sites for 15-deoxi-$\Delta^{12,14}$-PGJ_2 in α- and β-tubulin.**

Summarizing these data, the described effects of 15d-PGJ_2 on cytoskeleton add a new anti-tumoral role for 15d-PGJ_2 based on the ability to directly binding to cysteine residues in α- and β-tubulin independently of PPARγ. As a consequence, 15d-PGJ_2 disrupts the MT structure in the cytoplasm of interphase cells and the spindle apparatus of mitotic cells leading to a mitotic arrest at the metaphase/anaphase transition, an accumulation of cells in G_2/M phase, and ultimately breast cancer cell death.

4.- EFFECT OF PPARγ LIGANDS ON HUMAN BREAST CANCER STEM CELLS.

Cancer stem cells (CSCs) have been recently identified in leukaemia, and they are intensively searched in different solid tumours. The culture under non-adherent conditions and the utilization of cell surface expression markers has made possible their isolation from brain tissue, and therefore this strategy is being used for prospective isolation from other tissues such as breast, colon or pancreas, where neither the surface antigens nor the expression pattern characterizing the subset of CSCs have been well defined yet.

Our results indicate that all of the four cell lines tested (SKBR3, MCF-7, T47D and MDA-MB-231) were able to form mammospheres when grown under non-adherent conditions. Non-adherent culture is a widely accepted method to determine the existence of stem cells in mammary tissues. Strong evidence support that single stem cells from normal human mammary tissue, when grown under non-adherent conditions, originate spheres capable of generating the three lineages that constitute the tissues in the mammary gland: myoepithelial, luminal and acinar (Dontu et al., 2003). This property of mammary stem cells to originate spheres is not restricted to normal stem cells, but shared with cancer stem cells (Fillmore and Kuperwasser, 2008). Consequently, the fact that all cell lines give rise to the formation of mammospheres implies that cancer stem cells exists in SKBR3, MCF-7, T47D and MDA-MB-231 cell lines. Considering the number of spheres generated with the number of cells cultured, we conclude that cancer stem cells in these cell lines constitute approximately ≤1% of total population, even though frequency varies depending on the cell line. This frequency is in agreement with previous data reporting stem cells to be scarce, with

percentages lower than 1% of the whole cell population (Bonnet and Dick, 1997). Our results are further supported by similar observations by other groups, that describe stem-like properties in the cells composing mammospheres derived from MCF-7 cell line (Ponti et al., 2005).

Remarkably, our data demonstrate that PPARγ ligands significantly reduce cancer stem cell growth, since treatment with these compounds significantly diminish the number of spheres, with 15d-PGJ_2 and rosiglitazone showing the most significant effects. However, effects exerted by pioglitazone, although not so rapidly also cause a decrease in mammosphere number, and moreover, impairs self-renewal of cancer stem cells. Thus, the previously mentioned antineoplastic effects of PPARγ ligands are not limited to cells of the bulk of the tumour, but are also effective on the cancer stem cell subset.

In addition, the present study analyzes the reliability of other systems rather than mammosphere culture to study breast cancer stem cells. Although mammosphere formation is a widely accepted method to identify cancer stem cells, it accounts for the disadvantage of being an indirect method that indicates the presence of a cancer stem cells only after it has undergone division and formed a cluster of daughter cells composed by both stem and differentiated cells. Thus, although this method enormously purifies the culture in cancer stem cells, it is not capable of identifying single cancer stem cells, rending impossible their isolation. To this purpose, characterization of cancer stem cells by differential expression of membrane antigens has become a priority.

Serial dilution transplantation studies in immunocompromised mice established $CD44^{+}/CD24^{-/low}$ expression pattern as the defining-phenotype for breast cancer stem cells (Al-Hajj et al., 2003). However, our screening for this phenotype in human breast cancer cell lines revealed that SKBR3, MCF-7 and T47D cells are depleted of cells with this pattern, whereas MDA-MB-231 cells are nearly 100% positive for this profile. This data are in agreement with data from other authors. Sheridan et al. obtained similar percentages of $CD44^{+}/CD24^{-/low}$ cells in the four cell lines studied (Sheridan et al., 2006), and recently Crocker et al. reported similar percentages in MCF-7 (0.05 ± 0.01%) and MDA-MB-231 (79 ± 2.7%) cells (Croker et al., 2008). In addition, our

analysis by flow cytometry for CD44 and CD24 staining reveals that there is no enrichment in $CD44^{+}/CD24^{-/low}$ cells in mammospheres when compared to adherent cultures. However, culture as spheres has been shown to result in increased number of progenitor cells (Dontu et al., 2003). Therefore, our flow cytometry results opposed those obtained from the mammosphere-forming assays, that had revealed the existence on cancer stem cells in all four cell lines. Interestingly, SKBR3, MCF-7 and T47D share a common origin. These cell lines are derived from luminal tissue in the mammary gland, whereas MDA-MB-231 cells have a basal origin, suggesting that $CD44^{+}/CD24^{-/low}$ profile could be a marker for basal origin, instead of stemness. This conclusion is further supported by the fact that no statistical significance has been found for CD44 nor CD24 with any histopathologic characteristic (such as grade, size or type) in primary breast tumours (Abraham et al., 2005). Moreover, a study regarding 240 human breast primary tumours detected $CD44^{+}/CD24^{-/low}$ cells only in 31% of the tumours, the majority of which were of basal origin (Honeth et al., 2008). In addition, no correlation between $CD44^{+}/CD24^{-/low}$ profile and prognosis (Shipitsin et al., 2007) or metastatic capacity (Sheridan et al., 2006) has been found, whereas evidences correlating CD24 staining and luminal origin in normal mouse mammary gland cells (Sleeman et al., 2006) have been published. According to this, $CD24^{-}$ cells correspond to non-epithelial cells, whereas $CD24^{low}$ cells are myoepithelial and $CD24^{hi}$ are luminal.

The activity of the enzyme aldehyde dehydrogenase (ALDH) has been shown to identify cells with stem properties in several tissues, including breast and colon (Ginestier et al., 2007). However, the utilization of this marker in our studies in unviable due to the fact that ALDH gene expression has been reported to be upregulated by PPARγ ligands (Moreb et al., 2008), and the utilization of this marker would therefore bias our results.

Other authors consider the side population (SP) a model of cancer stem cells (Zhou et al., 2007) based on the observations that this population is enriched in tumorigenic stem-like cancer cells (Patrawala et al., 2005). However, the same authors state that tumorigenicity is not dependent on expression of the ABCG2 transporter, in charge of mediating the efflux of Hoechst 33342 that determines the apparition of the SP. Moreover, murine mammary stem cell have not been found to be preferentially in the

SP region (Stingl et al., 2006). We report that PPARγ ligands, which we prove to seriously affect growth of cancer stem cells, have no effect on the percentage of cells comprising the SP of MCF-7 cells. In addition, we conclude that SP is not a reliable model of cancer stem cells, since both cells in the SP and their non-SP counterparts are capable of originating spheres and exhibit similar tumorigenicity *in vivo*. Although there are evidences in several cancer types pointing to greater SP tumorigenity, several findings indicate that SP cells are capable of a better growth than non-SP cells at low density (Mitsutake et al., 2007).

Altogether, our work provides evidence that PPARγ ligands exert antiproliferative effects on human breast cancer stem cells throughout multiple mechanism including regulation of cancer stem cells.

CONCLUSIONS

CONCLUSIONS

1.- 15-deoxi-Δ^{12-14}-Prostaglandin J_2, rosiglitazone and pioglitazone cause a decrease in the viability of human breast cancer cells, together with a reduction of their proliferation and an increase in their apoptosis.

2.- Members of the thiadiazolidinones (TDZDs) family are efficient inducers of breast cancer cell death, causing a decrease in their viability and proliferation through a mechanism that possibly implies PPARγ activation.

3.- Src-Homology-2 domain-containing phosphatase 1 (SHP-1) mediates the dephosphorylation of ErbB2 and ErbB3 receptors in response to treatment with 15d- Δ^{12-14}-Prostaglandin J_2, causing a blockage of their signalling pathway.

4.- 15-deoxi-Δ^{12-14}-Prostaglandin J_2 induces cell cycle arrest in the G_2/M phase of the cell cycle and disruption of the microtubule network due to direct binding of this prostanoid to α- and β-tubulin and a subsequent mitotic arrest.

5.- 15-deoxi-Δ^{12-14}-Prostaglandin J_2, rosiglitazone and pioglitazone significantly inhibit cell growth and self-renewal of human breast cancer stem cells.

CONCLUSIONES

CONCLUSIONES

1.- 15-deoxi-Δ^{12-14}-Prostaglandina J_2, rosiglitazona y pioglitazona causan una reducción de la viabilidad de células humanas de cáncer de mama así como a una reducción de su proliferación y un aumento de su apoptosis.

2.- Los miembros de la familia de las tiadiazolidinonas (TDZDs) son eficientes promotores de la muerte de células de cáncer de mama, provocando un descenso de su viabilidad y proliferación mediante un mecanismo en el que posiblemente está implicada la activación de PPARγ.

3.- La fosfatasa 1 con dominios de homología a Src (SHP-1) media la defosforilación de los receptores ErbB2 y ErbB3 en respuesta al tratamiento con 15-deoxi-Δ^{12-14}-Prostaglandina J_2, causando el bloqueo de sus respectivas vías de señalización.

4.- 15-deoxi-Δ^{12-14}-Prostaglandina J_2 promueve la parada del ciclo celular en fase G_2/M, así como la desestructuración de la red de microtúbulos debido a la unión directa de este prostanoide a α- y β-tubulina y la consecuente parada mitótica.

5.- 15-deoxi-Δ^{12-14}-Prostaglandina J_2, rosiglitazona y pioglitazona inhiben significativamente el crecimiento celular y la auto-renovación de células madre humanas de cáncer de mama.

BIBLIOGRAFIA

REFERENCES

Abraham, B.K., Fritz, P., McClellan, M., Hauptvogel, P., Athelogou, M., and Brauch, H. (2005). Prevalence of CD44+/CD24-/low cells in breast cancer may not be associated with clinical outcome but may favor distant metastasis. Clin Cancer Res *11*, 1154-1159.

Agazie, Y.M., Movilla, N., Ischenko, I., and Hayman, M.J. (2003). The phosphotyrosine phosphatase SHP2 is a critical mediator of transformation induced by the oncogenic fibroblast growth factor receptor 3. Oncogene *22*, 6909-6918.

Al-Hajj, M., Wicha, M.S., Benito-Hernandez, A., Morrison, S.J., and Clarke, M.F. (2003). Prospective identification of tumorigenic breast cancer cells. Proc Natl Acad Sci U S A *100*, 3983-3988.

Badano, J.L., Teslovich, T.M., and Katsanis, N. (2005). The centrosome in human genetic disease. Nat Rev Genet *6*, 194-205.

Ball, E.H., and Singer, S.J. (1982). Mitochondria are associated with microtubules and not with intermediate filaments in cultured fibroblasts. Proc Natl Acad Sci U S A *79*, 123-126.

Baselga, J., and Swain, S.M. (2009). Novel anticancer targets: revisiting ERBB2 and discovering ERBB3. Nat Rev Cancer *9*, 463-475.

Basu-Modak, S., Braissant, O., Escher, P., Desvergne, B., Honegger, P., and Wahli, W. (1999). Peroxisome proliferator-activated receptor beta regulates acyl-CoA synthetase 2 in reaggregated rat brain cell cultures. J Biol Chem *274*, 35881-35888.

Bhatia, M., Wang, J.C., Kapp, U., Bonnet, D., and Dick, J.E. (1997). Purification of primitive human hematopoietic cells capable of repopulating immune-deficient mice. Proc Natl Acad Sci U S A *94*, 5320-5325.

Bonnet, D., and Dick, J.E. (1997). Human acute myeloid leukemia is organized as a hierarchy that originates from a primitive hematopoietic cell. Nat Med *3*, 730-737.

Bragt, M.C., and Popeijus, H.E. (2008). Peroxisome proliferator-activated receptors and the metabolic syndrome. Physiol Behav *94*, 187-197.

Bonofiglio, D., Aquila, S., Catalano, S., Gabriele, S., Belmonte, M., Middea, E., Qi, H., Morelli, C., Gentile, M., Maggiolini, M., *et al.* (2006). Peroxisome proliferator-activated receptor-gamma activates p53 gene promoter binding to the nuclear factor-kappaB sequence in human MCF7 breast cancer cells. Mol Endocrinol *20*, 3083-3092.

Britto, P.J., Knipling, L., and Wolff, J. (2002). The local electrostatic environment determines cysteine reactivity of tubulin. J Biol Chem *277*, 29018-29027.

Bruecher-Encke, B., Griffin, J.D., Neel, B.G., and Lorenz, U. (2001). Role of the tyrosine phosphatase SHP-1 in K562 cell differentiation. Leukemia *15*, 1424-1432.

Buey, R.M., Calvo, E., Barasoain, I., Pineda, O., Edler, M.C., Matesanz, R., Cerezo, G., Vanderwal, C.D., Day, B.W., Sorensen, E.J., *et al.* (2007). Cyclostreptin binds covalently to microtubule pores and lumenal taxoid binding sites. Nat Chem Biol *3*, 117-125.

Burstein, H.J., Demetri, G.D., Mueller, E., Sarraf, P., Spiegelman, B.M., and Winer, E.P. (2003). Use of the peroxisome proliferator-activated receptor (PPAR) gamma ligand troglitazone as treatment for refractory breast cancer: a phase II study. Breast Cancer Res Treat *79*, 391-397.

Chaffer, C.L., Thomas, D.M., Thompson, E.W., and Williams, E.D. (2006). PPARgamma-independent induction of growth arrest and apoptosis in prostate and bladder carcinoma. BMC Cancer *6*, 53.

Chen, H.E., Chang, S., Trub, T., and Neel, B.G. (1996). Regulation of colony-stimulating factor 1 receptor signaling by the SH2 domain-containing tyrosine phosphatase SHPTP1. Mol Cell Biol *16*, 3685-3697.

Citri, A., and Yarden, Y. (2006). EGF-ERBB signalling: towards the systems level. Nat Rev Mol Cell Biol *7*, 505-516.

Clay, C.E., Monjazeb, A., Thorburn, J., Chilton, F.H., and High, K.P. (2002). 15-Deoxy-delta12,14-prostaglandin J2-induced apoptosis does not require PPARgamma in breast cancer cells. J Lipid Res *43*, 1818-1828.

Croker, A.K., Goodale, D., Chu, J., Postenka, C., Hedley, B.D., Hess, D.A., and Allan, A.L. (2008). High aldehyde dehydrogenase and expression of cancer stem cell markers selects for breast cancer cells with enhanced malignant and metastatic ability. J Cell Mol Med.

Dontu, G., Abdallah, W.M., Foley, J.M., Jackson, K.W., Clarke, M.F., Kawamura, M.J., and Wicha, M.S. (2003). In vitro propagation and transcriptional profiling of human mammary stem/progenitor cells. Genes Dev *17*, 1253-1270.

Elnemr, A., Ohta, T., Iwata, K., Ninomia, I., Fushida, S., Nishimura, G., Kitagawa, H., Kayahara, M., Yamamoto, M., Terada, T., *et al.* (2000). PPARgamma ligand (thiazolidinedione) induces growth arrest and differentiation markers of human pancreatic cancer cells. Int J Oncol *17*, 1157-1164.

Elstner, E., Muller, C., Koshizuka, K., Williamson, E.A., Park, D., Asou, H., Shintaku, P., Said, J.W., Heber, D., and Koeffler, H.P. (1998). Ligands for peroxisome proliferator-activated receptorgamma and retinoic acid receptor inhibit growth and induce apoptosis of human breast cancer cells in vitro and in BNX mice. Proc Natl Acad Sci U S A *95*, 8806-8811.

Engelmann, K., Shen, H., and Finn, O.J. (2008). MCF7 side population cells with characteristics of cancer stem/progenitor cells express the tumor antigen MUC1. Cancer Res *68*, 2419-2426.

Evans, R.M. (1988). The steroid and thyroid hormone receptor superfamily. Science *240*, 889-895.

Ferlay, J., Autier, P., Boniol, M., Heanue, M., Colombet, M., and Boyle, P. (2007). Estimates of the cancer incidence and mortality in Europe in 2006. Ann Oncol *18*, 581-592.

Fillmore, C.M., and Kuperwasser, C. (2008). Human breast cancer cell lines contain stem-like cells that self-renew, give rise to phenotypically diverse progeny and survive chemotherapy. Breast Cancer Res *10*, R25.

Forman, B.M., Tontonoz, P., Chen, J., Brun, R.P., Spiegelman, B.M., and Evans, R.M. (1995). 15-Deoxy-delta 12, 14-prostaglandin J2 is a ligand for the adipocyte determination factor PPAR gamma. Cell *83*, 803-812.

Frank, C., Burkhardt, C., Imhof, D., Ringel, J., Zschornig, O., Wieligmann, K., Zacharias, M., and Bohmer, F.D. (2004). Effective dephosphorylation of Src substrates by SHP-1. J Biol Chem *279*, 11375-11383.

Fu, Y.G., Sung, J.J., Wu, K.C., Bai, A.H., Chan, M.C., Yu, J., Fan, D.M., and Leung, W.K. (2006). Inhibition of gastric cancer cells associated angiogenesis by 15d-prostaglandin J2 through the downregulation of angiopoietin-1. Cancer Lett *243*, 246-254.

Gensler, M., Buschbeck, M., and Ullrich, A. (2004). Negative regulation of HER2 signaling by the PEST-type protein-tyrosine phosphatase BDP1. J Biol Chem *279*, 12110-12116.

Ginestier, C., Hur, M.H., Charafe-Jauffret, E., Monville, F., Dutcher, J., Brown, M., Jacquemier, J., Viens, P., Kleer, C.G., Liu, S., *et al.* (2007). ALDH1 is a marker of normal and malignant human mammary stem cells and a predictor of poor clinical outcome. Cell Stem Cell *1*, 555-567.

Goodell, M.A., Brose, K., Paradis, G., Conner, A.S., and Mulligan, R.C. (1996). Isolation and functional properties of murine hematopoietic stem cells that are replicating in vivo. J Exp Med *183*, 1797-1806.

Grommes, C., Landreth, G.E., and Heneka, M.T. (2004). Antineoplastic effects of peroxisome proliferator-activated receptor gamma agonists. Lancet Oncol *5*, 419-429.

Grommes, C., Landreth, G.E., Sastre, M., Beck, M., Feinstein, D.L., Jacobs, A.H., Schlegel, U., and Heneka, M.T. (2006). Inhibition of in vivo glioma growth and invasion by peroxisome proliferator-activated receptor gamma agonist treatment. Mol Pharmacol *70*, 1524-1533.

Guzman, M.L., Li, X., Corbett, C.A., Rossi, R.M., Bushnell, T., Liesveld, J.L., Hebert, J., Young, F., and Jordan, C.T. (2007). Rapid and selective death of leukemia stem and progenitor cells induced by the compound 4-benzyl, 2-methyl, 1,2,4-thiadiazolidine, 3,5 dione (TDZD-8). Blood *110*, 4436-4444.

He, D., Song, X., Liu, L., Burk, D.H., and Zhou, G.W. (2005). EGF-stimulation activates the nuclear localization signal of SHP-1. J Cell Biochem *94*, 944-953.

Hellyer, N.J., Cheng, K., and Koland, J.G. (1998). ErbB3 (HER3) interaction with the p85 regulatory subunit of phosphoinositide 3-kinase. Biochem J *333 (Pt 3)*, 757-763.

Hennighausen, L., and Robinson, G.W. (2005). Information networks in the mammary gland. Nat Rev Mol Cell Biol *6*, 715-725.

Ho, T.C., Chen, S.L., Yang, Y.C., Chen, C.Y., Feng, F.P., Hsieh, J.W., Cheng, H.C., and Tsao, Y.P. (2008). 15-deoxy-Delta(12,14)-prostaglandin J2 induces vascular endothelial cell apoptosis through the sequential activation of MAPKS and p53. J Biol Chem *283*, 30273-30288.

Holbro, T., Beerli, R.R., Maurer, F., Koziczak, M., Barbas, C.F., 3rd, and Hynes, N.E. (2003a). The ErbB2/ErbB3 heterodimer functions as an oncogenic unit: ErbB2 requires ErbB3 to drive breast tumor cell proliferation. Proc Natl Acad Sci U S A *100*, 8933-8938.

Holbro, T., Civenni, G., and Hynes, N.E. (2003b). The ErbB receptors and their role in cancer progression. Exp Cell Res *284*, 99-110.

Hollmen, M., Maatta, J.A., Bald, L., Sliwkowski, M.X., and Elenius, K. (2009). Suppression of breast cancer cell growth by a monoclonal antibody targeting cleavable ErbB4 isoforms. Oncogene *28*, 1309-1319.

Home, P.D., Pocock, S.J., Beck-Nielsen, H., Curtis, P.S., Gomis, R., Hanefeld, M., Jones, N.P., Komajda, M., and McMurray, J.J. (2009). Rosiglitazone evaluated for cardiovascular outcomes in oral agent combination therapy for type 2 diabetes (RECORD): a multicentre, randomised, open-label trial. Lancet.

Honeth, G., Bendahl, P.O., Ringner, M., Saal, L.H., Gruvberger-Saal, S.K., Lovgren, K., Grabau, D., Ferno, M., Borg, A., and Hegardt, C. (2008). The CD44+/CD24- phenotype is enriched in basal-like breast tumors. Breast Cancer Res *10*, R53.

Huang, Y., Johnson, K.R., Norris, J.S., and Fan, W. (2000). Nuclear factor-kappaB/IkappaB signaling pathway may contribute to the mediation of paclitaxel-induced apoptosis in solid tumor cells. Cancer Res *60*, 4426-4432.

Hynes, N.E., and Lane, H.A. (2005). ERBB receptors and cancer: the complexity of targeted inhibitors. Nat Rev Cancer *5*, 341-354.

Jiang, C., Ting, A.T., and Seed, B. (1998). PPAR-gamma agonists inhibit production of monocyte inflammatory cytokines. Nature *391*, 82-86.

Jordan, M.A. (2002). Mechanism of action of antitumor drugs that interact with microtubules and tubulin. Curr Med Chem Anticancer Agents *2*, 1-17.

Jordan, M.A., Wendell, K., Gardiner, S., Derry, W.B., Copp, H., and Wilson, L. (1996). Mitotic block induced in HeLa cells by low concentrations of paclitaxel (Taxol) results in abnormal mitotic exit and apoptotic cell death. Cancer Res *56*, 816-825.

Jordan, M.A., and Wilson, L. (2004). Microtubules as a target for anticancer drugs. Nat Rev Cancer *4*, 253-265.

Kanthou, C., Greco, O., Stratford, A., Cook, I., Knight, R., Benzakour, O., and Tozer, G. (2004). The tubulin-binding agent combretastatin A-4-phosphate arrests endothelial cells in mitosis and induces mitotic cell death. Am J Pathol *165*, 1401-1411.

Keilhack, H., Tenev, T., Nyakatura, E., Godovac-Zimmermann, J., Nielsen, L., Seedorf, K., and Bohmer, F.D. (1998). Phosphotyrosine 1173 mediates binding of the protein-tyrosine phosphatase SHP-1 to the epidermal growth factor receptor and attenuation of receptor signaling. J Biol Chem *273*, 24839-24846.

Keller, H., and Wahli, W. (1993). Peroxisome proliferator-activated receptors A link between endocrinology and nutrition? Trends Endocrinol Metab *4*, 291-296.

Keshamouni, V.G., Reddy, R.C., Arenberg, D.A., Joel, B., Thannickal, V.J., Kalemkerian, G.P., and Standiford, T.J. (2004). Peroxisome proliferator-activated receptor-gamma activation inhibits tumor progression in non-small-cell lung cancer. Oncogene *23*, 100-108.

Kim, K.Y., Kim, S.S., and Cheon, H.G. (2006). Differential anti-proliferative actions of peroxisome proliferator-activated receptor-gamma agonists in MCF-7 breast cancer cells. Biochem Pharmacol *72*, 530-540.

Kim, E.H., and Surh, Y.J. (2006). 15-deoxy-Delta12,14-prostaglandin J2 as a potential endogenous regulator of redox-sensitive transcription factors. Biochem Pharmacol *72*, 1516-1528.

Kim, E.H., Na, H.K., Kim, D.H., Park, S.A., Kim, H.N., Song, N.Y., and Surh, Y.J. (2008). 15-Deoxy-Delta12,14-prostaglandin J2 induces COX-2 expression through Akt-driven AP-1 activation in human breast cancer cells: a potential role of ROS. Carcinogenesis *29*, 688-695.

Kliewer, S.A., Lenhard, J.M., Willson, T.M., Patel, I., Morris, D.C., and Lehmann, J.M. (1995). A prostaglandin J2 metabolite binds peroxisome proliferator-activated receptor gamma and promotes adipocyte differentiation. Cell *83*, 813-819.

Klingmuller, U., Lorenz, U., Cantley, L.C., Neel, B.G., and Lodish, H.F. (1995). Specific recruitment of SH-PTP1 to the erythropoietin receptor causes inactivation of JAK2 and termination of proliferative signals. Cell *80*, 729-738.

Kubota, T., Koshizuka, K., Williamson, E.A., Asou, H., Said, J.W., Holden, S., Miyoshi, I., and Koeffler, H.P. (1998). Ligand for peroxisome proliferator-activated receptor gamma (troglitazone) has potent antitumor effect against human prostate cancer both in vitro and in vivo. Cancer Res *58*, 3344-3352.

Lee-Hoeflich, S.T., Crocker, L., Yao, E., Pham, T., Munroe, X., Hoeflich, K.P., Sliwkowski, M.X., and Stern, H.M. (2008). A central role for HER3 in HER2-amplified breast cancer: implications for targeted therapy. Cancer Res *68*, 5878-5887.

Lehmann, J.M., Lenhard, J.M., Oliver, B.B., Ringold, G.M., and Kliewer, S.A. (1997). Peroxisome proliferator-activated receptors alpha and gamma are activated by indomethacin and other non-steroidal anti-inflammatory drugs. J Biol Chem *272*, 3406-3410.

Li, R.Y., Gaits, F., Ragab, A., Ragab-Thomas, J.M., and Chap, H. (1995). Tyrosine phosphorylation of an SH2-containing protein tyrosine phosphatase is coupled to platelet thrombin receptor via a pertussis toxin-sensitive heterotrimeric G-protein. EMBO J *14*, 2519-2526.

Lin, H.L., Chang, Y.F., Liu, T.Y., Wu, C.W., and Chi, C.W. (1998). Submicromolar paclitaxel induces apoptosis in human gastric cancer cells at early G1 phase. Anticancer Res *18*, 3443-3449.

Lorenz, U., Ravichandran, K.S., Burakoff, S.J., and Neel, B.G. (1996). Lack of SHPTP1 results in src-family kinase hyperactivation and thymocyte hyperresponsiveness. Proc Natl Acad Sci U S A *93*, 9624-9629.

Luna-Medina, R., Cortes-Canteli, M., Alonso, M., Santos, A., Martinez, A., and Perez-Castillo, A. (2005). Regulation of inflammatory response in neural cells in vitro by thiadiazolidinones derivatives through peroxisome proliferator-activated receptor gamma activation. J Biol Chem *280*, 21453-21462.

Luna-Medina, R., Cortes-Canteli, M., Sanchez-Galiano, S., Morales-Garcia, J.A., Martinez, A., Santos, A., and Perez-Castillo, A. (2007). NP031112, a thiadiazolidinone compound, prevents inflammation and neurodegeneration under excitotoxic conditions: potential therapeutic role in brain disorders. J Neurosci *27*, 5766-5776.

Mangelsdorf, D.J., Borgmeyer, U., Heyman, R.A., Zhou, J.Y., Ong, E.S., Oro, A.E., Kakizuka, A., and Evans, R.M. (1992). Characterization of three RXR genes that mediate the action of 9-cis retinoic acid. Genes Dev *6*, 329-344.

Martinez, A., Alonso, M., Castro, A., Perez, C., and Moreno, F.J. (2002). First non-ATP competitive glycogen synthase kinase 3 beta (GSK-3beta) inhibitors: thiadiazolidinones (TDZD) as potential drugs for the treatment of Alzheimer's disease. J Med Chem *45*, 1292-1299.

Miller, M.C., 3rd, Johnson, K.R., Willingham, M.C., and Fan, W. (1999). Apoptotic cell death induced by baccatin III, a precursor of paclitaxel, may occur without G(2)/M arrest. Cancer Chemother Pharmacol *44*, 444-452.

Minotti, A.M., Barlow, S.B., and Cabral, F. (1991). Resistance to antimitotic drugs in Chinese hamster ovary cells correlates with changes in the level of polymerized tubulin. J Biol Chem *266*, 3987-3994.

Mitsutake, N., Iwao, A., Nagai, K., Namba, H., Ohtsuru, A., Saenko, V., and Yamashita, S. (2007). Characterization of side population in thyroid cancer cell lines: cancer stem-like cells are enriched partly but not exclusively. Endocrinology *148*, 1797-1803.

Moreb, J.S., Baker, H.V., Chang, L.J., Amaya, M., Lopez, M.C., Ostmark, B., and Chou, W. (2008). ALDH isozymes downregulation affects cell growth, cell motility and gene expression in lung cancer cells. Mol Cancer *7*, 87.

Nabha, S.M., Mohammad, R.M., Dandashi, M.H., Coupaye-Gerard, B., Aboukameel, A., Pettit, G.R., and Al-Katib, A.M. (2002). Combretastatin-A4 prodrug induces mitotic catastrophe in chronic

lymphocytic leukemia cell line independent of caspase activation and poly(ADP-ribose) polymerase cleavage. Clin Cancer Res *8*, 2735-2741.

O'Brien, C.A., Pollett, A., Gallinger, S., and Dick, J.E. (2007). A human colon cancer cell capable of initiating tumour growth in immunodeficient mice. Nature *445*, 106-110.

O'Brien, J.J., Baglole, C.J., Garcia-Bates, T.M., Blumberg, N., Francis, C.W., and Phipps, R.P. (2009). 15-deoxy-Delta12,14 prostaglandin J2-induced heme oxygenase-1 in megakaryocytes regulates thrombopoiesis. J Thromb Haemost *7*, 182-189.

Oka, T., Yoshino, T., Hayashi, K., Ohara, N., Nakanishi, T., Yamaai, Y., Hiraki, A., Sogawa, C.A., Kondo, E., Teramoto, N., *et al.* (2001). Reduction of hematopoietic cell-specific tyrosine phosphatase SHP-1 gene expression in natural killer cell lymphoma and various types of lymphomas/leukemias : combination analysis with cDNA expression array and tissue microarray. Am J Pathol *159*, 1495-1505.

Oliva, J.L., Perez-Sala, D., Castrillo, A., Martinez, N., Canada, F.J., Bosca, L., and Rojas, J.M. (2003). The cyclopentenone 15-deoxy-delta 12,14-prostaglandin J2 binds to and activates H-Ras. Proc Natl Acad Sci U S A *100*, 4772-4777.

Ostman, A., and Bohmer, F.D. (2001). Regulation of receptor tyrosine kinase signaling by protein tyrosine phosphatases. Trends Cell Biol *11*, 258-266.

Palmer, C.N., Hsu, M.H., Griffin, H.J., and Johnson, E.F. (1995). Novel sequence determinants in peroxisome proliferator signaling. J Biol Chem *270*, 16114-16121.

Panigrahy, D., Singer, S., Shen, L.Q., Butterfield, C.E., Freedman, D.A., Chen, E.J., Moses, M.A., Kilroy, S., Duensing, S., Fletcher, C., *et al.* (2002). PPARgamma ligands inhibit primary tumor growth and metastasis by inhibiting angiogenesis. J Clin Invest *110*, 923-932.

Patrawala, L., Calhoun, T., Schneider-Broussard, R., Zhou, J., Claypool, K., and Tang, D.G. (2005). Side population is enriched in tumorigenic, stem-like cancer cells, whereas ABCG2+ and ABCG2- cancer cells are similarly tumorigenic. Cancer Res *65*, 6207-6219.

Paulson, R.F., Vesely, S., Siminovitch, K.A., and Bernstein, A. (1996). Signalling by the W/Kit receptor tyrosine kinase is negatively regulated in vivo by the protein tyrosine phosphatase Shp1. Nat Genet *13*, 309-315.

Pei, D., Lorenz, U., Klingmuller, U., Neel, B.G., and Walsh, C.T. (1994). Intramolecular regulation of protein tyrosine phosphatase SH-PTP1: a new function for Src homology 2 domains. Biochemistry *33*, 15483-15493.

Phulwani, N.K., Feinstein, D.L., Gavrilyuk, V., Akar, C., and Kielian, T. (2006). 15-deoxy-Delta12,14-prostaglandin J2 (15d-PGJ2) and ciglitazone modulate Staphylococcus aureus-dependent astrocyte activation primarily through a PPAR-gamma-independent pathway. J Neurochem *99*, 1389-1402.

Pighetti, G.M., Novosad, W., Nicholson, C., Hitt, D.C., Hansens, C., Hollingsworth, A.B., Lerner, M.L., Brackett, D., Lightfoot, S.A., and Gimble, J.M. (2001). Therapeutic treatment of DMBA-induced mammary tumors with PPAR ligands. Anticancer Res *21*, 825-829.

Pignatelli, M., Cortes-Canteli, M., Lai, C., Santos, A., and Perez-Castillo, A. (2001). The peroxisome proliferator-activated receptor gamma is an inhibitor of ErbBs activity in human breast cancer cells. J Cell Sci *114*, 4117-4126.

Pignatelli, M., Cocca, C., Santos, A., and Perez-Castillo, A. (2003). Enhancement of BRCA1 gene expression by the peroxisome proliferator-activated receptor gamma in the MCF-7 breast cancer cell line. Oncogene *22*, 5446-5450.

Pignatelli, M., Sanchez-Rodriguez, J., Santos, A., and Perez-Castillo, A. (2005). 15-deoxy-Delta-12,14-prostaglandin J2 induces programmed cell death of breast cancer cells by a pleiotropic mechanism. Carcinogenesis *26*, 81-92.

Pihan, G.A., Purohit, A., Wallace, J., Knecht, H., Woda, B., Quesenberry, P., and Doxsey, S.J. (1998). Centrosome defects and genetic instability in malignant tumors. Cancer Res *58*, 3974-3985.

Pihan, G.A., Purohit, A., Wallace, J., Malhotra, R., Liotta, L., and Doxsey, S.J. (2001). Centrosome defects can account for cellular and genetic changes that characterize prostate cancer progression. Cancer Res *61*, 2212-2219.

Plutzky, J., Neel, B.G., and Rosenberg, R.D. (1992). Isolation of a src homology 2-containing tyrosine phosphatase. Proc Natl Acad Sci U S A *89*, 1123-1127.

Ponti, D., Costa, A., Zaffaroni, N., Pratesi, G., Petrangolini, G., Coradini, D., Pilotti, S., Pierotti, M.A., and Daidone, M.G. (2005). Isolation and in vitro propagation of tumorigenic breast cancer cells with stem/progenitor cell properties. Cancer Res *65*, 5506-5511.

Poole, A.W., and Jones, M.L. (2005). A SHPing tale: perspectives on the regulation of SHP-1 and SHP-2 tyrosine phosphatases by the C-terminal tail. Cell Signal *17*, 1323-1332.

Qu, C.K., Nguyen, S., Chen, J., and Feng, G.S. (2001). Requirement of Shp-2 tyrosine phosphatase in lymphoid and hematopoietic cell development. Blood *97*, 911-914.

Quintana, E., Shackleton, M., Sabel, M.S., Fullen, D.R., Johnson, T.M., and Morrison, S.J. (2008). Efficient tumour formation by single human melanoma cells. Nature *456*, 593-598.

Ricote, M., Li, A.C., Willson, T.M., Kelly, C.J., and Glass, C.K. (1998). The peroxisome proliferator-activated receptor-gamma is a negative regulator of macrophage activation. Nature *391*, 79-82.

Rossi, A., Kapahi, P., Natoli, G., Takahashi, T., Chen, Y., Karin, M., and Santoro, M.G. (2000). Anti-inflammatory cyclopentenone prostaglandins are direct inhibitors of IkappaB kinase. Nature *403*, 103-108.

Sankaran, S., and Parvin, J.D. (2006). Centrosome function in normal and tumor cells. J Cell Biochem *99*, 1240-1250.

Sato, H., Ishihara, S., Kawashima, K., Moriyama, N., Suetsugu, H., Kazumori, H., Okuyama, T., Rumi, M.A., Fukuda, R., Nagasue, N., *et al.* (2000). Expression of peroxisome proliferator-activated receptor (PPAR)gamma in gastric cancer and inhibitory effects of PPARgamma agonists. Br J Cancer *83*, 1394-1400.

Schneeweiss, A., Sinn, H.P., Ehemann, V., Khbeis, T., Neben, K., Krause, U., Ho, A.D., Bastert, G., and Kramer, A. (2003). Centrosomal aberrations in primary invasive breast cancer are associated with nodal status and hormone receptor expression. Int J Cancer *107*, 346-352.

Schneider, Y., Chabert, P., Stutzmann, J., Coelho, D., Fougerousse, A., Gosse, F., Launay, J.F., Brouillard, R., and Raul, F. (2003). Resveratrol analog (Z)-3,5,4'-trimethoxystilbene is a potent anti-mitotic drug inhibiting tubulin polymerization. Int J Cancer *107*, 189-196.

Sergina, N.V., Rausch, M., Wang, D., Blair, J., Hann, B., Shokat, K.M., and Moasser, M.M. (2007). Escape from HER-family tyrosine kinase inhibitor therapy by the kinase-inactive HER3. Nature *445*, 437-441.

Sertznig, P., Seifert, M., Tilgen, W., and Reichrath, J. (2007). Present concepts and future outlook: function of peroxisome proliferator-activated receptors (PPARs) for pathogenesis, progression, and therapy of cancer. J Cell Physiol *212*, 1-12.

Sheridan, C., Kishimoto, H., Fuchs, R.K., Mehrotra, S., Bhat-Nakshatri, P., Turner, C.H., Goulet, R., Jr., Badve, S., and Nakshatri, H. (2006). CD44+/CD24- breast cancer cells exhibit enhanced invasive properties: an early step necessary for metastasis. Breast Cancer Res *8*, R59.

Shipitsin, M., Campbell, L.L., Argani, P., Weremowicz, S., Bloushtain-Qimron, N., Yao, J., Nikolskaya, T., Serebryiskaya, T., Beroukhim, R., Hu, M., *et al.* (2007). Molecular definition of breast tumor heterogeneity. Cancer Cell *11*, 259-273.

Singh, S.K., Hawkins, C., Clarke, I.D., Squire, J.A., Bayani, J., Hide, T., Henkelman, R.M., Cusimano, M.D., and Dirks, P.B. (2004). Identification of human brain tumour initiating cells. Nature *432*, 396-401.

Slamon, D.J., Godolphin, W., Jones, L.A., Holt, J.A., Wong, S.G., Keith, D.E., Levin, W.J., Stuart, S.G., Udove, J., Ullrich, A., *et al.* (1989). Studies of the HER-2/neu proto-oncogene in human breast and ovarian cancer. Science *244*, 707-712.

Sleeman, K.E., Kendrick, H., Ashworth, A., Isacke, C.M., and Smalley, M.J. (2006). CD24 staining of mouse mammary gland cells defines luminal epithelial, myoepithelial/basal and non-epithelial cells. Breast Cancer Res *8*, R7.

Sohda, T., Momose, Y., Meguro, K., Kawamatsu, Y., Sugiyama, Y., and Ikeda, H. (1990). Studies on antidiabetic agents. Synthesis and hypoglycemic activity of 5-[4-(pyridylalkoxy)benzyl]-2,4-thiazolidinediones. Arzneimittelforschung *40*, 37-42.

Srsen, V., and Merdes, A. (2006). The centrosome and cell proliferation. Cell Div *1*, 26.

Stingl, J., Eirew, P., Ricketson, I., Shackleton, M., Vaillant, F., Choi, D., Li, H.I., and Eaves, C.J. (2006). Purification and unique properties of mammary epithelial stem cells. Nature *439*, 993-997.

Straus, D.S., and Glass, C.K. (2001). Cyclopentenone prostaglandins: new insights on biological activities and cellular targets. Med Res Rev *21*, 185-210.

Straus, D.S., Pascual, G., Li, M., Welch, J.S., Ricote, M., Hsiang, C.H., Sengchanthalangsy, L.L., Ghosh, G., and Glass, C.K. (2000). 15-deoxy-delta 12,14-prostaglandin J2 inhibits multiple steps in the NF-kappa B signaling pathway. Proc Natl Acad Sci U S A *97*, 4844-4849.

Tapley, P., Shevde, N.K., Schweitzer, P.A., Gallina, M., Christianson, S.W., Lin, I.L., Stein, R.B., Shultz, L.D., Rosen, J., and Lamb, P. (1997). Increased G-CSF responsiveness of bone marrow cells from hematopoietic cell phosphatase deficient viable motheaten mice. Exp Hematol *25*, 122-131.

Tenev, T., Keilhack, H., Tomic, S., Stoyanov, B., Stein-Gerlach, M., Lammers, R., Krivtsov, A.V., Ullrich, A., and Bohmer, F.D. (1997). Both SH2 domains are involved in interaction of SHP-1 with the epidermal growth factor receptor but cannot confer receptor-directed activity to SHP-1/SHP-2 chimera. J Biol Chem *272*, 5966-5973.

Tomic, S., Greiser, U., Lammers, R., Kharitonenkov, A., Imyanitov, E., Ullrich, A., and Bohmer, F.D. (1995). Association of SH2 domain protein tyrosine phosphatases with the epidermal growth factor receptor in human tumor cells. Phosphatidic acid activates receptor dephosphorylation by PTP1C. J Biol Chem *270*, 21277-21284.

Tonks, N.K. (2006). Protein tyrosine phosphatases: from genes, to function, to disease. Nat Rev Mol Cell Biol *7*, 833-846.

Tontonoz, P., Hu, E., Graves, R.A., Budavari, A.I., and Spiegelman, B.M. (1994). mPPAR gamma 2: tissue-specific regulator of an adipocyte enhancer. Genes Dev *8*, 1224-1234.

Tontonoz, P., Singer, S., Forman, B.M., Sarraf, P., Fletcher, J.A., Fletcher, C.D., Brun, R.P., Mueller, E., Altiok, S., Oppenheim, H., *et al.* (1997). Terminal differentiation of human liposarcoma cells induced by ligands for peroxisome proliferator-activated receptor gamma and the retinoid X receptor. Proc Natl Acad Sci U S A *94*, 237-241.

Uchida, T., Matozaki, T., Noguchi, T., Yamao, T., Horita, K., Suzuki, T., Fujioka, Y., Sakamoto, C., and Kasuga, M. (1994). Insulin stimulates the phosphorylation of Tyr538 and the catalytic activity of PTP1C, a protein tyrosine phosphatase with Src homology-2 domains. J Biol Chem *269*, 12220-12228.

Vambutas, V., Kaplan, D.R., Sells, M.A., and Chernoff, J. (1995). Nerve growth factor stimulates tyrosine phosphorylation and activation of Src homology-containing protein-tyrosine phosphatase 1 in PC12 cells. J Biol Chem *270*, 25629-25633.

Vogel, W., Lammers, R., Huang, J., and Ullrich, A. (1993). Activation of a phosphotyrosine phosphatase by tyrosine phosphorylation. Science *259*, 1611-1614.

Williams, C.C., Allison, J.G., Vidal, G.A., Burow, M.E., Beckman, B.S., Marrero, L., and Jones, F.E. (2004). The ERBB4/HER4 receptor tyrosine kinase regulates gene expression by functioning as a STAT5A nuclear chaperone. J Cell Biol *167*, 469-478.

Wilson, L., and Jordan, M.A. (1995). Microtubule dynamics: taking aim at a moving target. Chem Biol *2*, 569-573.

Woods, C.M., Zhu, J., McQueney, P.A., Bollag, D., and Lazarides, E. (1995). Taxol-induced mitotic block triggers rapid onset of a p53-independent apoptotic pathway. Mol Med *1*, 506-526.

Wu, C., Guan, Q., Wang, Y., Zhao, Z.J., and Zhou, G.W. (2003). SHP-1 suppresses cancer cell growth by promoting degradation of JAK kinases. J Cell Biochem *90*, 1026-1037.

Wu, C.J., O'Rourke, D.M., Feng, G.S., Johnson, G.R., Wang, Q., and Greene, M.I. (2001). The tyrosine phosphatase SHP-2 is required for mediating phosphatidylinositol 3-kinase/Akt activation by growth factors. Oncogene *20*, 6018-6025.

Yang, J., Liu, L., He, D., Song, X., Liang, X., Zhao, Z.J., and Zhou, G.W. (2003). Crystal structure of human protein-tyrosine phosphatase SHP-1. J Biol Chem *278*, 6516-6520.

Yi, T., Mui, A.L., Krystal, G., and Ihle, J.N. (1993). Hematopoietic cell phosphatase associates with the interleukin-3 (IL-3) receptor beta chain and down-regulates IL-3-induced tyrosine phosphorylation and mitogenesis. Mol Cell Biol *13*, 7577-7586.

Yu, Z., Su, L., Hoglinger, O., Jaramillo, M.L., Banville, D., and Shen, S.H. (1998). SHP-1 associates with both platelet-derived growth factor receptor and the p85 subunit of phosphatidylinositol 3-kinase. J Biol Chem *273*, 3687-3694.

Zhang, Z., Shen, K., Lu, W., and Cole, P.A. (2003). The role of C-terminal tyrosine phosphorylation in the regulation of SHP-1 explored via expressed protein ligation. J Biol Chem *278*, 4668-4674.

Zhou, J., Wulfkuhle, J., Zhang, H., Gu, P., Yang, Y., Deng, J., Margolick, J.B., Liotta, L.A., Petricoin, E., 3rd, and Zhang, Y. (2007). Activation of the PTEN/mTOR/STAT3 pathway in breast cancer stem-like cells is required for viability and maintenance. Proc Natl Acad Sci U S A *104*, 16158-16163

Zhou, X.D., and Agazie, Y.M. (2008). Inhibition of SHP2 leads to mesenchymal to epithelial transition in breast cancer cells. Cell Death Differ *15*, 988-996.

Zhou, X., and Agazie, Y.M. (2009). Molecular mechanism for SHP2 in promoting HER2-induced signaling and transformation. J Biol Chem *284*, 12226-12234.

ANEXOS

CV